Chesapeake Bay Trust Restoration Research Award 19278

Climate Change Impacts to Restoration Practices – Final Report

Jonathan B. Butcher[1], David Sample[2], Theresa Thompson[2], Sami Towsif-Khan[2], and Afshin Shabani[1]

September 4, 2023

ABSTRACT

Climate change models predict that frequency and intensity of rain events will increase, that the growing season will lengthen, and that other processes related to the Chesapeake community's approved set of stormwater control measures (SCMs) will change. Increased rainfall intensity under future climate is likely to increase flood risk, alter stream stability, and potentially affect stream restoration structures. Should standards for stormwater practices, stream restoration, and other SCMs also change? There are multiple global climate models (GCMs) and multiple warming scenarios. Further variability is introduced by ways in which the model output is downscaled to a local spatial scale and daily or finer time scale relevant to evaluation of stormwater practices.

In prior work sponsored by CBT Butcher (2021) developed methods and applied them across Maryland to update the rainfall intensity-duration-frequency (IDF) curves used in SCM design based on GCM output with local bias correction. In the current work we address three important issues: (1) To what extent does downscaling method bias results? (2) Do Maryland's Environmental Site Design (ESD) requirements need to be changed to maintain similar levels of hydrologic control in a warming world? (3) How do results for protecting stream stability based on IDF analysis compare to continuous simulations of future climate? This works shows that different commonly used downscaled climate archives do contain systematic relative biases and that potential risks should be evaluated across multiple downscaling products. The ensemble simulation results indicate that the application of ESD concepts and requirements could remain effective in mitigating the impacts of increased runoff resulting from changing climate conditions when evaluated on an individual SCM basis. However, when considering the cumulative effects of development using continuous rainfall simulation of future climate scenarios in a well-studied watershed, it is clear that ESD does not replicate the hydrology of "woods in good condition" and will not protect channel stability over multiple decades under current or future climate conditions.

[1] Tetra Tech, Inc., Research Triangle Park, NC

[2] Biological Systems Engineering, Virginia Tech, Blacksburg, VA

(This page left intentionally blank.)

CONTENTS

TABLES

FIGURES

1.0 INTRODUCTION

This work addresses the CBT 2020 Restoration Research Question B.4: Climate Impacts to Restoration Practices: *Climate change models predict that frequency and intensity of rain events will increase, that [the] growing season will lengthen, and that other processes related to the Chesapeake community's approved set of BMPs will change. As a result, some suggest that standards for stormwater practices, stream restoration, and other BMPs should change (e.g., plan to treat a two-inch rain event versus a one-inch rain event; design stream restoration practices for more frequent storms).*

A topic of particular concern for the Chesapeake Bay watershed is the performance of stormwater control measures (SCMs) that are designed to protect receiving water quality by addressing precipitation events that occur on a relatively frequent basis. Maryland Department of the Environment's (MDE) 2000 Stormwater Design Manual presented calculations for a water quality volume (WQv) and a channel protection volume (CPv) for the design of SCMs. With the 2009 revisions to the Design Manual, MDE moved to the more holistic approach of Environmental Site Design (ESD), which combines the WQv and CPv objectives to produce a unified approach to stormwater design and management based on the net effects of all stormwater controls present on a site (MDE, 2009, Chapter 5).

"Environmental site design" (ESD) is defined as "using small–scale stormwater management practices, nonstructural techniques, and better site planning to mimic natural hydrologic runoff characteristics and minimize the impact of land development on water resources" (Md. Code Ann., Environment Article 4 § 201.1; 2007). ESD encompasses Low Impact Development (LID) but is broader in intent and more specific in application. LID practices are small-scale practices that use infiltration and other processes to capture the water quality storm event, normally 1 in. The general concept of ESD is to control runoff from a developed site in response to the 1-year 24-hour storm so that it is no greater than the runoff that would be expected for the same site with a cover of undeveloped woods in good condition, considering the distribution of hydrologic soil groups on the site. Woods in good condition was selected because it represents the best case (i.e., smallest amount of runoff) and, for most soil types, is basically a zero surface runoff requirement. ESD does not require detailed simulation modeling of developed and undeveloped conditions. Rather, a simplified method was developed for sizing practices to ease implementation on smaller sites, based on the relative change in Curve Number used in the National Resources Conservation Service TR-55 method (NRCS, 1986). The difference in responses to the 1-yr 24-hr event determines the excess runoff that needs to be treated (Q_E). In units of depth, $Q_E = P_E \times R_V$. R_V is the surface runoff fraction, defined as $R_V = 0.005 + 0.009 \times I$, where I is the impervious fraction expressed as a percentage. P_E is then the excess rainfall amount that needs to be treated. Rather than calculating P_E, simple lookup tables are provided (one for each of the four hydrologic soil groups, A, B, C, and D). P_E is listed in the table in increments of 0.2 inches and imperviousness in increments of 5% and incorporates a single assumption about the 1-yr 24-hr storm across all of Maryland. The estimates of P_E that these tables provide are not exact but are sufficient to achieve the desired level of control on average, especially when weighted across multiple subareas of a site with varying soil and development characteristics.

The approach of controlling site runoff to levels expected for woods in good condition is in theory climate neutral because both developed and woods runoff will change if climate changes. However, the table that is used to determine P_E is rooted in specific assumptions about the magnitude of the 1-yr 24-hr storm event that are likely to change under future climate conditions. Additionally, stream channels will respond to any change in hydrology, regardless of land cover (e.g., channels with forested watersheds may also undergo geomorphic changes in response to climate change). The underlying assumption is that by overmanaging the runoff from the 1 yr, 24-hr event, the bankfull discharge (typically between the 1-yr. and 2 yr. storm) is also managed.. The CPv calculations assume that, by maintaining bankfull and sub-bankfull discharges at levels that occur in a forested watershed, channel stability will be maintained. However, the theory that bankfull discharge can represent the geomorphic work produced by the full range of flows is founded on the assumption that the channel is stable. Given the history of impacts to streams in the eastern US (Walter and Merritts, 2008) and the time required for streams to respond to disturbances, many streams in the Chesapeake Bay watershed are still in a state of adjustment. Later research subsequent to the development of the CPv approach (e.g., Annable et al., 2011) suggests that discharge for urbanized streams that have not reached equilibrium with altered watershed conditions can exceed bankfull stage multiple times per year.

This research builds upon two previous CBT Restoration Research grants: Under Award 16928, Tetra Tech developed methods to precipitation Intensity-Duration-Frequency (IDF) curves for future climate projections and calculated future IDF relationships and predicted storm runoff for all Maryland stations in NOAA Atlas 14 (Bonnin et al., 2006). These results suggest greater changes for larger, low recurrence runoff events, suggesting that current guidance for road culverts may be inadequate to prevent flooding over their expected design life. However, impacts on stream stability and water quality SCMs may be less severe due to smaller anticipated changes in high recurrence events (Butcher, 2021; Butcher et al., 2021).

Under Award 15829, Virginia Tech is evaluating the impacts of traditional ESD on channel stability using data from Minebank Run and Tributary 109 to Seneca Creek. SWMM models of each watershed were developed and used to create continuous streamflow data for each watershed. A sediment transport model was developed and calibrated to simulate the geomorphic behavior of a 2000-ft. reach within the Tributary 109 watershed of Clarksburg, Maryland. This watershed has an intensive application of ESD. The sediment transport model was built using Hydrologic Engineering Center River Analysis System (HEC-RAS) 6.2 and calibrated using field cross-section data and observations during field visits. Analysis of HEC-RAS model results revealed that even with the extensive application of ESD design, the study reach is expected to degrade over time under current climate conditions. The effectiveness of ESD in protecting channel stability in the future, given the anticipated hydrologic changes due to climate change, were not addressed in this project.

Previous work based on IDF curves raised a variety of data and methodological issues in need of further exploration. First, the prior work used the localized constructed analogs (LOCA; Pierce et al., 2014) statistically downscaled set of Coupled Model Intercomparison Project Phase 5 (CMIP5) climate products, and results are conditional on LOCA's assumptions and biases. Second, evaluation of stream stability based on climate-modified IDF curves and design storms may not be sufficient to evaluate stream responses to continuous future weather time series.

To evaluate these issues, the current was organized around three research hypotheses:

H1. Problems in the LOCA methodology introduce biases in the estimation of future 1-year, 24-hour rainfall events used to calculate ESD. If the null hypothesis of no significant differences is not supported, analysis based on LOCA alone is not sufficient to address H2.

H2. Despite changes in precipitation by mid-century, current ESD requirements will be sufficient to mitigate effects associated with anthropogenic development. Note that this focuses on anthropogenic stresses, which are the result of the difference between post-development and good condition forest. There will still be climate effects because the forest baseline will also move.

H3. ESD concepts and requirements are applicable and appropriate to management of real watersheds under future climate. Most conclusions to date are based on simplified analyses using design storms and estimates of runoff from unit-area runoff models. To what extent do those conclusions remain applicable under continuous simulation with complex real watersheds? How will channel stability respond to forecast changes in hydrology? Three sub-hypotheses are:

- **H3a**. The historical flow duration curve for Tributary 109 will not change under future climate. Analysis of flow duration curves will facilitate the identification of the magnitude and frequency of storms that diverge most from historical time series.
- **H3b**. Watersheds developed under current stormwater management regulations and climate will not experience increased channel erosion, comparing the historical CMIP5 dataset with various GCMs and scenario combinations. This is a key question in assessing if the current ESD design criteria are protective of the stream when climate change is considered.
- **H3c**. Retrofitting existing stormwater management using the future 1-yr, 24-hour design storm will protect channel stability when comparing the historical CMIP5 dataset with various GCMs and scenario combinations. Assuming that the 1-year, 24-hour design storm changes with CC, is the revised 1-year, 24-hour design storm protective, given a redesign of all SCMs on site with the revised design storm?

(This page left intentionally blank.)

2.0 FUTURE CLIMATE ANALYSES

2.1 INTRODUCTION: DOWNSCALING METHODS

Conclusions from Award 16928 are conditional on the LOCA statistically downscaled interpretation of climate model output produced for the 5th round Coupled Model Intercomparison Project (CMIP5) of the Intergovernmental Panel on Climate Change, which uses a constructed analogs approach to convert output from 32 GCMs to a daily time step and a spatial resolution of 1/6 degree latitude and longitude (approximately 6.9 x 5.4 km at the latitude of Baltimore, MD).

Wang et al. (2020) presented evidence suggesting a potential problem in the LOCA analysis for extreme precipitation events when compared to the Multivariate Adaptive Constructed Analogs (MACA-Ave2) downscaling (Abatzoglou and Brown, 2012). For 1-day annual maxima, the "magnitude of both absolute and relative changes are much smaller in LOCA than in MACA." The difference in extreme precipitation estimates is due to the training data. LOCA uses the Livneh et al. (2015) reanalysis data set, which has an inherent problem due to the use of a linear split of each recorded 24-hr precipitation amount into two days, rather than using non-overlapping 24-hr records, which results in an apparent under-estimation of 24-hr extreme precipitation. The MACA Ave2 training dataset does not have this problem. There are also questions as to whether use of any constructed analog approach introduces biases by assuming that general weather temporal sequences in the future can be inferred from past history. The potential problems with the LOCA product suggested the need to compare ESD results from other statistical downscaling (e.g., MACA) as well as dynamical downscaling methods to help resolve if and to what extent conclusions based on LOCA may be biased.

Simulation models for climate change are essentially global in nature because they must incorporate the interactions between atmosphere, oceans, and the land surface worldwide. Although computer power and data storage capacity continue to increase, the need to simulate such a large domain restricts the spatial and temporal resolution that is feasible to be obtained in a global simulation that covers multiple decades. On the other hand, many of the effects of climate change to which adaptation may be needed are inherently regional or local in scale, ranging from questions about future water balance and water supply (typically basin scale, temporal resolution of months to years) to impacts on stormwater infrastructure in response to intense precipitation events (typically at the neighborhood or block scale with a desired temporal resolution of minutes to hours). In addition, global climate models (GCMs) are generally trained to reproduce large-scale spatial responses that may not accurately reflect conditions at a specific location either because the global-scale models do not consider important local modifiers of weather such as orographic effects or because crucial phenomena, such as convective storms, occur at temporal and spatial scales not resolved by the global models.

To convert output from a GCM to a form useful for local impact and adaptation studies requires three things: (1) bias correction to ensure correct representation for the area of interest, (2) spatial downscaling from the GCM grid scale to a more local scale, and (3) temporal disaggregation from the GCM output time step to the time step of interest. For evaluating responses of stormwater that depend on extreme precipitation events further adjustments are needed to augment the skill of GCMs in simulating such events. This can take the form of further temporal and spatial downscaling to match the timing and spatial extent of severe convective storms; however, the most common approach is to use climate products (usually ones that are already downscaled to a local level) to make inferences about changes in the probability distribution of extreme precipitation, often summarized through a rainfall intensity-duration-frequency (IDF) curve for a specific location. Development of a climate-modified IDF curve may thus be thought of as another type of downscaling and bias correction to the local stormshed scale.

The most commonly used methods of GCM downscaling are statistical downscaling and dynamical downscaling.

Statistical downscaling is based on relationships that interpolate large-scale GCM output to observations of historical weather and climate (Wood et al., 2004). Advances in statistical downscaling, such as the LOCA (Pierce et al., 2014) and MACA (Abatzoglou and Brown, 2012) CMIP5 products, use a constructed analogs approach, in which a library of historical observation series is used to scale from monthly to daily time step, ensuring a reasonable representation of the temporal structure of local rainfall. The downscaling process incorporates a bias correction step and ensures that local, daily time series projections exhibit patterns similar to historical observed data. This achieves a spatial resolution of 1/6 degree (approximately 6.9 x 5.4 km at the latitude of Baltimore). The LOCA downscaling approach was developed to address some shortcomings of the older bias-correction constructed analog approaches to avoid damping of local precipitation extremes; however, a criticism of constructed analog statistical downscaling is that future results may be overly dependent on the temporal characteristics of the training data. The statistical downscaling process is automated, so results are available for the majority of GCMs, and greenhouse gas scenarios produced in CMIP5.

Dynamical downscaling uses GCM output as boundary conditions to drive a smaller-scale regional climate model (RCM), or even smaller scale local area model (LAM) that presumably has better predictive capabilities for local rainfall events. Future climate time series are then obtained directly from the RCM or LAM output. Dynamical downscaling is computationally expensive but has become more available due to the CORDEX (Coordinated Regional Climate Downscaling Experiment; http://www.cordex.org/) effort. Examples include Li et al. (2017), Vu et al. (2018), Kristvik et al. (2019), and Cannon and Innocenti (2019). The advantages of this approach depend on the level of accuracy that is achieved by the smaller-scale model. One problem with direct use of RCMs is that they generally still do not explicitly model small-scale cloud processes that cause intense convective storms, for which LAMs with horizontal scales finer than about 3 km may be needed (Arnbjerg-Nielsen et al., 2013). Because of the computational expense only a limited number of potential GCM-RCM combinations are available in the North American component of the international Coordinated Regional Downscaling Experiment (NA-CORDEX) data repository (Mearns et al., 2017), which do not provide full replication of the MACA and LOCA data sets.

2.2 METHODS AND DATA FOR IDF ANALYSIS

In the current work we use both LOCA and MACA statistically downscaled climate archives from CMIP5. The statistical downscaling methods obtain a spatial resolution of around 6 km in Maryland. They also incorporate bias-correction adjustments to gridded training data for the historical period that represent a partial further downscaling to an individual station basis. The currently available products also provide output at a daily time step, so further temporal downscaling is needed.

Our studies use a conditional IDF approach to complete temporal and spatial downscaling. In this approach (Butcher et al., 2021), the IDF curves published in NOAA Atlas 14 (Bonnin et al., 2006, for Maryland) for individual weather stations are updated to reflect the relative change predicted in downscaled climate products such as LOCA. Local model biases are addressed through equidistant quantile mapping, in which the modeled change in the cumulative distribution of storm events from historical to future conditions is used to adjust the extreme value fit used for IDF curve development. The Atlas 14 IDF curves are based on site data (with some regional smoothing of higher moments); thus, this process implicitly scales from the downscaled climate product (e.g., 6 km scale) to the hyper-local scale of an individual rain gauge. Temporal disaggregation is also incorporated because the NOAA IDF estimation process incorporates extreme value fits from the sub-hourly to the multi-day scale.

We analyzed downscaled precipitation products in several ways: through direct analysis of downscaled output, through the development of IDF relationships, and through rainfall-runoff simulations developed through the application of additional local bias correction.

Stormwater infrastructure includes a mix of conveyances, storage facilities, and treatment practices that are designed to meet diverse public safety and environmental goals. Achieving these goals in new urban construction or redevelopment is typically codified in design standards that in turn are based on a consideration of the range of anticipated storm events. Design standards represent a tradeoff between the risks of inadequate sizing and costs of over-design. Design storms of a given frequency and probability (e.g., the 24-hour storm event anticipated to recur, on average, once in 10 years) are used to translate a given level of risk and cost into stormwater design standards.

Design storms are most often derived from an analysis of historic climate observations at a given location (e.g., IDF curves) to incorporate the numerous factors that influence local weather. This approach assumes that climate is stationary in the sense that the past provides a useful guide to the future. As many researchers have noted, climate change suggests the stationarity assumption may be inappropriate to inform infrastructure design at many locations (e.g., Milly et al., 2008; Jakob, 2013).

In many jurisdictions in the U.S., including Maryland, the selection of design storms is based on precipitation IDF curves published in NOAA Atlas 14 (Bonnin et al., 2006, 2007) for analysis of larger events with recurrence interval greater than one year coupled with local analysis of more frequent storms (e.g., 90^{th} percentile rainfall event) for water quality practice design. (Atlas 14 does not provide estimates for events with recurrence interval less than one year but these events and their relative change under future climate can be estimated with a peaks-over-threshold approach analogous to the estimate of future IDF curves but using a generalized Pareto distribution as described in Butcher et al. (2021)).

Atlas 14 IDF curves are developed from extreme value distribution statistical modeling of observed precipitation maxima series and thus provide design information based solely on past data. The Clausius-Clapeyron relationship implies that there is an increase in the potential water-holding capacity of the atmosphere by about 7% for every 1 °C rise in temperature (Trenberth et al., 2003), so increasing intensity of the most extreme storms is expected even where total annual precipitation volume may decrease (Janssen et al., 2016; Hayhoe et al., 2018; Ragno et al., 2018; Papalexiou et al., 2019); however, the effects on more frequent precipitation events are less clear. Under future climate, design standards based on historic observations may thus fail to meet desired levels of performance and risk management.

An alternative to statistical downscaling is dynamical downscaling with RCMS. RCMs can directly provide output at subdaily scales; however, one of the challenges in dynamical downscaling with RCMs is that the resulting spatial scale is still somewhat large. We examined this effect through the RCM-derived results from CMIP5 reported for the NA-CORDEX experiments (Mearns et al., 2017). The CORDEX analyses were undertaken at two different spatial scales, with grid resolution of 0.22 and 0.44° (approximately 19 and 38 km at the latitude of MD). The difference in these results provides an indication of the effects of changing spatial scale.

Overall, there are 66 pairs of CORDEX simulations at 0.22 and 0.44° resolution. We compared IDF results for the predicted 2-, 10-, and 100-yr 24-hr events, combining the mid-century (ca. 2055) and late century (ca. 2085) analyses as an indicator of the changes in the overall distribution of storm events. On average the CORDEX 0.22° event depths are larger than CORDEX 0.44 results for all three recurrences, although the differences are small (Figure 2-1).

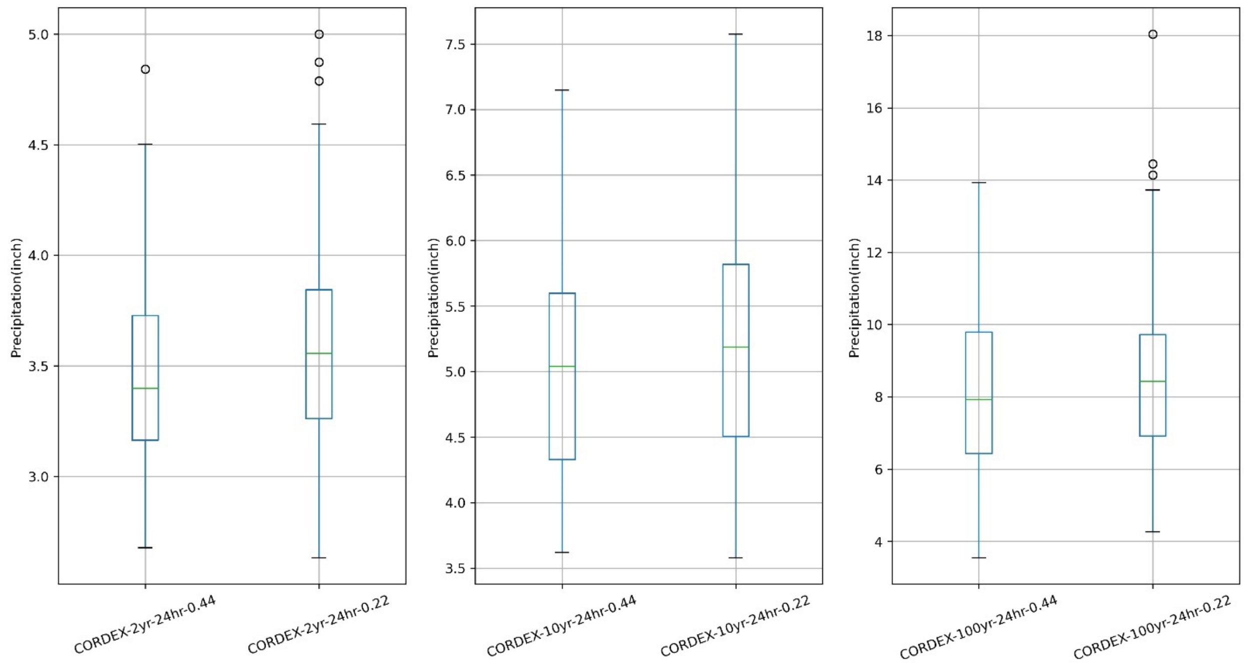

Figure 2-1. Boxplots Comparing CORDEX 0.22° and 0.44° Results for 24-hr Events with 2-, 10-, and 100-yr Recurrence

There is on average an increase in precipitation intensity when going to the smaller (0.22°) scale. Paired sample t tests show that the difference is statistically significant at the 5% level for the 2-year and 10-year events (Table 2-1). The largest percent difference is for the 100-year event, but this is not statistically significant. This primarily reflects the high uncertainty and resulting variance associated with estimating the 100-year recurrence event from short (30-year) time series.

Table 2-1. T Test Results for CORDEX 0.44° versus 0.22° Events

Recurrence (24-hr event)	Average Difference	T statistic	p-value (2-tail)
2-yr	-5.08%	-3.737	0.0004
10-yr	-4.37%	-2.180	0.0329
100-yr	-9.08%	-0.908	0.3670

The CORDEX analyses suggest that there is a scale-induced bias toward under-estimation of extreme precipitation events that likely persists below the 0.22° scale such that greater intensity would likely be predicted at smaller scales more closely approximating the size of convective storm cells. Note that this effect persists despite the IDF estimation procedure adjustment to local rain gauge data that likely helps compensate for spatial bias but not non-linear scale-dependent biases on the relationship between intensities at different recurrence probabilities.

2.3 IDF ANALYSIS RESULTS

We analyzed downscaled precipitation products in several ways: through direct analysis of downscaled output, through the development of IDF relationships, and through rainfall-runoff simulations developed through the application of additional local bias correction.

In previous work for CBT under grant #16928 (Butcher et al., 2020) we developed IDF curves by applying the methods described in Butcher et al. (2021) to the LOCA CMIP5 statistically downscaled climate results for all stations in Maryland. To evaluate differences between the LOCA and MACA products we applied the same methods to calculate IDF curves from the MACA dataset.

The comparison between LOCA and MACA is focused on the 24-hr predictions for storm events of 2 to 100-year recurrence frequency as the sub-daily results have fewer supporting data and are subject to greater uncertainty. The prior analyses using LOCA (Butcher et al., 2020) presented results for four climate scenarios (characterized as approximating the 10th percentile overall, 90th percentile overall, and the two median estimates from the ensemble of RCP 4.5 and RCP 8.5 climate scenarios under CMIP5) and examined the 2-year, 10-year, 100-year event predictions. Of the 632 station/model/time horizon combinations included in Phase 1 for Maryland stations, 302 are also available in MACA. (MACA includes a smaller set of GCMs as it is restricted to those GCMs that reported meteorological variables beyond precipitation and temperature).

Table 2-2. Comparison of Difference in IDF Curves Derived from LOCA and MACA

Time Horizon	2-year			10-year			100-year		
	average	median	RMSE (in.)	average	median	RMSE (in.)	average	median	RMSE (in.)
2055	5.49%	5.24%	0.36	9.27%	8.31%	0.95	13.18%	13.93%	3.72
2085	3.92%	4.69%	0.33	6.55%	7.09%	0.75	8.66%	13.48%	2.81

Results are based on MACA-derived IDF curves minus LOCA IDF curves for all station/GCM combinations available in both data sets. Differences are evaluated as MACA minus LOCA. RMSE = root mean squared error.

On average, the MACA results for a given recurrence interval are higher than those obtained from LOCA, consistent with the analysis provided by Wang et al. (2020). Further, the difference appears to increase for longer recurrence intervals; however, the differences are not consistent for individual station/GCM combinations. Differences are similar for the 2055 and 2085 time horizons.

MACA and LOCA predictions for individual station/GCM combinations for the 2-year, 10-year, and 100-year events are shown in Figure 2-2 through Figure 2-4. These reveal a large spread in predictions from the two methods that increases with recurrence interval. The two methods are in fair agreement for the 2-year event but deviate to a large degree for the 100-year event, with the MACA product producing some extreme predictions not seen in LOCA that reduce the R^2 for a regression between the two methods to less than zero.

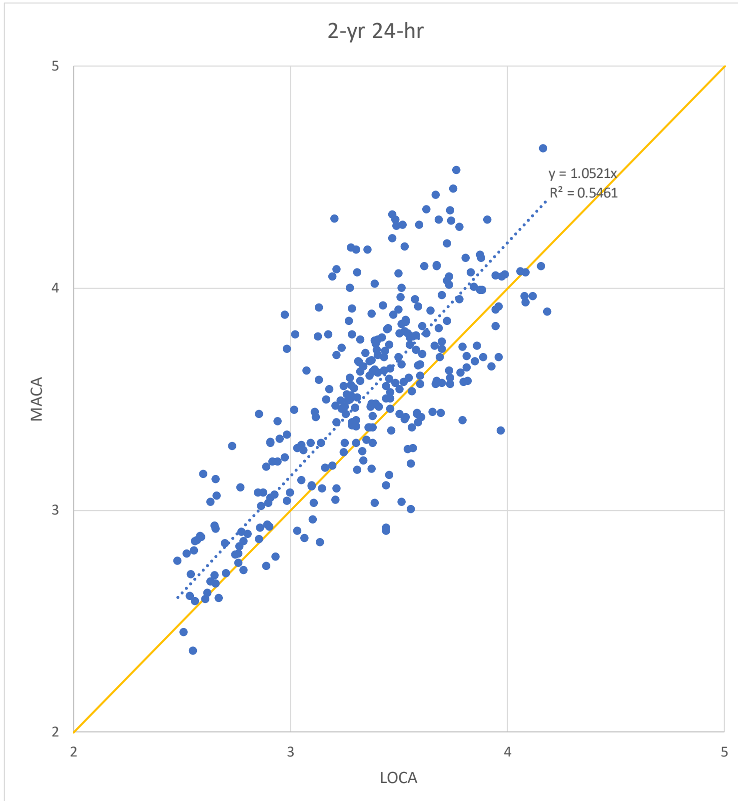

Figure 2-2. Comparison of MACA and LOCA Predictions for Future 2-year Event (ca. 2055 and 2085)

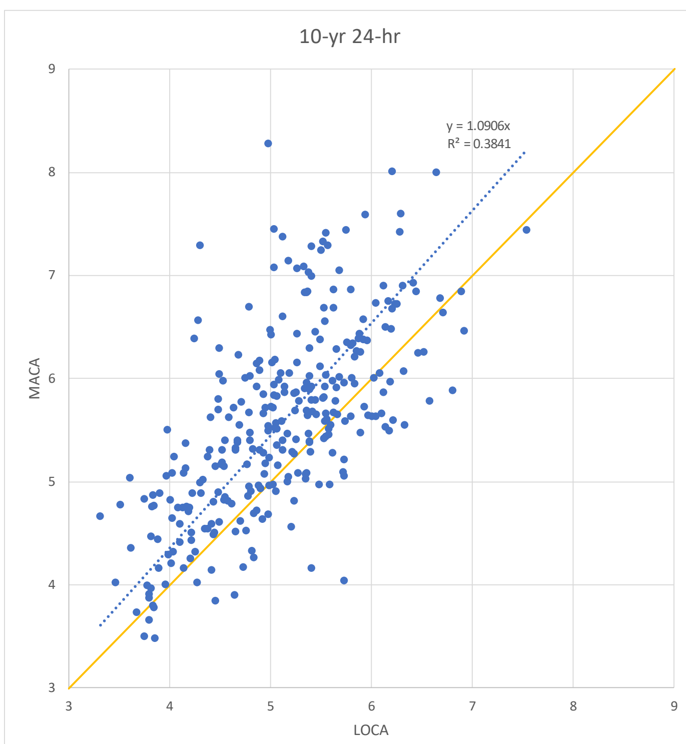

Figure 2-3. Comparison of MACA and LOCA Predictions for Future 10-year Event (ca. 2055 and 2085)

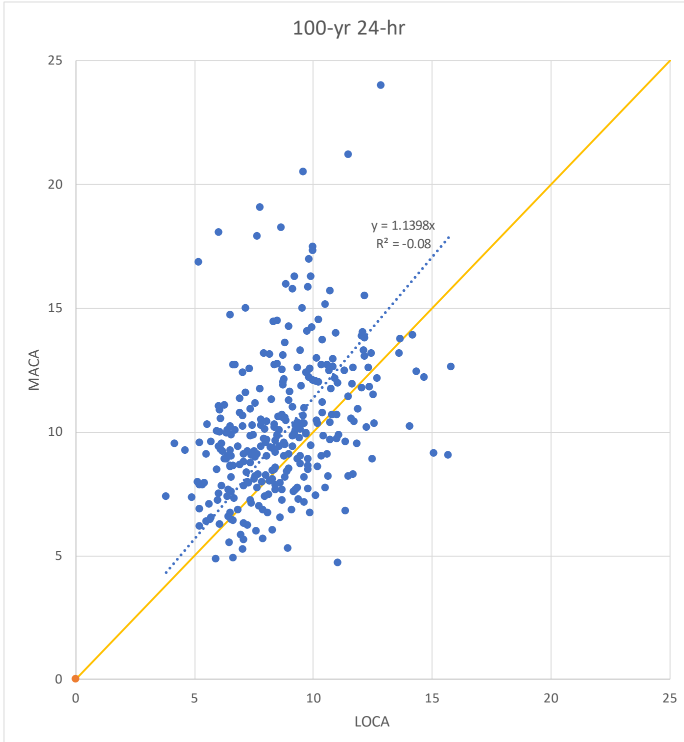

Figure 2-4. Comparison of MACA and LOCA Predictions for Future 100-year Event (ca. 2055 and 2085)

MACA and LOCA are both constructed analog approaches that downscale coarse GCM projections of future climate to finer-scale projections at a daily time scale by comparison to “analog” periods of past recorded weather but use different training data and apply the training data at a different scale. In addition, MACA searches for analogs based on multiple weather variables including humidity and cloud cover in addition to precipitation and temperature, whereas LOCA analogs are based on precipitation and temperature only.

Statistical tests of the significance of relative bias between LOCA and MACA was evaluated with a null hypothesis of no significant difference using a nested or hierarchical analysis of variance (ANOVA) and also a non-parametric method, the Wilcoxon Signed-Rank test, for 24-hour rainfall event with different return periods of 1, 2, 5, 10, 25, 50, 100, 200, 500, and 1000 years. The results of both tests rejected the null hypothesis at the 5 percent level and demonstrated that downscaling method is a significant contributor to the total variance of estimated 24-hour rainfall events. Therefore, the results of LOCA and MACA downscaled precipitations are different from each other in a statistical sense.

For the hierarchical ANOVA, the relative contribution of downscaling method (LOCA or MACA) to the future estimation of 24- hour rainfall events using the IDF approach was analyzed using the method of Box and Tiao (1992). The analysis evaluated three levels of variance components (downscaling method, GCM, and sample site), and was conducted for the 79 Maryland climate stations included in NOAA Atlas 14. There are 18 GCMs in common between LOCA and MACA, all of which are available for both the RCP 4.5 and RCP 8.5 emission scenarios. IDF results were generated for 2055 and 2085, resulting in a total of 72 GCM-RCP-time horizon pairs (“GCM scenarios”). The ANOVA matrix was constructed using two main groups (downscaling methods), 72 subgroups (GCM scenarios), and 79 elements (station samples) and the matrix was evaluated based on the future estimates of 24-hour rainfall event. Further details are provided in Butcher (2022).

Contributions to the total variance attributed to the three levels of the ANOVA analysis are presented in Table 2-3. For all recurrence intervals, the relative contribution of downscaling method to the total variance is greater than 5 percent; however, the largest source of variance is site variability, reflecting the uncertainty in estimating the generalized extreme value distribution, followed by the GCM. Among all 24-hour rainfall events, the downscaling method contributes the largest fraction of variance to the 10-year event, while the smallest relative contribution is for the 1000-year event, reflecting the higher level of uncertainty in predicting extreme events.

Table 2-3. Total and Relative Variance of Estimated 24-hour Rainfall (inches) Contributed by Site Variability, GCM Selection and Downscaling Method

Recurrence	Due to site variability	Due to GCM	Due to downscaling	Total	Percent from downscaling
1-yr	0.07	0.02	0.01	0.10	7.03%
2-yr	0.13	0.04	0.02	0.17	10.08%
5-yr	0.28	0.08	0.05	0.39	12.62%
10-yr	0.52	0.15	0.10	0.73	13.47%
25-yr	1.26	0.39	0.22	1.76	12.79%
50-yr	2.54	0.80	0.40	3.54	11.43%
100-yr	5.19	1.61	0.71	7.14	9.90%
200-yr	10.55	3.17	1.21	14.31	8.47%
500-yr	26.64	7.61	2.43	35.41	6.86%
1000-yr	53.06	14.44	4.08	69.44	5.87%

The Wilcoxon Signed-Rank (WSR) is a commonly applied non-parametric test to determine if two independent samples with non-normal or skewed distribution are significantly different from each other (Corder and Foreman, 2009). The test is similar to the t-test applied for the comparison of samples with normal error distributions but does not impose the normality constraint. The null hypothesis (H_0) for the WSR test is that the two samples are drawn from the same distribution. Rejecting the null hypothesis indicates that the distributions from which the two samples are drawn are significantly different from one another. For the WSR analysis, the paired samples were averaged values of LOCA and MACA 24-hour rainfall across 79 Maryland climate stations for 72 GCMs. The WSR analysis was performed for all recurrence times individually using the Wilcoxon function in the Python SciPy v.1.8.0 package (SciPy documentation — SciPy v1.8.0.dev0+2099.3f05efb Manual).

WSR results in Table 2-4 indicate LOCA and MACA estimated precipitation depths are significantly different. Wilcoxon's statistic represents a mean signed-rank for two observations and the greater value of the parameter shows larger differences. The non-parametric WSR is thus in agreement with the

ANOVA result that indicates that choice of downscaling method contributes significantly to the estimated depth of extreme rainfall events.

Table 2-4. Wilcoxon Signed-Rank Statistic and Probability Value

Recurrence	Wilcoxon Statistic	Probability Value
1-yr	176	1.7×10^{-10}
2-yr	118	1.9×10^{-11}
5-yr	99	9.2×10^{-12}
10-yr	114	1.6×10^{-11}
25-yr	202	4.37×10^{-10}
50-yr	278	6.11×10^{-9}
100-yr	354	7.15×10^{-8}
200-yr	414	4.4×10^{-7}
500-yr	477	2.64×10^{-6}
1000-yr	532	1.14×10^{-5}

2.4 METHODS AND DATA FOR CONTINUOUS SIMULATION

A comprehensive analysis of the implications of future changes in the cumulative distribution function of rainfall events on SCM performance requires the use of continuous simulation, not just analysis of the response to events of a specified recurrence frequency.

An example of such a study is Job et al. (2020), which used continuous model simulations to evaluate site conditions and SCM performance under future climate conditions in five U.S. locations, including Harford County, MD. The analysis provides insights into the potential impacts of changes in the characteristics of precipitation time series (rather than just extreme events) on stormwater infrastructure performance and allows comparison of how the responses may differ between conventional stormwater detention and GI practices.

When is continuous simulation for stormwater warranted? For the most extreme and rare events, the impact at the local scale in urban settings with significant imperviousness is largely determined by the intensity of the individual storm as initial conditions are overwhelmed by the magnitude of the event. (This of course does not hold for fluvial flooding where initial volumes at the start of a storm are of high importance.) Analyses of local or pluvial responses to the most extreme events can thus be adequately assessed using event-based extreme value analysis, such as IDF curves. Smaller, more frequent storm events are more strongly influenced by antecedent conditions. Events with recurrence intervals less than 2 years generally account for much of the physical work done on the channel and are thus of high importance for channel morphology and for water quality control. Use of continuous rainfall-runoff simulation is likely most valuable for this class of events.

In this project we developed continuous meteorological time series (air temperature and precipitation) for future climate conditions that can be used in rainfall-runoff models such as the Storm Water Management

Model (SWMM) and Hydrologic Engineering Center – River Analysis System (HEC-RAS). The required air temperature series for these models are daily maximum and minimum temperature, while the precipitation series are needed at sub-hourly intervals.

For these applications, the daily output provided by LOCA and MACA is temporally downscaled to a 5-minute time step. We also undertook additional spatial bias correction to improve the match to the point gage used to drive the model calibration described in Section 3.0 by applying empirical quantile mapping (eQM). The eQM approach (Amengual et al., 2012) does not assume a specific parametric statistical distribution and is applicable to bias adjustment of any time series. Given model output for the historical time series (*H*), an unadjusted time series for a future prediction period (*F*), and a time series of local observations for the historical period (*O*), the approach locates the quantile of the prediction *F* within the cumulative distribution function of the training data, *H*, then transfers this position to the same quantile within the cumulative distribution function of the local observations, *O*, thus creating a prediction (*P*) that is bias-corrected to the local observations. The general method developed by Amengual et al. expresses the quantile adjustment or shift as $P_i = O_i + g\,\bar{\Delta} + f\,\Delta_i$, where $\bar{\Delta}$ is the mean regime shift and Δ_i, is the difference between the future and historical *i*th quantile. The parameters *g* and *f* allow for adjustments that weight the influence between the overall regime shift and the shift in individual quantiles. We adjusted the quantiles with recurrence greater than or equal to 1 year based on the IDF results while adjusting lower quantiles directly based on historical vs. future constructed analog output. Python code for this method is available at svn.oss.deltares.nl/repos/openearthtools/trunk/python/applications/hydrotools/hydrotools/statistics/bias_correction.py.

MACA and LOCA provide data at daily time steps and the eQM bias correction method was applied to the daily time step. To convert 24-hour totals to realistic sub-hourly precipitation we use random multiplicative cascades (RMC; Menabde et al., 1997; Molnar and Burlando, 2005; Kumar et al., 2009). The RMC method distributes mass of the initial time interval successively over regular subdivisions as a fractal process (usually subdivided by factors or two). The initial time scale rainfall depth is multiplied by a cascade generator at each subdivision (multiplied by more cascade generators as further subdivisions occur). The distribution of the scaling generator(s) determines the scaling properties of the rainfall. Therefore, the main goal in the random cascade is to establish the distribution of the cascade generator. As explained in Kumar et al. (2009), this method first aggregates the provided time series by a factor of two, up to five times, to generate the moments, varying from zero to five. For this case, the provided daily rainfall time series is aggregated in series to a two, four, eight, sixteen, and thirty-two-day timestep. Sample moments are defined as:

$$M_n(q) = \sum_{i=1}^{b^n} \mu_n^q(\Delta_n^i)$$

Here q is the moment order, the i^{th} interval after *n* levels of subdivision is shown as Δ_n^i (*i*=1, ..,b^n intervals at level *n*). In this case, the branching number *b* = 2 and there are 32 constituent intervals at level *n* = 5. μ_n is the rainfall mass in "subcube" Δ_n^i (the i^{th} interval in the n^{th} subdivision) is defined as:

$$\mu_n(\Delta_n^i) = R_0 \lambda_n \prod_{i=1}^{n} W_j(i)$$

where R_0 is the initial rainfall depth at level *n*=0.

The slope of the ensemble moments scaling relationship (X_b) is called the Mandelbrot-Kahane-Peyriere (MKP) function (Mandelbrot, 1974; Kahane and Peyriere, 1976), calculated as:

$$X_b(q) = 1 - q + \log_b \mathrm{E}(W^q)$$

The MKP contains information about the cascade generator (*W*) and, therefore, contains information about the scaling properties of the rainfall.

The slope of the sample moment scaling relationship ($\tau(q)$) is defined as:

$$\tau(q) = \lim_{\lambda_n \to 0} \frac{\log M_n(q)}{-\log \lambda_n}$$

Here λ_n is the dimensionless spatial scale defined as $\lambda_n = b^{-n}$.

$\tau(q)$ is used to approximate $X_b(q)$, and thus the distribution of a cascade generator can be determined by fitting $\tau(q)$ as a function of sample moments, and then using the probability density function of that distribution. The cascade generator is then able to estimate a realistic hourly timestep rainfall series from a daily timestep rainfall that is consistent with the rainfall pattern across daily to monthly scales.

The disaggregation method calculates the weights that define each successive split of precipitation depth into constituent time units using a log Poisson distribution (as recommended by Kumar et al. (2009)) that reflects the fractal properties of observed precipitation from periods of length one, two, four, eight, sixteen, and thirty-two days. The log Poisson scaling function is constrained to be greater than zero, thus every split in the cascade assigns some non-zero portion of the volume to each successor time interval. The result would be that on a day with precipitation at least some non-zero amount of precipitation will be assigned to every hour. Obviously, this is not a desirable outcome. This issue is addressed as in Molnar and Burlando (2009) by adding an intermittency factor that determines whether the cascade splitting weight is equal to zero.

The weighting factors in the RMC code (W) are constructed as composite variables W = BY, where B is a (0,1) intermittency or dry-period factor within a day with rain and Y is a strictly positive random variable – such as the log Poisson model. The probability that B = 0 is defined as 1 – $b^{-\beta}$, where b is the splitting order (2 in the common case) and β is a parameter. Molnar and Burlando show that it is sufficient to construct a canonical, mass-preserving model in which β is a constant defined as 1 – τ(0), where τ(0) is the slope of the sample moment of the Mandelbrot-Kahane-Peyriere equation at moment order zero.

Given τ(0), the probability of a dry period can be calculated. Consider an example where τ(0) = 0.6376 and p(dry) ≈ 0.222. Splitting can be accomplished through the use of a (0,1) discrete random Bernoulli variable with probability equal to *p*(dry). A splitting cascade must also address the possibility that the parent cell contains a positive volume of rainfall, but the random Bernoulli variables for both daughter cells are “dry”. In that case, it is appropriate to assign all the precipitation volume in the parent cell to one of the daughter cells based on a random (0,1) choice. To retain the correct probability of p(dry) for individual daughter cells after this adjustment it is necessary to adjust the initial p(dry) to p(dry)*(1 + p(dry)) given that p(dry)*p(dry) instances will be shifted to a state where one of the daughter cells is not dry.

RMC proceeds by successive splits of a data step by 2. The final step length (in minutes) in downscaling from 1 day is thus constrained to be a function of whole powers of 2, or 1440/2^n minutes. A challenge this creates is that progressive division of 1,440 minutes by powers of 2 does not resolve to an integer value below 45 and thus cannot directly produce a 5-minute time step. (The method can be developed with a basis different from 2, but this tends to degrade the information extracted from the daily to monthly-scale results). A close approximation is achievable by setting n = 11, resulting in a timestep of 0.70315 minutes, then aggregating seven consecutive intervals to obtain a step length of 4.922 minutes. If a step of exactly 5 minutes is required, this can be done by re-interpolating the cumulative distribution of the 4.922-minute steps to exact 5-minute intervals.

2.5 CONTINUOUS SIMULATION RESULTS

Butcher (2021) evaluated performance of ESD under future climate conditions throughout Maryland by examining the changes in precipitation and the resulting difference in runoff between developed and good condition woods for the future 1-yr 24-hr event, as predicted by TR-55 (NRCS, 1986). These results suggested that by end of century there is a risk of an increasing magnitude of the 1-yr 24-hr event and associated runoff as a result of which the storm volume for which the capture volume required to achieve the same design performance for stormwater management components such as bioretention cells might need to increase. The changes, however, were predicted to be small in magnitude, suggesting that the water quality functions of ESD are likely to remain intact. This occurs despite a majority of climate scenarios predicting a substantial increase in total precipitation volume because most of those increases are projected to occur in larger, less frequent rainfall events with a recurrence interval greater than one year.

These same analyses can be used to examine continuous dynamic simulation of runoff and SCM performance to evaluate how responses will change across the full range of future weather, account for the effects of antecedent events, and evaluate potential effects of changes in seasonal storm patterns. This was done by routing continuous weather series through unit-area SWMM simulations across all Atlas 14 stations in MD.

The statewide SWMM simulations combine a unit-area (1 acre) watershed area with a bioretention SCM designed consistent with MDE (2009) recommendations. The generic specification for bioretention includes a 9-inch surface ponding depth, 24 inches of growing media, and 12 inches of stone drainage layer. The system is assumed to have an underdrain (4-inch pipe in the middle of drainage layer that controls outflow. The growing media consists of 25% compost and 75% sandy soil with a porosity of 0.529. The drainage layer has a void ratio of 0.54 and a drainage coefficient of 0.18 for a drain height of 41 inches and drain time of 72 hours. Storage volume includes the ponding depth and the storage in the media (taking porosity into account). The depth of storage is thus 0.75 ft ponding + 2 ft media x 0.529 porosity = 1.808 ft. The analysis assumes sandy clay loam Hydrologic Soil Group C soils, typical of many areas in Maryland, and climate conditions for 2070-2100, i.e., centered at 2085.

MDE uses pre-calculated estimates of WQv for current conditions and specifies two "rainfall zones" – a western zone and eastern zone that use a 0.9 in storm and 1.0 in storm, respectively, for the WQv calculation. A key metric for the ESD evaluation is a comparison of the amount and frequency of surface runoff flow that bypasses the SCM relative to the design capture depth specification, Q_E. The target Q_E is the runoff to be treated from the 1-year 24-storm relative to woods in good condition. Although the design storm varies geographically, when using the simplified procedures in MDE (2009) with imperviousness set to 50% on hydrologic soil group C, Q_E for bioretention design under current conditions always comes out as 0.9 inches regardless of the rainfall zone. Specifically, the tabled estimates of the design storm, P_E, is 1.8" when using Table 5.3 in MDE (2009) regardless of the zone. Under those assumptions $R_V = 0.05 + 0.009 \times I = 0.05 + 0.009 \times 50 = 0.5$, and $Q_E = P_E \times R_V = 0.9$".

The MDE design guidance establishes the minimum required area of the bioretention SCM per acre (43,560 ft^2) of the area treated using the Simple method as Area (ft^2) = P_E (in) x 43,560 (ft^2/ac) x (0.05 +

0.009 x I)/12/SD, where SD is the surface storage depth, defined in the design setup as 1.808 ft. For P_E of 1.8”, this works out to a bioretention cell area of 1,807 ft^2. Note that the Simple method calculation is inherently conservative. Direct calculation based on setting P_E equal to a 90th percentile 24-hr rainfall event depth of 1 inch and applying the curve number method leads to a smaller design footprint of 1,003 ft^2.

The full analysis includes each available CMIP5 climate scenario using RCP 4.5 and 8.5 in the LOCA and MACA datasets for a total of 4,687 station-GCM combinations. Detailed results are shown first for a single GCM scenario (LOCA downscaling of MIROC5, RCP 8.5 for station 18-1032 [Boyds 2 NW]). This is also the station in Montgomery Co., MD that is used in the detailed SWMM simulations of Tributary 109 described in Section 3.0. The predicted future daily runoff series (flow entering the SCM in inches over the watershed) is shown in Figure 2-5.

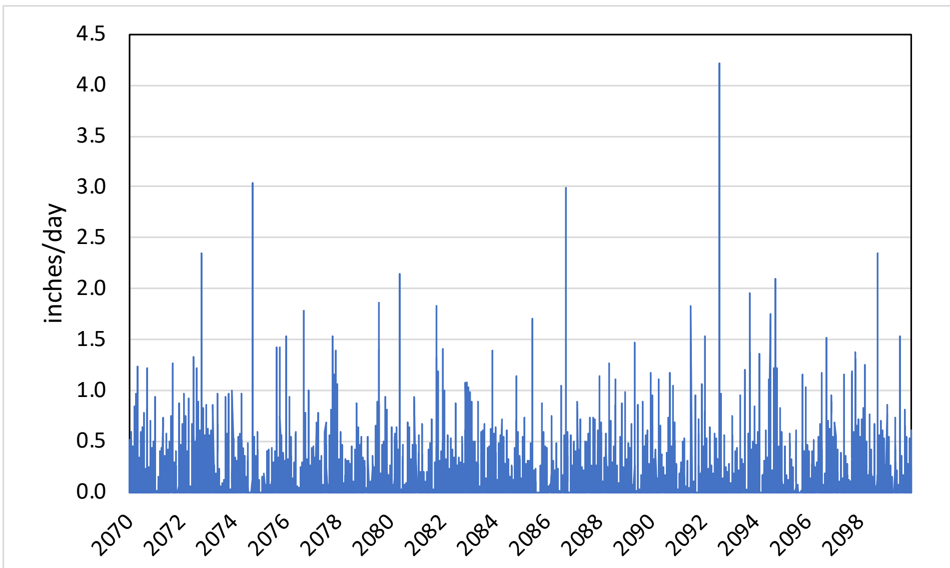

Figure 2-5. Daily Runoff Series, Station 18-1032, C soils, 50% Impervious, LOCA Scenario MIROC5 RCP8.5, 2070-2100

Flow entering the bioretention cell can exit in 4 ways:

- Evapotranspiration to the atmosphere,
- Discharge downstream through the controlled underdrain,
- Exfiltration to groundwater through the base of the cell, or
- Surface runoff that exceeds the storage capacity of the cell and thus bypasses treatment.

Figure 2-6 summarizes the disposition of the volume influent to the cell. The untreated bypass flow accounts for about 7 percent of the influent volume.

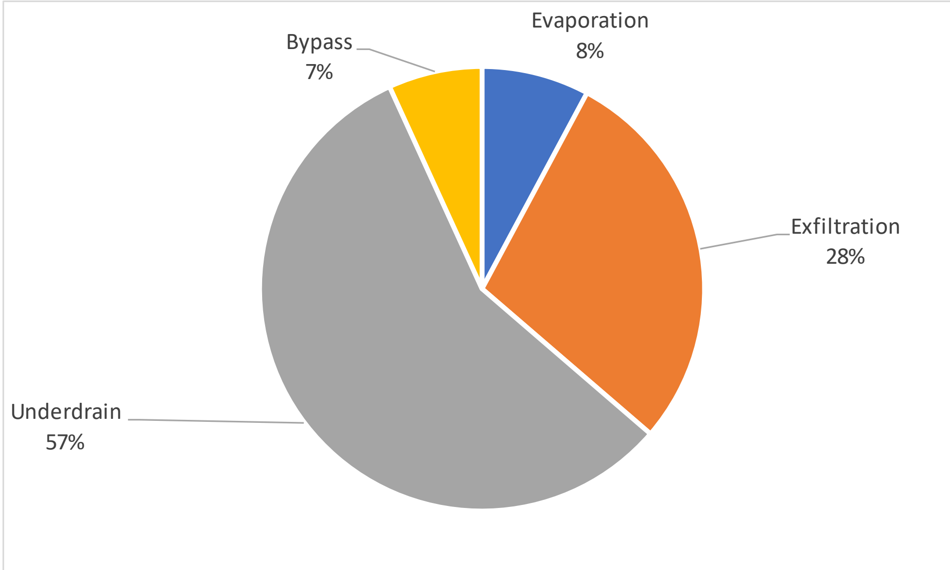

Figure 2-6. Bioretention Cell Disposition of Inflow, Station 18-1032, C soils, 50% Impervious, LOCA Scenario MIROC5 RCP8.5, 2070-2100

Figure 2-7 shows the cumulative distribution functions for projections of late century (ca. 2085) conditions at station 18-1032 for LOCA Scenario MIROC5 RCP8.5. The X axis shows the percent of days on which a given level of flow is exceeded. The axis is plotted on a logit or log odds scale, in which the intervals on the axis are based on LN [p/(1-p)], where p is the probability of exceedance, which expands the axis and tends to linearize the relationship, allowing visualization of the tails of the distribution.

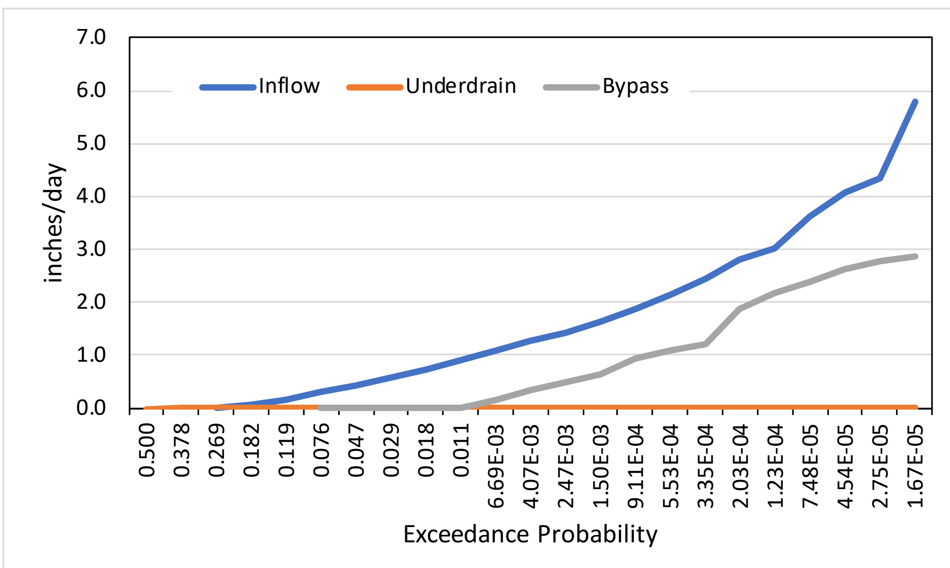

Figure 2-7. Cumulative Distribution Functions for Bioretention Cell Outflow (in/day) for Station 18-1032, C soils, 50% Impervious, LOCA Scenario MIROC5 RCP8.5, 2070-2100

The bypass flows occur on a relatively small number of days. For this scenario, inflow of at least 0.01 in/day is projected to occur on 14.5 percent of individual days, while bypass flow of 0.01 in/yr is projected to occur on 0.81 percent of all days – equivalent to bypass occurring on 5.6 percent of days with runoff above an 0.01 in threshold. This meets or exceeds the ESD objective of controlling all flows greater than the natural background for the 90th percentile event.

The downscaled future climate projections suggest relatively little change in the magnitude of the 90th percentile 24-hr storm event, which in turn indicates that the number of bypass events per year for an SCM built according to current design guidelines will not change much; however, the analysis also projects that there may be substantial increases in the magnitude of precipitation and runoff events with a recurrence of 2 years or greater. As a result, the total volume of bypassed flow is likely to increase.

Across all GCMs for station 18-1032 the projected amounts of SCM bypass flow fall into a relatively small range with an annual average bypass flow volume of 1.66 in/yr (7.1% of inflow) for LOCA scenarios and 1.69 in/yr (7.3% of inflow) for MACA scenarios (Figure 2-8). Bypasses of at least 0.01 inch are predicted for 5.6% of days with inflow for LOCA and 5.2% of days with inflow for MACA. These results are consistent with the objective of controlling or treating flow from the 90th percentile 24-hr event. The bypass volumes predicted from MACA downscaling tend to be slightly greater than those from LOCA downscaling, but there is strong overlap between the two and no statistically significant difference. It thus appears that ESD design requirements based on current conditions are indeed likely to provide similar levels of treatment in terms of the percentage of events treated through the end of the century.

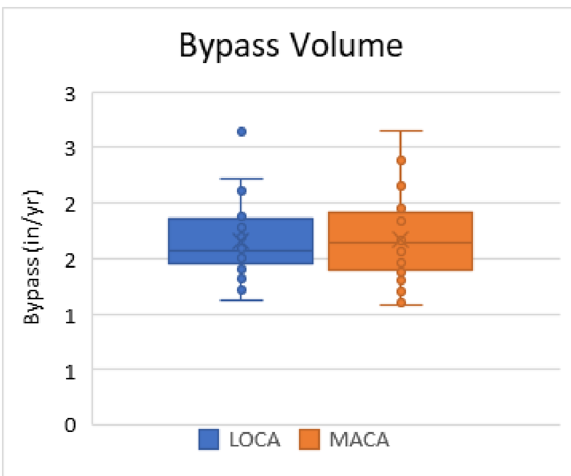

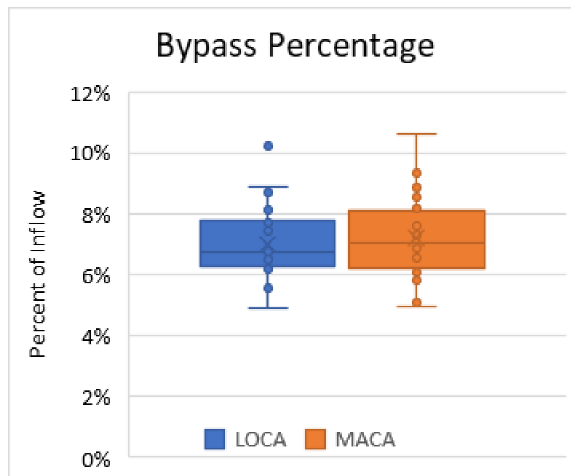

Figure 2-8. Boxplots of Projected Bioretention Cell Bypass Flows, Station 18-1032, C soils, 50% Impervious, All LOCA and MACA Scenarios, 2070-2100

Note: Box shows interquartile range with median.

Results for all Atlas 14 stations across the state are summarized in Table 2-5, first for LOCA, then for MACA. The results are based on the 2070-2100 average for each site/climate scenario combination. The results are similar to those shown above for the Boyds 2 NW and fall into a relatively small range, with a coefficient of variation (standard deviation divided by the mean) around 0.3 for bypass flow volumes. RCP 8.5 appears to yield somewhat larger average total inflows and bypass flows than RCP 4.5, but the difference is not statistically significant.

Results from MACA and LOCA are also similar, as shown in Figure 2-9 (boxplot) and Figure 2-10 (scatterplot of average results by station). The regression of MACA versus LOCA bypass volumes is tight, with a slope of 0.927 and an R^2 of 92%. This result is significant because it indicates that, while MACA and LOCA appear to have various biases for more extreme rainfall events, the choice of the downscaling approach has little effect on the projected amount of flow that will bypass bioretention SCMs built according to current design guidance as climate evolves over the century. The observation further supports our previous inference that ESD guidelines will continue to perform as intended (in terms of the proportion of stormwater volume that is treated) under future climate conditions.

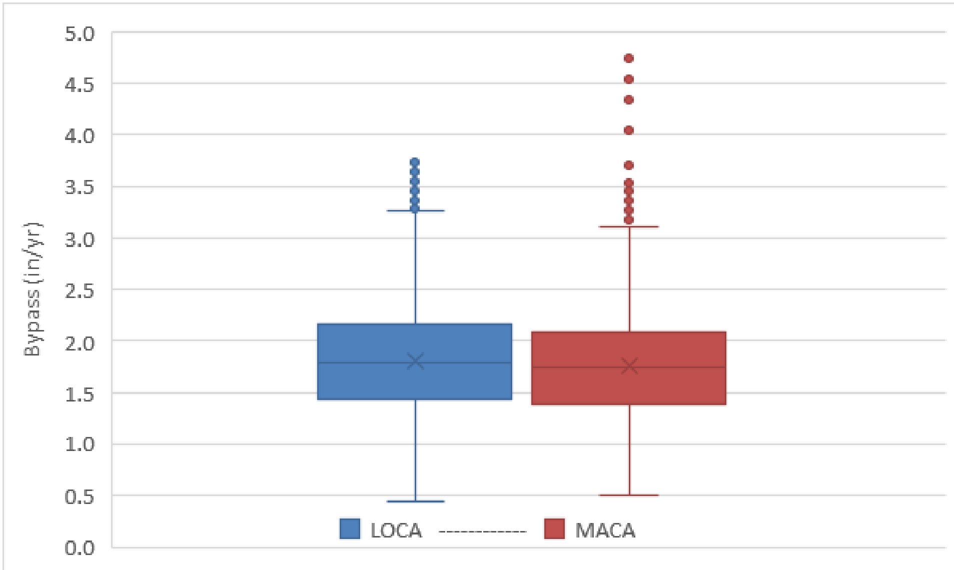

Figure 2-9. Boxplot Comparison of LOCA and MACA Results for Simulation of Bioretention Performance based on Current Design Guidance for C soils, 50% Impervious, for 2070-2100 Climate Conditions, All Maryland NOAA Atlas 14 Stations

Table 2-5. Statewide Results for Simulation of Bioretention Performance based on Current Design Guidance for C soils, 50% Impervious, for 2070-2100 Climate Conditions (in/yr)

LOCA		Inflow	Evaporation	Exfiltration	Drain	Bypass	Bypass % of inflow	Bypass % of precip
ALL	average	24.33	1.74	6.77	13.99	1.81	7.4%	3.5%
	median	24.39	1.74	6.73	14.05	1.79	7.4%	3.5%
	max	31.17	2.02	10.24	18.57	3.74	13.3%	6.6%
	min	18.40	1.33	5.61	9.76	0.44	1.9%	0.9%
	stdev	2.06	0.10	0.56	1.44	0.57	1.9%	1.0%
RCP 4.5	average	23.70	1.69	6.82	13.57	1.60	6.7%	3.2%
	median	23.75	1.70	6.78	13.60	1.61	6.8%	3.3%
	stdev	1.95	0.09	0.56	1.37	0.47	1.7%	0.8%
RCP 8.5	average	24.97	1.79	6.73	14.41	2.02	8.0%	3.9%
	median	25.04	1.81	6.65	14.51	2.01	8.1%	3.9%
	stdev	1.98	0.09	0.56	1.38	0.58	1.9%	1.0%
MACA		**Inflow**	**Evaporation**	**Exfiltration**	**Drain**	**Bypass**	**Bypass % of inflow**	**Bypass % of precip.**
ALL	average	23.72	1.72	6.94	13.28	1.75	7.3%	3.5%
	median	23.72	1.74	6.88	13.36	1.75	7.4%	3.5%
	max	31.18	2.00	10.58	17.88	4.75	16.5%	8.1%
	min	17.86	0.30	5.59	9.16	0.51	2.2%	1.0%
	stdev	2.01	0.14	0.63	1.42	0.55	1.9%	0.9%
RCP 4.5	average	23.27	1.68	7.01	12.96	1.60	6.8%	3.3%
	median	23.22	1.70	6.98	13.01	1.62	7.0%	3.3%
	stdev	1.99	0.14	0.64	1.40	0.49	1.8%	0.9%
RCP 8.5	average	24.17	1.77	6.87	13.61	1.90	7.8%	3.7%
	median	24.22	1.80	6.77	13.67	1.87	7.8%	3.7%
	stdev	1.94	0.13	0.61	1.37	0.57	1.9%	1.0%

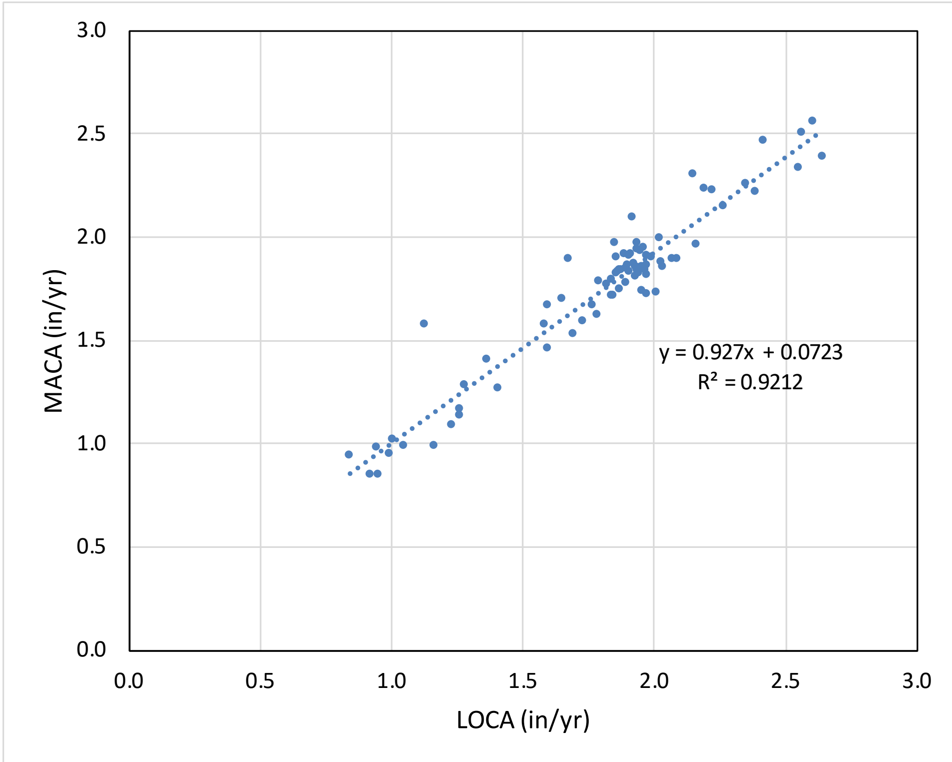

Figure 2-10. Station-by-station Comparison of LOCA and MACA Simulations of Bioretention Bypass Volumes based on Current Design Guidance for C soils, 50% Impervious, for 2070-2100 Climate Conditions

3.0 STREAM STABILITY IN TRIBUTARY 109, CLARKSBURG, MD

The site chosen to evaluate channel stability under changing climate is a small, urbanized catchment (211 ac.) located in Montgomery County, Maryland, USA, within the Piedmont Physiographic Province. The entire catchment falls within the Clarksburg Special Protection Area (CSPA) (

Figure 3-1), a designated area subject to strict development guidelines and restrictions requiring the implementation of ESD to protect its high-quality or unusually sensitive water resources (Jarnagin and Jennings 2004). The land-use and land-cover (LULC) of the catchment transitioned from predominately agriculture to suburban development from 2006 to 2017.

The current (post 2017) LULC within the catchment area comprises a blend of detached single-family homes and attached townhouses, complemented by widespread implementation of SCMs adhering to Maryland Department of the Environment (MDE) ESD regulations. These SCMs encompass a range of practices, including conventional end-of-pipe techniques like detention ponds, as well as decentralized SCMs that promote infiltration (SCM density = 1.4 per ac.). Catchment SCMs were placed in treatment trains where overflows from one SCM are redirected to another SCM before being stored in detention ponds at the outlet of each subwatershed. Runoff generated from all impervious areas of the study site is routed through a SCM before discharging to the main stem of the channel flowing through the catchment, resulting in a directly connected impervious area (DCIA) of nearly zero. The infiltration-based SCMs of the catchment were designed to capture peak flows from a 1 in. precipitation event whereas the detention ponds were designed to retain a 2.6 in., 1-yr., 24-hr. event for 24 hours (MDE, 2009). In addition to the SCMs, the entire riparian zone of the channel is undeveloped and can be considered a nonstructural BMP.

A watershed-level Stormwater Management Model (SWMM version 5.1.013; Rossman 2015) was developed to simulate current (post-2017) hydrologic conditions in the watershed, including most of the SCMs . A total of 70 SCMs were explicitly simulated in the model (26 micro-bioretention cells, 10 infiltration trenches, 5 ponds, 11 sand filters, and 18 underground storage facilities). Small street tree boxes were not simulated to reduce model complexity. The SWMM model was calibrated utilizing the 5-minute interval precipitation record of the “Black Hill” rain gauge maintained by Montgomery County, MD and discharge data from the U.S. Geological Survey (USGS) streamflow station located just upstream of the watershed outlet (station # 01644372 on Little Seneca Creek Tributary at Brink, Maryland; Figure 3-1). Details of the SWMM hydrologic calibration are documented in Alsmadi et al. (2022).

A 2,010-ft. long study reach downstream of Snowden Farm Parkway was chosen to evaluate the effects of ESD on stream stability. The study reach has a gravel-bed, riffle-pool morphology with a 1.1% bed slope. Bed material ranges from sands to small boulders. A 1-D quasi-unsteady hydraulic model of the reach was built utilizing HEC-RAS 6.3 (Brunner 2022) and was calibrated using gage height from the USGS gage.

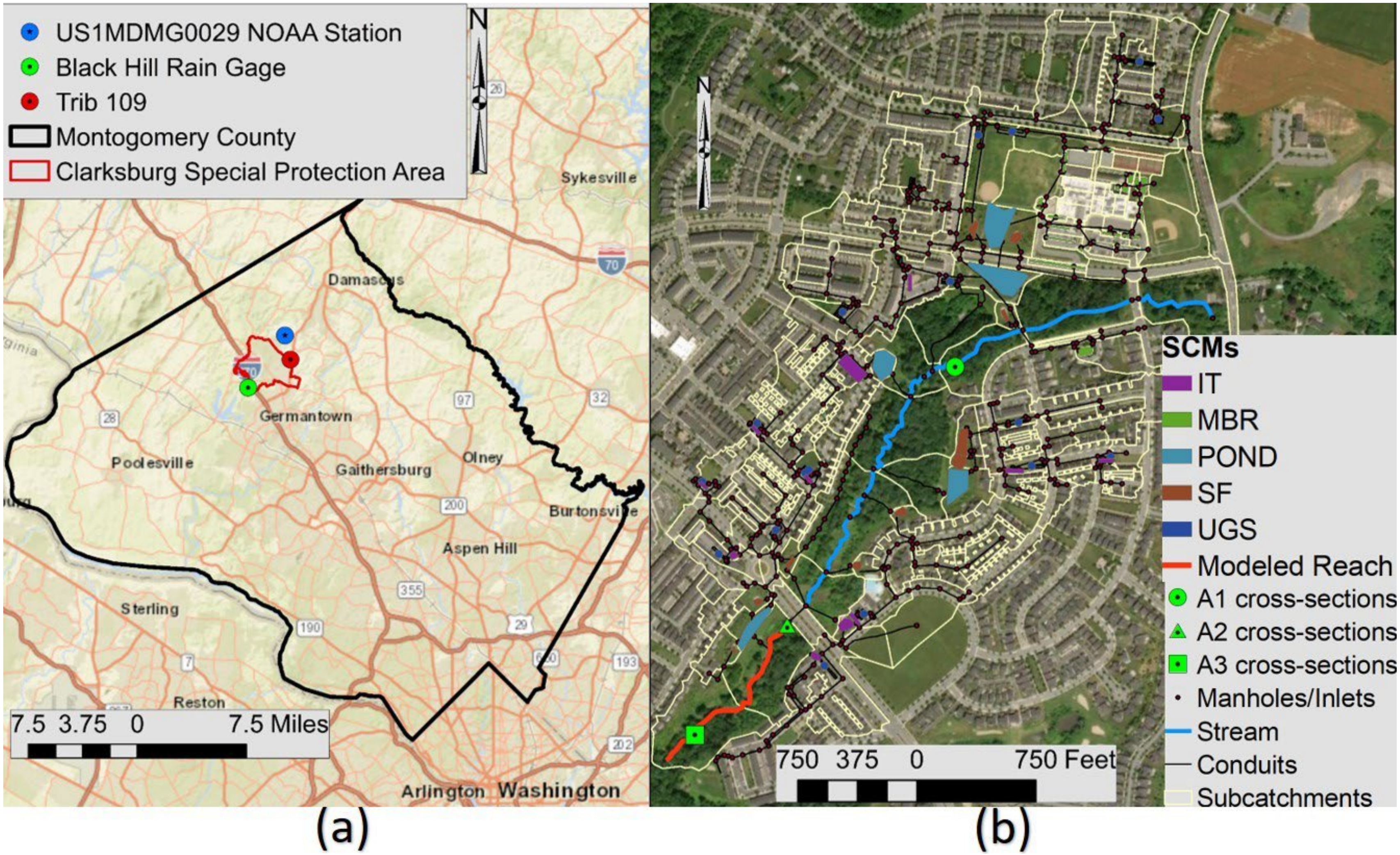

Figure 3-1. Site Map. a) Tributary 109 site along with the Black Hill rain gauge and b) stormwater conveyance and stormwater control methods (SCMs) of the study site (IT= infiltration trenches, MBR=micro bioretention cells, SF=sand filters, UGS=underground storage).

Note: Cross-sections were measured by Montgomery County, MD.

3.1 MODELING APPROACH

A coupled hierarchical modeling approach (Figure 3-2) utilizing the calibrated SWMM and HEC-RAS models was developed and applied to address the research questions under Hypotheses 3a-c of this study. Details of the approach are described in the following sections.

3.1.1 Evaluation of ESD Hydrology under Changing Climate

Virginia Tech received downscaled precipitation and temperature time series for projected climate conditions of the Tributary 109 watershed from Tetra Tech (Butcher, 2022). These included 5-min. interval air temperature and precipitation time series from 2040-2099 for 16 global climate models (GCMs). The datasets contained series from two downscaling methods, LOCA (Pierce et al. 2014) and MACA (Abatzoglou and Brown 2012). Each of these series in turn contained two series for representative concentration pathways (RCP 4.5 and RCP 8.5) reflecting different future greenhouse gas radiative forcing assumptions. The precipitation time series in the dataset contained values lower than 0.01 in. as a result of spatial-temporal downscaling from 24-hr. rainfall depths to 5-min. depths. However, these trace rainfall amounts greatly increased SWMM model run times while having minor impact on storm runoff rates. Additionally, since most rain gauges cannot record trace rainfall below this threshold, these data points are not physically realistic and were therefore excluded from the analysis. This data filtering process significantly improved the computational efficiency of the SWMM model. Nevertheless, it is important to note that removing these trace rainfall depths led to a reduction in the calculated average annual precipitation by 6.0 to 7.2 in. The edited precipitation and temperature time series of these 64 climate change (CC) scenarios were incorporated into the calibrated SWMM model to obtain streamflow time series under future climate. The streamflow time series under the current climate was obtained by running the calibrated model with the measured precipitation record from 2004-2020 at the Black Hill rain gauge.

The stream flow time series at the watershed outlet for current and future climate simulations were exported to R, an open-source, freely available system that can be used for statistical analysis and programming (Wickham et al. 2019). A script was written in R utilizing the RSWMM package to read the binary output files created by SWMM and extract only the flow time series at the watershed outlet to evaluate the change in watershed hydrology with changing climate (Alamdari and Sample 2019). The R script was executed in the Linux operating system to reduce the computation time required to read the large binary files generated by SWMM.

Two CC scenarios, MIROC-ESM MACA RCP 8.5 and 9 CSIRO-Mk3-6-0 LOCA RCP 4.5, with the highest and lowest rainfall total, respectively, with and without trace rain removal, were incorporated into the SWMM model to compare the effects of the rain time series truncation on the simulated flows. Our findings demonstrate that the cumulative flow volume decreased by approximately 15% as a result of this data filtering. However, it is important to note that this filtering did not have any effect on the annual maxima or peak flows of individual storm events.

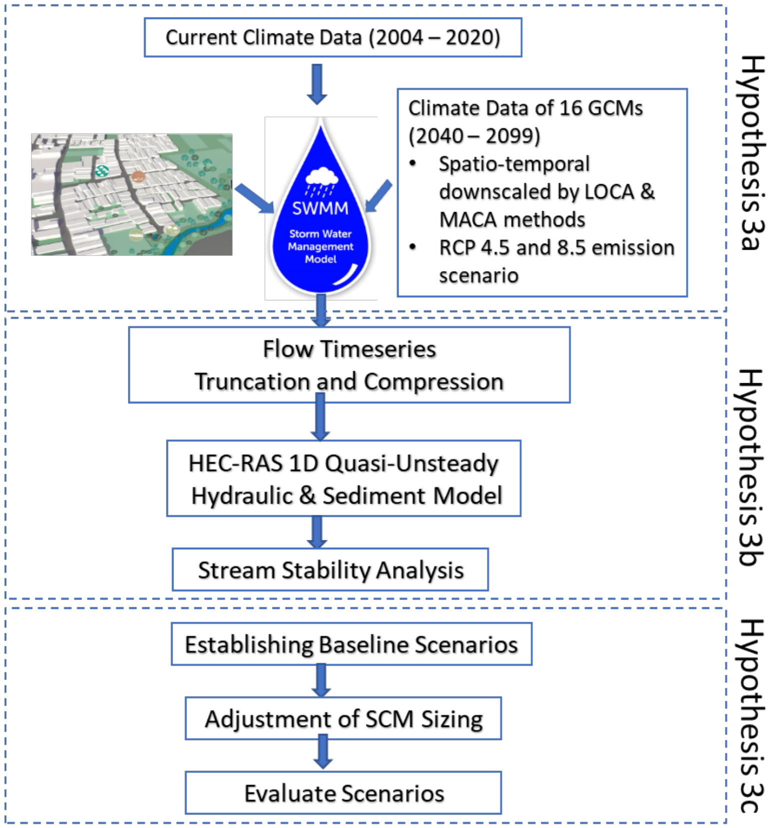

Figure 3-2. Methodological Framework for Addressing Hypotheses 3a-c

Note: GCM=Global Climate Model

3.1.1.1 Projected Changes in Storm Event-based Streamflow

To quantify the changes in storm event-based streamflow with changing climate, a frequency analysis was conducted on storm event peak discharge. Storm events were identified based on the 5-min. interval precipitation record, employing a rainfall total threshold of 0.1 in. and a 6-hr. inter-event period, for both the current and CC scenarios. To capture the peak discharge accurately, the ending time of each storm event was extended by 1 hr. This adjustment was necessary due to the typical time lag between the peak rainfall and peak discharge in urbanized streams (Hood et al. 2007).

Frequency analysis of storm event peak discharge was conducted by calculating the probability of exceedance by sorting each of the variables from largest to the smallest, then assigning a rank, r, to each value and then exceedance probability, P, was calculated using the following equation:

$$P = \frac{\mathrm{r}}{n} \times 100$$

where *n* is the number of values of each of the variables.

The 2%, 5%, 10%, 25% and 50% exceedance values, along with the maximum value, of storm event peak discharge were extracted from the respective frequency curves for each climate change (CC) scenario. Subsequently, a one-sample t-test was performed to assess the differences between the extracted values of storm event peak discharge of the CC scenarios with the corresponding value observed in the current climate.

3.1.1.2 Flood-Frequency Analysis

Flood-frequency analysis (FFA) provides information about the magnitude and frequency of flood discharges based on records of annual maximum series (AMS) (England Jr. et al. 2019). The annual maximum flood series was calculated for each of the CC scenarios and the current climate stream flow based on the instantaneous maximum peak flow for each year. The analysis was performed using standard techniques specified in "Guidelines for Determining Flood Flow Frequency, Bulletin 17C" (England Jr. et al. 2019). Estimates of instantaneous annual maximum peak flows having recurrence intervals of 10, 50, and 100 yrs. were extracted from the flood frequency curve to evaluate potential shifts in the magnitude of peak flows of different CC scenarios from current climate conditions. Discharge for flood recurrence intervals of 0.5, 0.75, 1, 2, and 5 yrs. was calculated from the partial duration series (PDS) by fitting the peak discharge data to a Gumbel distribution (Van Campenhout et al. 2020). The lowest flow value from the AMS and an inter-event time of 7 days were used as the thresholds for constructing the partial duration series.

Differences in the flood probability distributions of the AMS for each of the CC scenarios were compared to historic conditions using the Kullback-Leibler Divergence (KLD). KLD is a measure of the difference or relative entropy between two probability distributions of the same variable, which in this case is the annual maximum peak flow distribution (Kullback and Leibler 1951). The probability densities of the annual peak flows at different recurrence intervals calculated from the flood frequency analysis were utilized to obtain the KLD between each CC scenario and the current climate. KLD can take values from 0 to ∞, where a value of 0 indicates that the two distributions match exactly. KLD is formally defined as:

$$KLD_{(H\|C)} = \sum_{i=1}^{N} H(x_i) \log\left(\frac{H(x_i)}{C(x_i)}\right)$$

where:
N = Number of selected flows
H(x) = Probability density of annual peak flows for the current climate
C(c) = Probability density of annual peak flows for each of the CC scenarios

A similar analysis was conducted to assess the impact of the edits to the precipitation time series on study results.

3.1.2 Evaluation of Stream Channel Stability under Changing Climate

The existing 1-D unsteady HEC-RAS 6.3 hydraulic model was run in quasi-unsteady mode to evaluate the channel stability of the studied reach. The quasi-unsteady mode was utilized because it was more stable than the fully unsteady mode when modeling the extreme precipitation intensity of some of the CC scenarios. Model parameterization and calibration are outlined in Figure 3-3 and briefly described in the following sections. A more detailed description of this process is available in Technical Memo 8A (Sample et al. 2022).

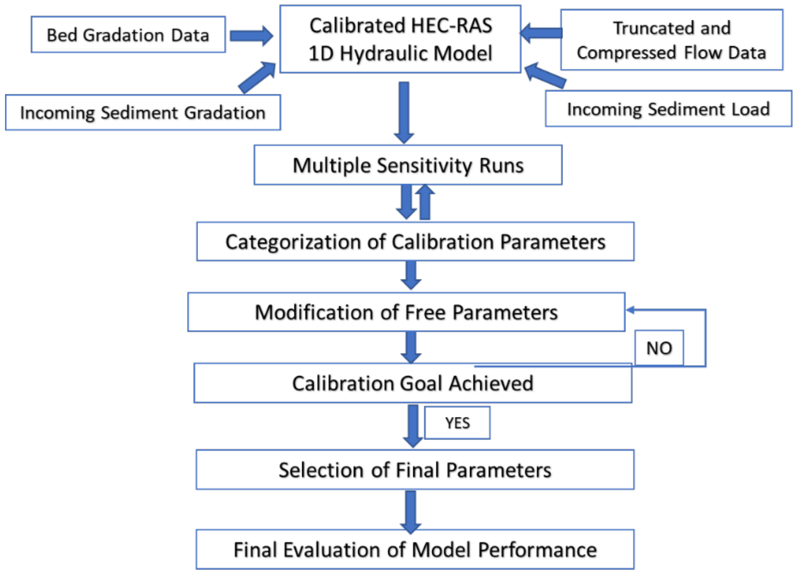

Figure 3-3. Workflow for Sediment Model Development and Calibration

3.1.2.1 Sediment Transport Model Parameterization

Sediment transport was simulated using the Wilcock and Crowe (2003) model and the Active Layer method since these options best represent the modeled reach (Wilcock and Crowe 2003). To decrease the computational time in HEC-RAS, the 5-min. interval stream flow time series for current and future climate conditions were truncated at 1 cfs, given that no bed material transport occurs at low flows. The truncated flow time series were further compressed by grouping flows less than 10 cfs while also conserving the sediment mass delivery at the upstream model boundary and maintaining the total flow duration but not the flow volume. The flow compression was necessary to reduce the flow time series to 40,000 entries, which is a limitation of HEC-RAS.

To model sediment transport through a stream reach, an input sediment rating curve (tons/day versus discharge) and sediment gradation must be specified at the upstream model boundary. The incoming sediment load was estimated from suspended sediment measurements at six USGS gages with similar geology, climate, and LULC. Sediment rating curves for each of the six gages were developed using the Sediment Rating Curve Analysis Tool within HEC-RAS version 6.3, which uses an unbiased power regression method. The sediment load values in tons/day at 1, 40, 319, 600, and 1,300 cfs stream discharges were then estimated for the study reach based on the six gage sediment rating curves and the relative channel widths. The median of these values was used to construct the initial sediment rating curve for the study reach, which was adjusted during the calibration process. A discharge value of 40 cfs was included in the rating curve because USGS staff noted gravel transport in Tributary 109 at similar flows (Baker, 2022a). Because the largest flood during the calibration period had a peak discharge of 319 cfs, the sediment rating curve beyond 319 cfs was unknown.

Urbanization affects not only watershed hydrology, but also the supply of coarse bedload sediment to the channel. Nearby hillslopes, zero-order colluvial channels, and the upstream channel bed are major sources of coarse sediment. This coarse sediment is critical to bed stability. During development, hillslopes are stabilized with vegetation or retaining walls, intermittent channels are buried, and other channels are piped, reducing the supply of coarse sediment to downstream reaches and exacerbating problems with channel erosion. To simulate the impact of potential changes in coarse sediment supply following development within the Tributary 109 watershed, two different sediment rating curves were developed, one assuming increasing sediment load with increasing stream discharge and one assuming sediment supplies to the channel are limited and do not increase at the same rate at higher discharges. These two sediment rating curves were constructed for flows beyond the 319 cfs value – one with the median and another with the minimum of the measured loads from the six USGS gages, which represented a “sediment starved” condition where sediment supplies from the watershed are exhausted during extreme floods (Figure 3-4). Bulk subsurface sediment samples were collected from the reach, sieved, and weighed to characterize the gradation of the incoming sediment load for flows equal to and greater than 40 cfs (Figure 3-5).

3.1.2.2 Sediment Model Calibration and Evaluation

Due to the difficulty of measuring bedload sediment transport rates, sediment transport models are typically calibrated using observed cross-section data collected across multiple locations and years. In addition to replicating the observed channel changes, these cross-sections can be converted to a cumulative reach volume change, which represents the cumulative downstream sediment load (Gibson et al. 2017). This sediment loss is then also used to calibrate the sediment transport parameters. Montgomery County measured pool and riffle cross sections annually, as well as bed surface particle size distributions, at three locations along Tributary 109 between 2005 and 2017 (locations A1-A3); the A2 and A3 cross sections (Figure 3-1) showed signs of aggradation during construction, followed by 1-2 ft. of degradation post-construction (Williams et al. 2022). To represent the final built conditions in the watershed, the sediment transport model was calibrated using cross-section data at location A3 from 2017 to 2020 and field observations of reach-level changes during the study period. During field visits it was noted that there was no sedimentation or flood debris on the floodplain. Conversations with a USGS technician maintaining the gage confirmed that Tributary 109 rarely inundates the floodplain (Baker, 2022b). Due to the construction of a stream restoration project in the upper 1048 ft. of the reach in 2017, the A2 cross sections were not utilized in model calibration. The stream restoration project was not simulated in the HEC-RAS model to avoid the confounding effects of the restoration project on study results.

To avoid potential equifinality errors, which are common in sediment transport calibration, a subset of calibration parameters, known as “free parameters”, was isolated to modify while the rest of the parameters were kept fixed throughout the calibration process. These selections were made based on multiple model sensitivity runs, field observations, and recommendations in the HEC-RAS technical reference manual (Brunner 2022). The categorization of the sediment transport parameters based on these assessments is summarized in Table 3-1. The free parameters were modified to replicate the general bed changes documented in the A3 cross sections.

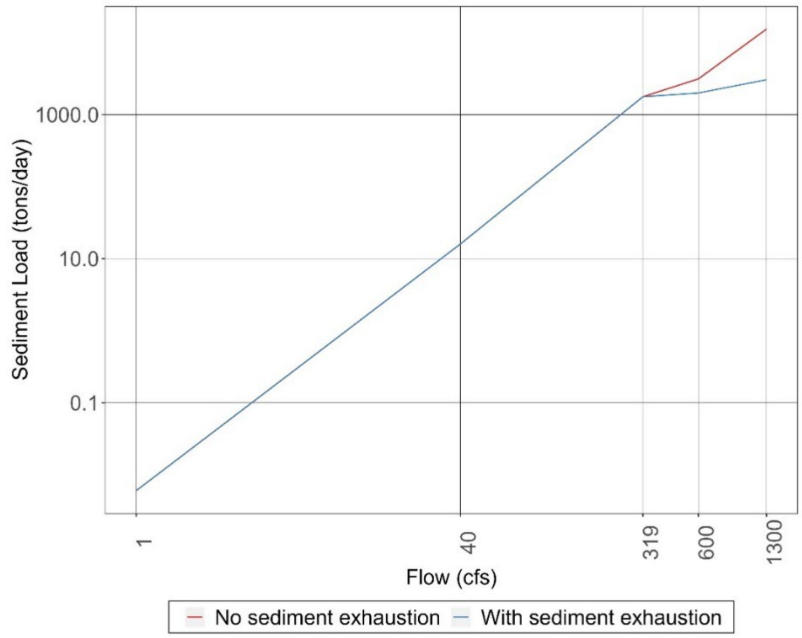

Figure 3-4. Calibrated Inflow Sediment Rating Curve

Note: The axes are drawn in log-log space.

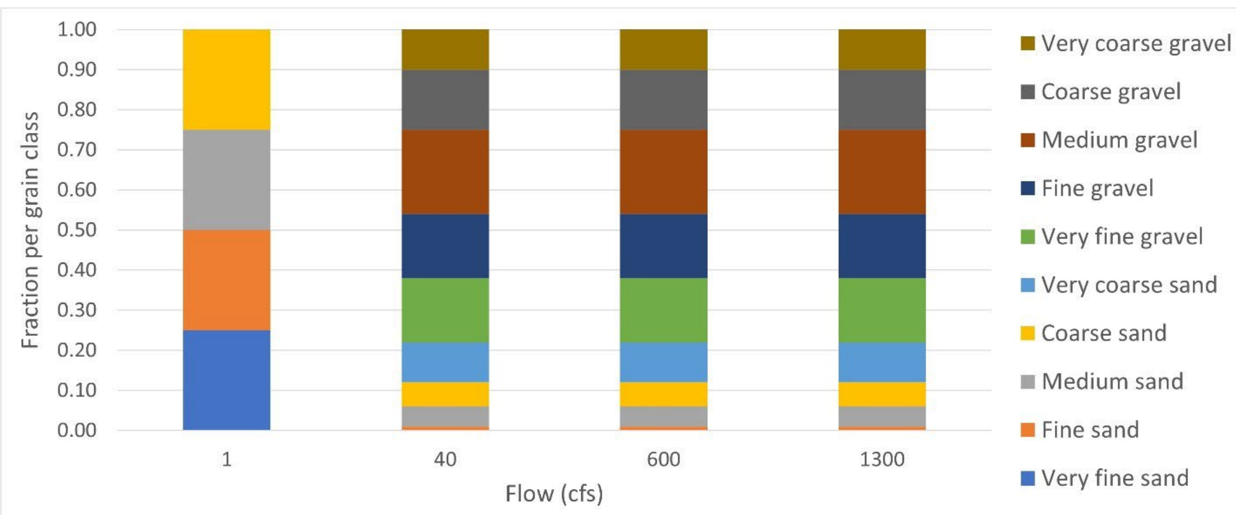

Figure 3-5. Calibrated Inflow Sediment Load Gradation

Table 3-1. Summary of Calibration Settings

Uncertainty	Low Sensitivity	High Sensitivity
Low	Bed Mixing Algorithm Fall Velocity *Moveable Bed Limits*	Transport Function *Incoming Sediment Gradation*
High		Active Layer Thickness *Incoming Sediment Load Transport Function Scaling Factor*

Note: Italics identify free parameters.

The 1-D sediment transport model in HEC-RAS is a decadal scale model and is more robust when used for more than 10 years of calibration and projections. Since a 10-yr. observed post-construction flow record was unavailable for our study site, the simulated stream flow time series, developed using precipitation from 2005-2020 as an input to the post-development SWMM model, was used to evaluate the HEC-RAS model performance for long-term simulation; the HEC-RAS model was further calibrated so that there was no long-term channel aggradation or overbank deposition within the reach.

3.1.2.3 Sediment Model Setup for Climate Change Simulations

Unlike hydraulics, the sediment transport dynamics in fluvial systems are heavily influenced by the sequence of storm events over longer timespans, a phenomenon called historical contingency (Wohl 2018). Therefore, to compare the sediment transport dynamics of the CC scenarios with the current climate, the length of the inflow discharge time series must be equal. To create a 59-yr. long flow time series for the current conditions, the measured precipitation record from 2004-2020 at the Black Hill station was repeated in series to develop a 59-year long continuous precipitation time series. This synthetic time series was used as an input to the post-development calibrated SWMM model to generate a continuous streamflow time series for the current climate. This discharge time series at the watershed outlet was then used as an input to the calibrated HEC-RAS model to allow comparisons of channel change under the current climate conditions. Each of the CC simulated discharge time series was modeled with and without the sediment exhaustion condition, which resulted in 128 CC HEC-RAS models.

The effect of trace rain removal on the HEC-RAS simulation results was evaluated for the CC scenarios with the highest and lowest rainfall totals. The predicted channel profile resulting from the precipitation and discharge series with the trace rain removal was similar to the channel profile without the editing: the channel end profile varied as little as 0.3 feet for some cross-sections and the majority of cross-sections were the same.

3.1.2.4 Stream Stability Analysis

Continuous time series of cross-section shape, longitudinal bed profile, and sediment transport rate and gradation were exported from the standard HEC-RAS HDF file to *R* (Wickham et al. 2019) to evaluate the effects of the CC scenarios on sediment transport dynamics and channel morphology. To quantify and compare the change in channel morphology, three indices were calculated from the cross-section data of each of the non-interpolated model river stations, including channel width:depth ratio, change in cross-sectional area, and change in invert elevation. In addition to the three indices of channel morphological change, effective discharge (Q_{eff}) was also calculated for the current conditions and the 128 CC scenarios, following the methods of Biedenharn et al. (2000b). Since a Shapiro-Wilk test (Shapiro and

Wilk 1965) showed evidence of non-normality, a non-parametric two-sample test (Rey and Neuhäuser 2011) was then conducted for each of the three indices to determine if the central tendency of an index for a particular CC scenario was significantly different from the central tendency of an index for the current climate. The CC scenario model results were grouped based on the downscaling method, representative concentration pathway of the global climate model (GCM), and type of sediment rating curve, which resulted in eight sets of CC scenario HEC-RAS model results. An alpha level of 0.05 was used for all of the statistical tests.

3.1.3 ESD Adjustments for Stream Stability

Ensemble simulation results showed that even with the extensive implementation of ESD, the studied reach is expected to degrade further over the next several decades under both current and future climate conditions. This result indicates the modification of stormwater regulations is necessary to address the sediment-transport characteristics of the receiving stream, as well to control the runoff from impervious surfaces. To address this need, a four-step approach (Figure 3-6) was developed using the well-calibrated SWMM and HEC-RAS models. Details of the approach are described in the following sections. A more detailed version of this approach is available in Technical Memo 8a (Sample et al. 2022).

Step 1: Establish baseline scenarios

- Develop and calibrate appropriate rainfall-runoff model for pre-development condition
- Generate flow time series for pre-development condition for design storms

Step 2: Estimate erosion potential (E_p)

- Select design storms and site-specific sediment transport methods
- Estimate Ep for pre-development, current ESD and retrofitted ESD scenarios
- Adjust retrofitted ESD sizing to minimize Ep for selected design storms

Step 3: Estimate erosional hour (E_h) and effective work (E_w)

- Estimate critical shear stress for representative bed particle size (d_{50} or d_{84})
- Estimate E_h ,E_w for pre-development, current ESD and retrofitted ESD scenarios
- Adjust retrofitted ESD sizing to minimize E_h ,E_w for selected design storm

Step 4: Evaluate scenarios

- Generate continuous flow time series for all scenarios under current and future climate conditions using the calibrated SWMM model
- Examine sediment transport dynamics using previously calibrated HEC-RAS model for all stormwater management and climate scenario combinations

Figure 3-6. Methodological Framework for ESD Adjustments

3.1.3.1 Establishing Pre-development Conditions

An additional SWMM model was developed for the study watershed utilizing available LULC (Williams et al. 2018) and a 3-ft. resolution digital elevation model (DEM) (Metes and Jones 2021) from the year 2002; this model was then used to establish the baseline conditions of the receiving stream. This pre-development SWMM model of the study area was calibrated to a single storm event using discharge data from the USGS gage. Due to the short time span between when the gage was established and the initiation of development, only one storm event was suitable for model calibration. The groundwater parameters of the pre-development SWMM model were set to the same values as those of the floodplain in the calibrated SWMM model, which reflects the LULC of the post-2017 period. These parameters were not varied during the calibration of the pre-development model, as the floodplain had not undergone any modifications during the construction period from 2006 to 2017. In this pre-development scenario, all the delineated subcatchments of the pre-development watershed were assumed to be 100% pervious, and their physical properties were obtained from the DEM of the watershed in 2002. The main purpose of this model was to generate a runoff time series in response to specific design storm rainfall for the calculation of the pre-development cumulative bedload transport amount and shear stress exceedance criteria, which are described in the following section.

3.1.3.2 Existing SCM Retrofits

Maintaining channel stability following urbanization requires design requirements that address bedload transport in the receiving stream. Two methods were evaluated at a single stable cross section within the reach. The Erosion Potential criterion by Bledsoe (2002) requires the cumulative bedload transported pre- and post-development be equal. A second method maintains the magnitude and duration of shear stress exceedance (Pomeroy et al. 2008). This approach is referred to as the Shear Stress method. An outline of both methods is provided in Table 3-2.

The existing SCMs in the watershed were retrofitted according to the specifications outlined in Table 3-2 to achieve the design requirements set by the respective methods. These targets were established for a range of standard design storms commonly used in stormwater management, including 24-hr. storm events with recurrence intervals of 1, 2, 5, 10, 25, 50, and 100 yr. Calculations were completed in R with the cross-section data of river station 1357, which was generally stable in the model simulations. The analysis determined that the design targets of both methods for storm events with a recurrence interval greater than 5 yrs. were met by the existing SCMs, likely because the most significant increase in sediment transport post-development occurred during flows at or below the bankfull stage (Rosburg et al. 2017). Consequently, the SCM updates focused exclusively on the design storms with recurrence intervals of 1, 2, and 5 yrs. The rainfall depths were obtained Maryland Department of the Environment's (MDE) Stormwater Design Manual (MDE, 2009) and are shown in Table 3-3. The 24-hr. rainfall depths after trace rain removal for recurrence intervals less than 25 yr. were significantly less for the climate change scenarios as compared to the storm depths prescribed in the design manual, so no additional SCM modification was necessary for the climate change scenarios.

Table 3-2. Summary of “Erosion Potential” and “Shear Stress” Design Methods

Attribute	**Erosion Potential**	**Shear Stress**
Key variable(s) calculated	Channel bed cumulative sediment transport capacity in tons (Q_s) employing any suitable, reach-representative sediment transport capacity equation.	Magnitude (E_w) and duration (E_h) of critical shear stress exceedance of a representative bed particle size, typically d_{50} or d_{84}.
Design Target	Keep Q_s the same as pre-development conditions by retrofitting existing and/or designing new SCMs for selected design storms.	Keep E_w and E_w the same or less than pre-development conditions using adjusted and/or new SCMs for selected design storms.
Data Requirement	• Grain size distribution of the channel bed. • Channel cross section geometry and bed slope.	• Grain size distribution of the channel bed, • Channel cross section geometry and bed slope.
Limitations	• Results are highly sensitive to the chosen sediment transport capacity equation. • Calculation intensive.	• Considers the mobility of selected particle size only. • Does not consider the effect of bed gradation on sediment mobility.
SCM Modifications Required	• Modification of inlet and outlet structures (both size and elevation) of existing ponds and the SCMs paired with the ponds. The invert elevations of the outlet orifices and weirs were raised by 5-7 ft. to provided extended detention for the ponds. • Restructuring the flow connectivity of decentralized SCMs. The outlet orifices of SCMs immediate upstream of existing dry ponds were raised by 2-4 ft. to decrease the inflow rate of existing dry ponds. • Addition of low stage orifice to ponds. These low stage orifices were sized as per minimum allowable diameter (6 in.; MDE, 2009). • Addition of new in-line pond	• Modification of inlet and outlet structures (both size and elevation) of existing ponds and the SCMs paired with the ponds. • Restructuring the flow connectivity of decentralized SCMs • Addition of low stage orifice to ponds

Table 3-3. Rainfall Depth of Storm Events of Different Return Periods (MDE, 2009)

Return Period (yr.)	1	2	5	10	25	50	100
24-hr Rainfall Depth (in.)	2.6	3.2	4.2	5.1	5.6	6.3	7.2

3.1.3.3 Evaluation of Retrofit Scenarios

The calibrated HEC-RAS model was employed to evaluate the performance of the retrofit scenarios in protecting channel stability under current and future climate conditions. The 59-year long precipitation record of the “CSIRO-Mk3-6-0 MACA RCP 4.5” CC scenario was used to represent future climate conditions; this scenario had the highest amount of rainfall among all the 64 CC scenarios. The SWMM model of the retrofit SCM scenarios was run with the precipitation record of current conditions for the 2004-2020 period and with the precipitation record of the chosen CC scenario. The 16-yr long simulated flow time series at current climate conditions of the retrofit scenarios was extended to 59 yr. to make the current conditions flow time series comparable with the CC scenario. A continuous time series of cross-section shape, longitudinal bed profile, and sediment transport rates were exported from the standard HEC-RAS HDF file to *R* (Wickham et al., 2019) to evaluate the effects of the retrofit scenarios on sediment transport dynamics and channel morphology.

3.2 RESULTS

3.2.1 Evaluation of ESD hydrology

Figure 3-7 presents boxplots of the average total annual precipitation for the 64 climate change (CC) scenarios, both without and with trace rain removal, in comparison to the current climate period of 2005-2020. It is evident that all of the GCMs project an increase in annual rainfall, regardless of the downscaling method and RCP emission scenario, when compared to the climate normal. However, a decrease in annual rainfall was predicted for the GCMs with RCP 4.5 for both of the downscaling methods when compared with the current climate period of water years 2005 to 2020. During the current climate period (2005-2020), the Black Hill rain gauge recorded a significantly higher average annual rainfall compared to the NOAA climate normal (1991-2020) for the US1MDMG0029 station, situated 1.9 miles away from the watershed (Vose et al. 2014). The average annual rainfall at the Black Hill rain gauge was approximately 2.5 in. higher than the 30-year NOAA climate normal.

Figure 3-8 presents a boxplot illustrating the 24-hr. rainfall depths of typical recurrence intervals (RI) for the CC scenarios, with data from the Black Hill rain gauge. The frequency analysis conducted using precipitation records, which include trace rain data from the CC scenarios, reveals interesting insights. Notably, for the current climate, the 24-hr. rainfall depths for RIs less than 25 yr. were considerably higher, ranging from 0.4 to 1.1 in., in comparison to the median values of the CC scenarios. Conversely, certain extreme CC scenarios exhibited 24-hr. rainfall depths for RIs exceeding 25 yr. that were nearly double those observed at the Black Hill rain gauge.

It is noteworthy that the exclusion of trace rain records (<0.01 in. in 5 min.) resulted in a decrease in the average annual precipitation by approximately 6.0 to 7.2 in. This data filtering process removed approximately 15% of the total rainfall volume, which has the potential to introduce distortions in the statistical analysis of cumulative rainfall and runoff at daily, monthly, or yearly time scales. Because the trace rain records, which are typically observed towards the start or end of storm events, produce minimal runoff, the exclusion of these data does not impact extreme value or flood frequency analysis. Thus, while this data filtering may affect certain aspects of rainfall-runoff statistics, it does not compromise the assessment of extreme values or flood frequency analysis.

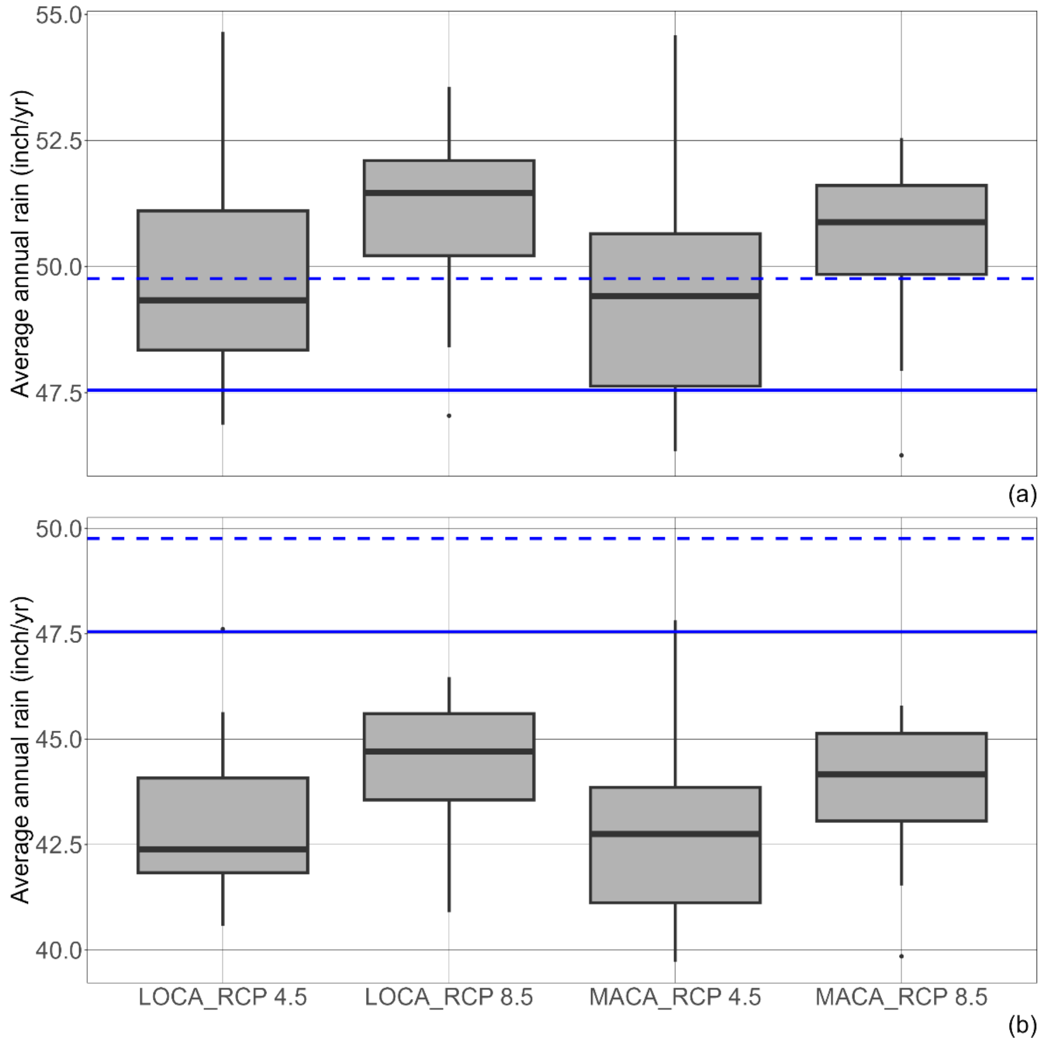

Figure 3-7. Boxplot of Average Annual Rainfall of 16 Global Climate Models (GCMs) for Water Years 2041 to 2099 (a) Without trace rain removal and (b) With trace rain removal

Note: The dashed line represents the precipitation recorded at the Black Hill rain gauge and the solid line represents the climate normal (1991-2020) for NOAA station US1MDMG0029.

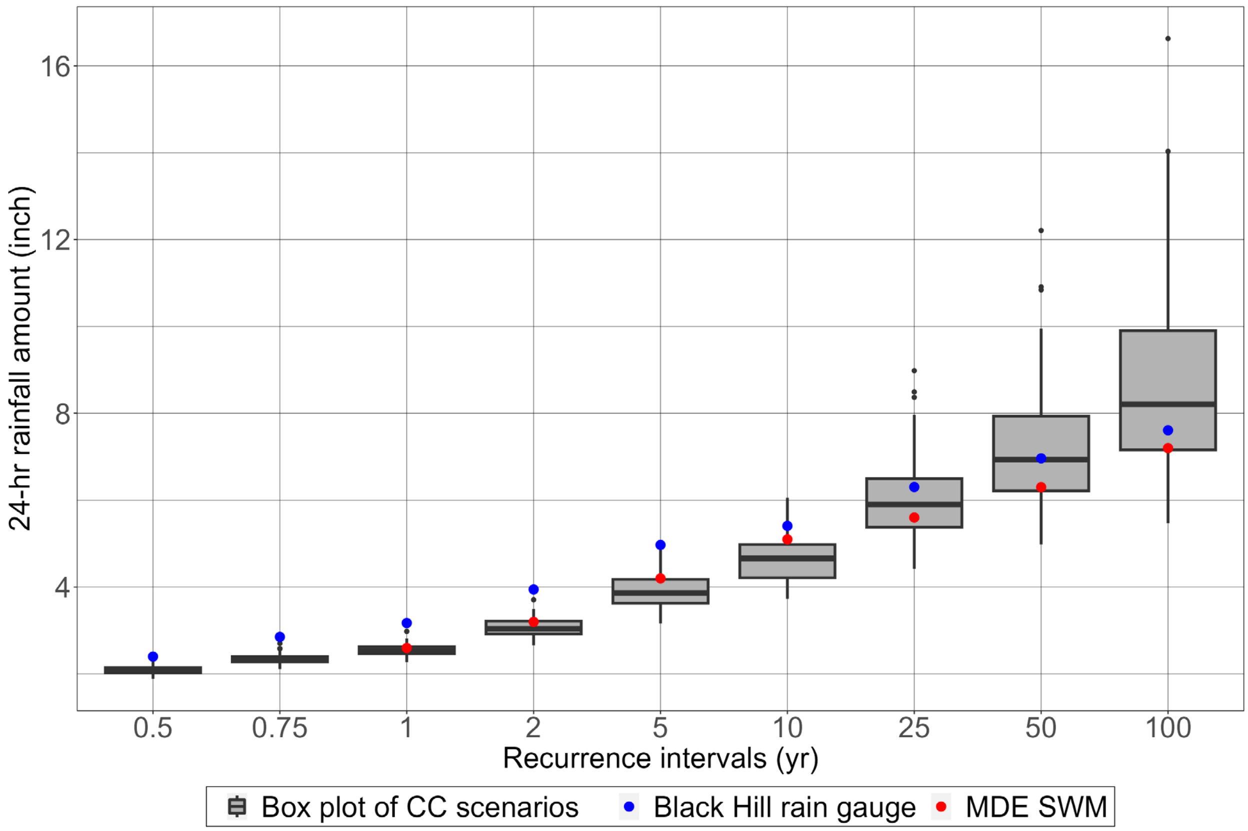

Figure 3-8. 24-hr. Rainfall Depth at Different Recurrence intervals for the Climate Change (CC) Scenarios, Black Hill Rain Gauge, and for Montgomery County as Reported in the Maryland Stormwater Management Manual (MDE 2009)

Frequency analysis was conducted to examine the changes in storm event-based streamflow responses under a changing climate (Figure 3-9). The 2%, 5%, 10%, 25%, and 50% exceedance values, along with the maximum value, of storm event peak discharge were extracted from the respective frequency curves and plotted in Figure 3-10. It is evident from the boxplot that the median peak flows of storms events with an exceedance of less than 25% are expected to increase in future.

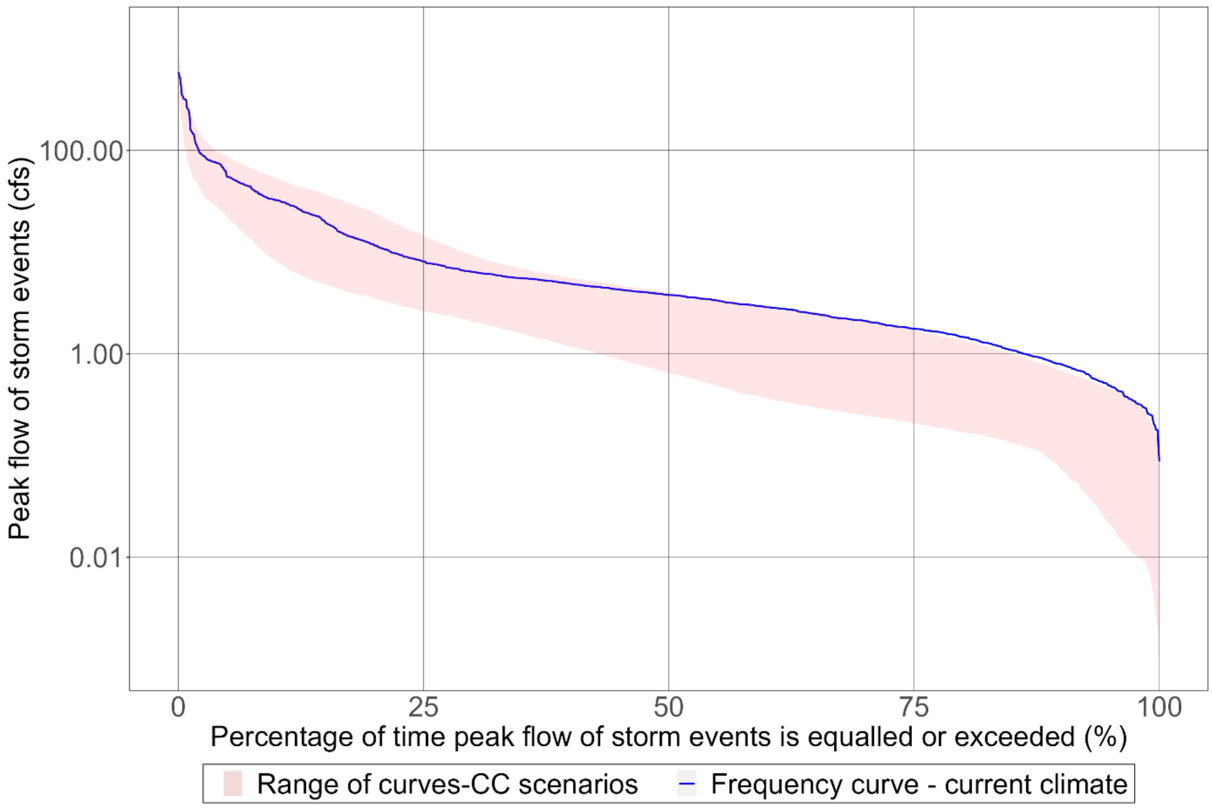

Figure 3-9. Frequency Curves of Storm Event Peak Flow

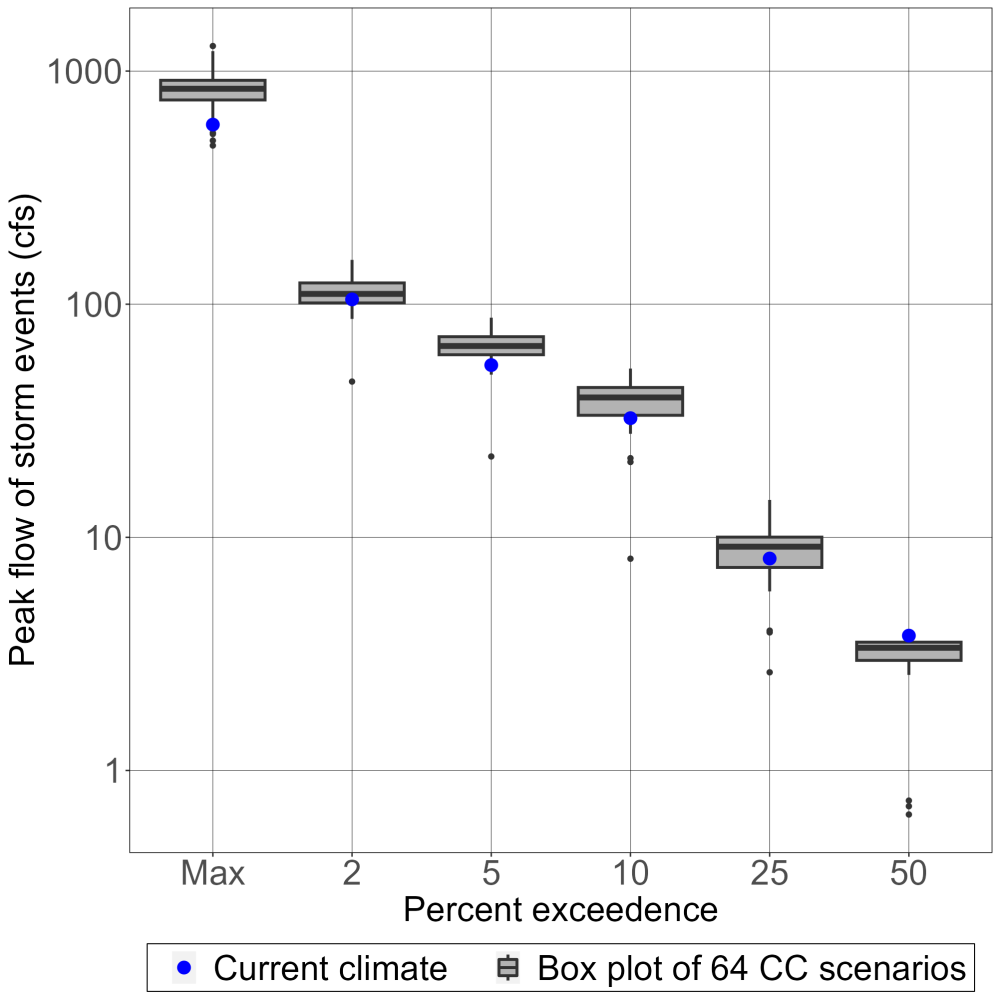

Figure 3-10. Storm Event Peak Flow for Selected Percent Exceedance Values

The flood frequency analysis conducted using the Annual Maximum Series (AMS) projected decrease in peak flows with a recurrence interval equal to or exceeding 10 yr. (Figure 3-11). However, it is important to acknowledge that the flood frequency analysis with the AMS was performed utilizing a log Pearson type III distribution, which tends to overestimate flood peaks of high return periods when the record length of the AMS is less than 20 years (Hamzah et al. 2021). In this study, the AMS for the current climate consisted of a record length of 16 years, while the CC scenario incorporated a flow time series spanning 59 years. Additionally, precipitation during 2005-2020 was higher than normal. This discrepancy in record length between the current climate and CC scenario and the abnormally wet current climate period limits the analysis and highlights the need for a careful interpretation of the results.

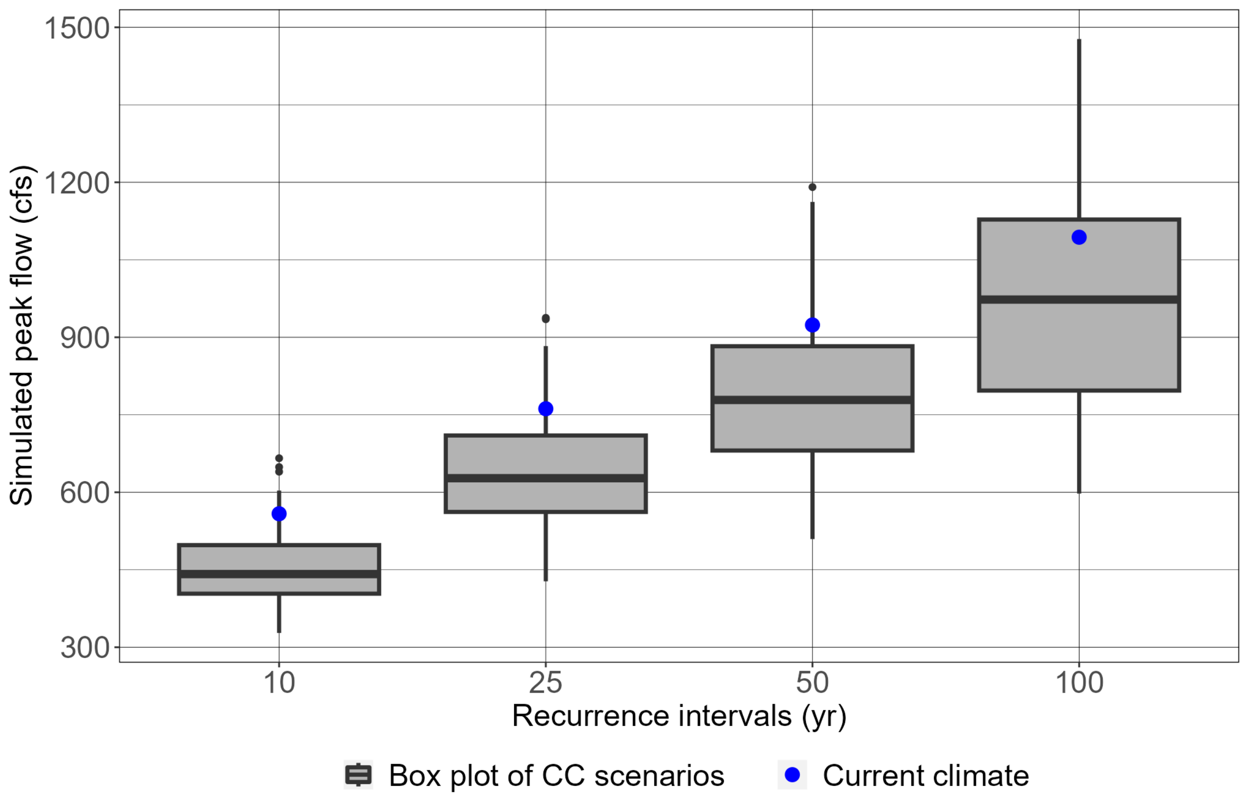

Figure 3-11. Range of Flood Recurrence Intervals Derived from Annual Maximum Series (AMS)

The Kullback-Leibler Divergence (KLD) between the AMS flood probability distributions for the CC scenarios and the current climate are shown in Figure 3-12. The lower the KLD score in Figure 3-12, the less peak flood distributions are expected to change due to CC. The KLD score for the scenario “CCSM4: MACA RCP 8.5” had the lowest KLD score (0.01) and the “CCSM4: LOCA RCP 8.5" scenario had the highest score (0.24), illustrating the impact of downscaling method on precipitation magnitude. The low KLD indicates that GCM CCSM4, with the MACA downscaling method, and RCP 8.5, closely matched the distribution of historic annual maximum peak runoff while CCSM4 using LOCA downscaling and an RCP of 8.5 predicted the greatest change in the flood distribution. The average annual precipitation total of these two CC scenarios differed by only 1 in.; however, the mean of the annual maxima varied significantly. It should also be noted that the KLD for RCP 4.5 is frequently greater than the KLD for RCP 8.5 for a given GCM, indicating that the distribution of annual maxima is more similar to the current climate under the scenarios with greater increases in future radiative forcing and thus more intense climate change. This finding could be due to the fact the precipitation record used to generate the current climate flow time series had several years with extremely high rainfall amounts, resulting in an AMS with a higher mean than all the GCMs. Figure 3-13 shows a boxplot of the AMS flow records for the above two CC scenarios and the current climate. The AMS of the current climate has a higher mean than both of the CC scenarios and the median of the current climate AMS is closer to the upper bound of the boxplot than the both of the CC scenarios, which indicates the distribution is right-skewed. These results indicate that the weather patterns experienced in the Clarksburg, Maryland during 2005-2020 are likely representative of the future climate.

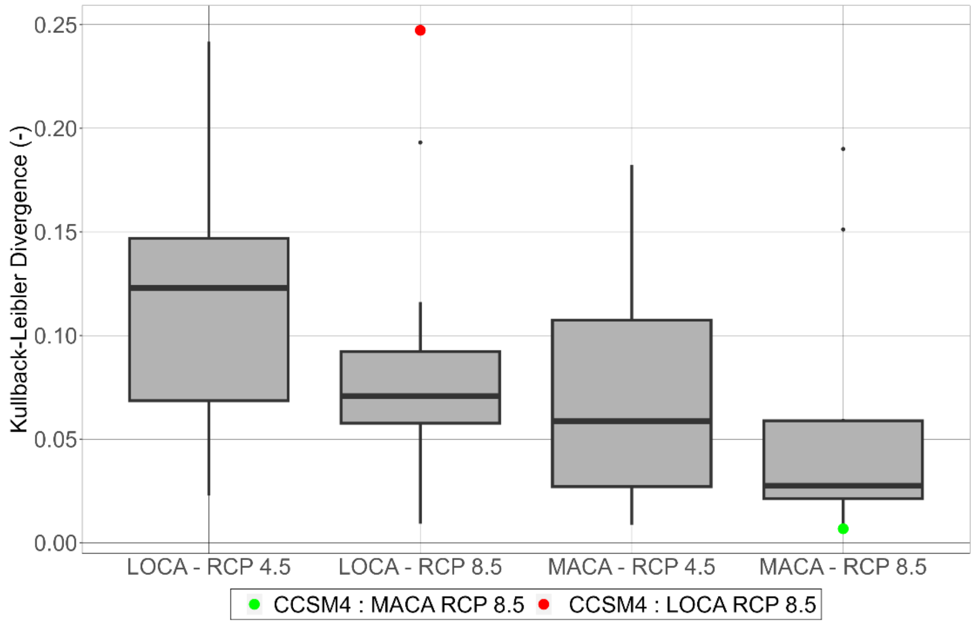

Figure 3-12. Kullback-Leibler Divergence of Flood Probability Distribution between the CC Scenarios and the Current Climate

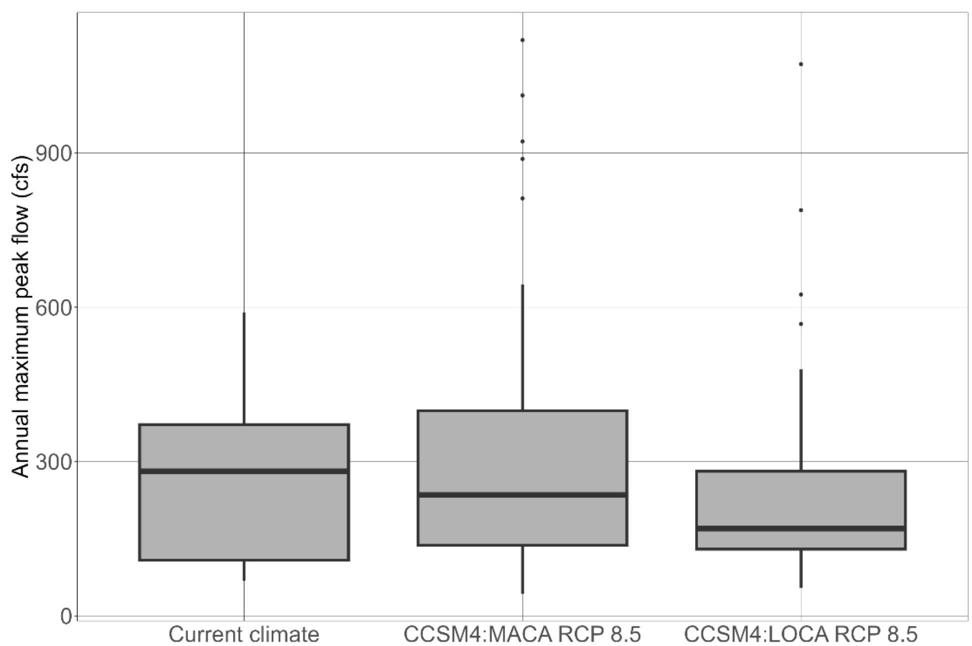

Figure 3-13. Annual Maximum Peak Flows for the Current Climate, “CCSM4: LOCA RCP 8.5" and “CCSM4: MACA RCP 8.5” Scenarios

The peaks over threshold analysis [partial duration series (PDS)] indicated a decrease in peak flows with a recurrence interval of 0.75 yr. and greater in the future (Figure 3-14). However, peak flows with a recurrence interval of less than 1 year under the current climate were within the interquartile range of the CC scenarios.

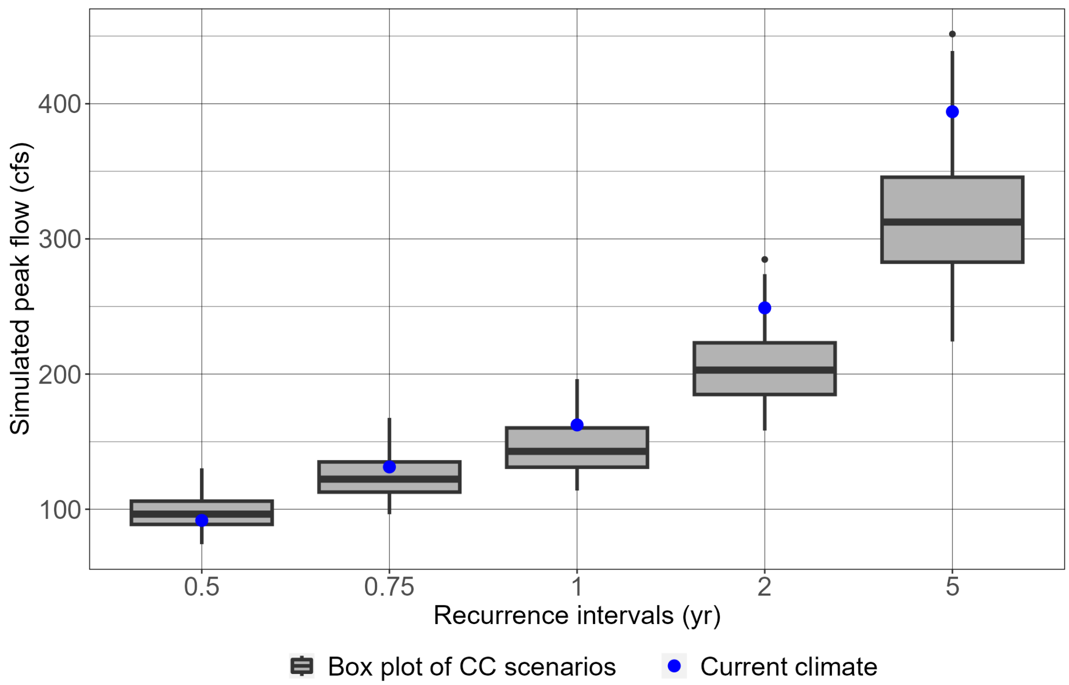

Figure 3-14. Flood Recurrence Intervals Derived from Partial Duration Series (PDS)

3.2.2 Evaluation ESD Stream Stability

The calibrated HEC-RAS model successfully captured the overall behavior and erosional characteristics of the reach for the calibration time span of 2017-2020 and reproduced the observed trends in channel geomorphology over the 16 years of available local precipitation data.

3.2.2.1 Predicted Long-term Changes in the Channel Profile

Under the current climate conditions, even with the existing ESD, which is over-designed by current Maryland stormwater standards, it is predicted that over the next 59 years the initial post-development channel degradation observed in the field along Tributary 109 will continue (Figure 3-15). The overall bed profile shows a decrease in bed slope due to a combination of channel degradation and aggradation, indicating the channel is adjusting to the increased runoff from development in the watershed, even with ESD. Due to the increased high flows following development, larger bed particles that were stable pre-development, are mobilized. Model results indicate cobbles (128-256 mm) generally become mobile at flows above 125-150 cfs, while small boulders (512-1024 mm) are entrained at flows over the range of 250-275 cfs. At RS 754 the channel narrows, causing backwater effects around RS 793, a reduction in sediment transport capacity, and deposition of coarse bed material mobilized from the upper reach. Figure 3-16b-c show that the bed coarsens at RS 793 (both d_{50} and d_{90} increase in size) due to the deposition of large clasts, creating a steep riffle at this location. Downstream of RS 793, the channel incises. In the most downstream section, the channel bed erodes to bedrock (estimated as 3 ft. below the initial channel invert elevation, Figure 3-16b), and a knickpoint forms between RS 388 and RS 428. It is anticipated that the channel would continue to degrade as this knickpoint migrates upstream over time. Similar channel dynamics were predicted both with and without sediment exhaustion at discharges greater than 319 cfs.

To better illustrate the sediment transport dynamics, the model results shown in Figure 3-16 are zoomed in for 1 year between the 6th and 7th year of the simulation period (Figure 3-17). During the two high flow events, the bed is scoured during the rising limb of the hydrograph at river stations 484, 1144, and 1566 as fine sediment is removed from the bed, leading to an increase in d_{50} and d_{90}. At river stations where aggradation is occurring (e.g., RS 793), the increased flow and erosion of the upstream bed, increases the bed elevation and decreases the bed particle size distribution at those locations. This graph illustrates the dynamic nature of sediment transport and channel morphology in stream channels.

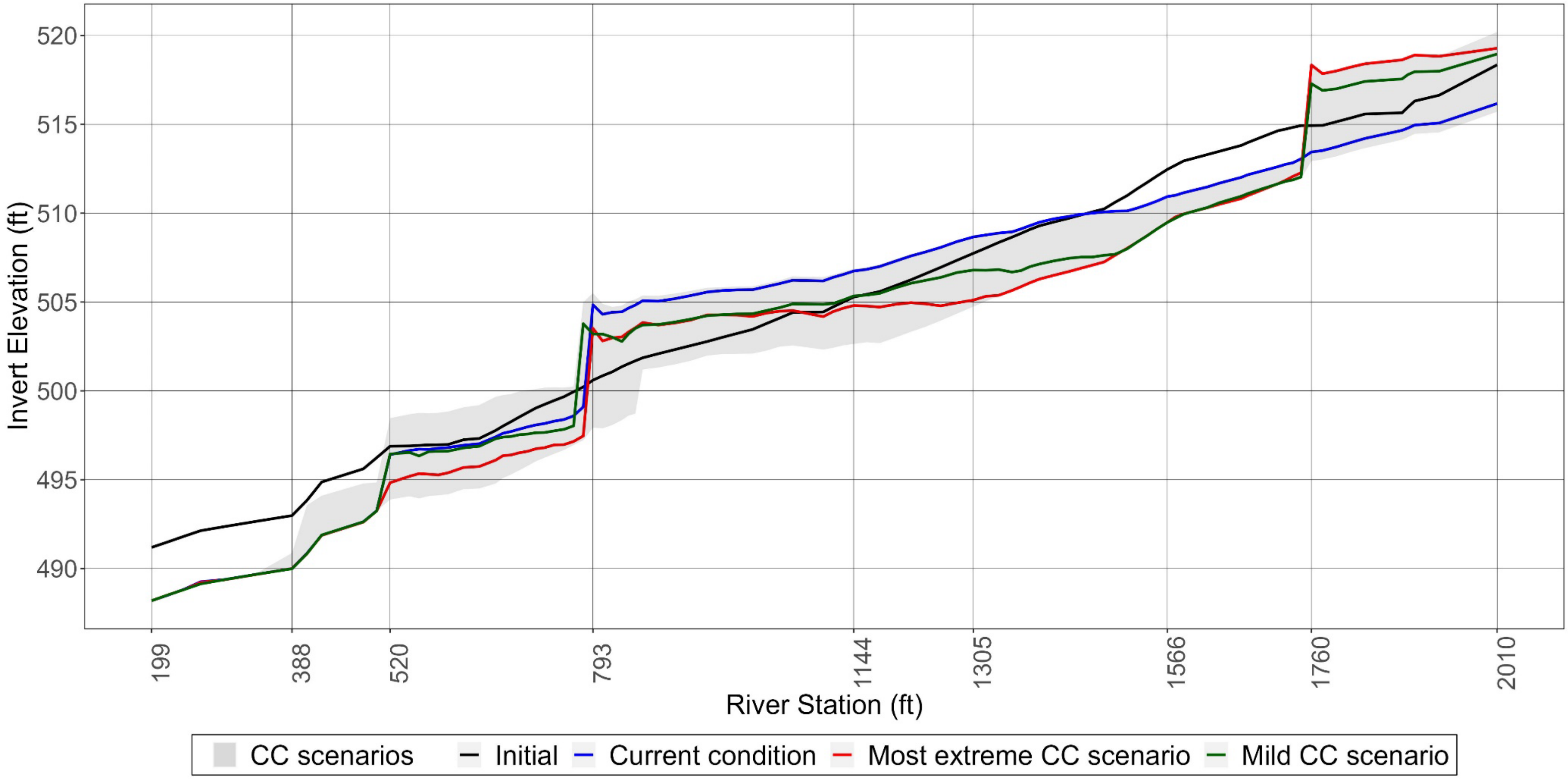

Figure 3-15. Predicted Channel Longitudinal Profile for the Current Climate, Most Extreme Climate Change (CC) Scenario (CSIRO-Mk3-6-0 MACA RCP 4.5), Mild CC Scenario (MRI-CGCM3 MACA RCP 4.5), and all CC Scenarios (shown as a grey band) without Sediment Exhaustion

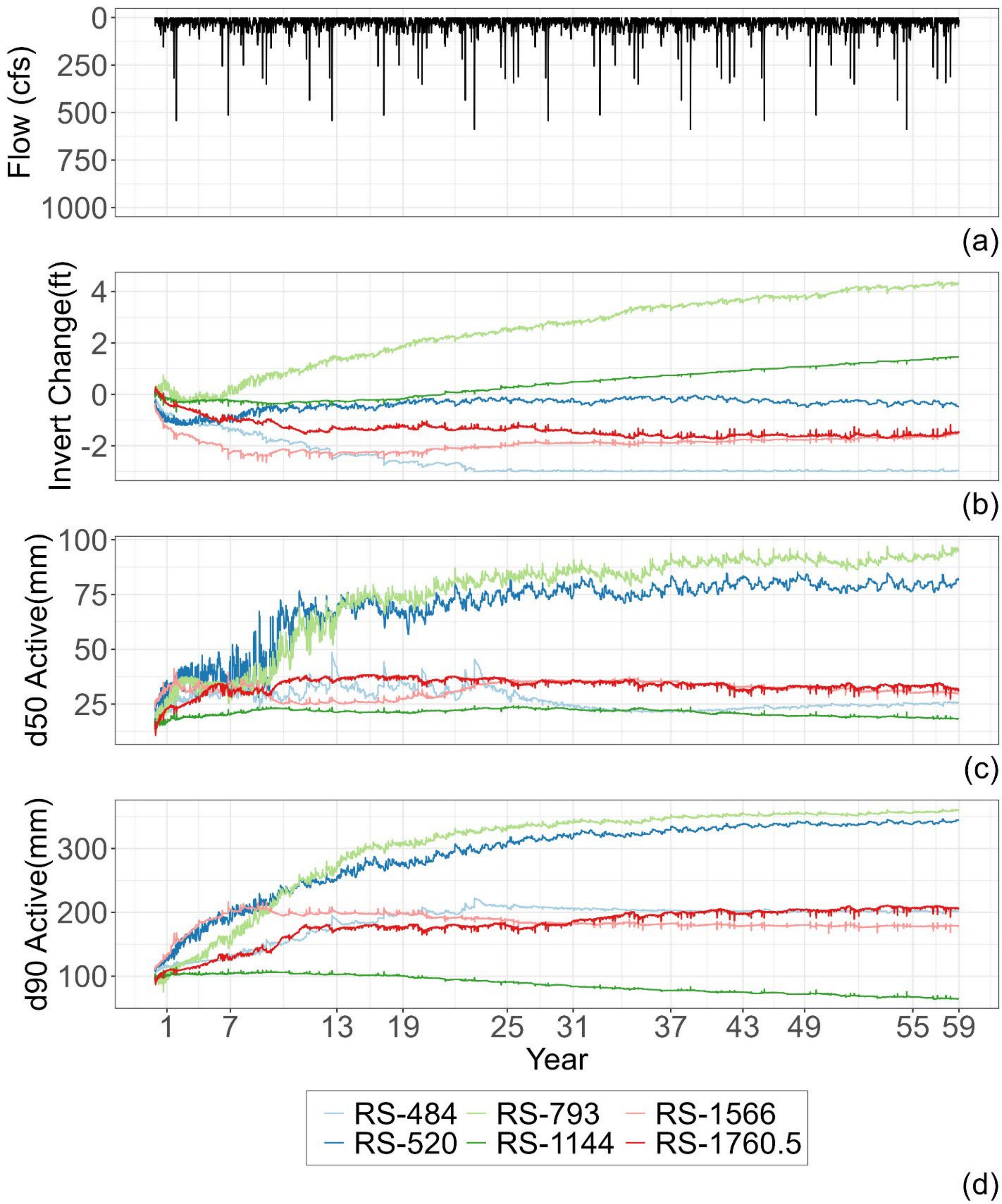

Figure 3-16. Simulated Time Series of a) Flow; b) Channel Invert Elevation Change; c) Bed Material d_{50}; and, d) Bed Material d_{90} for the Current Climate over 59 Years

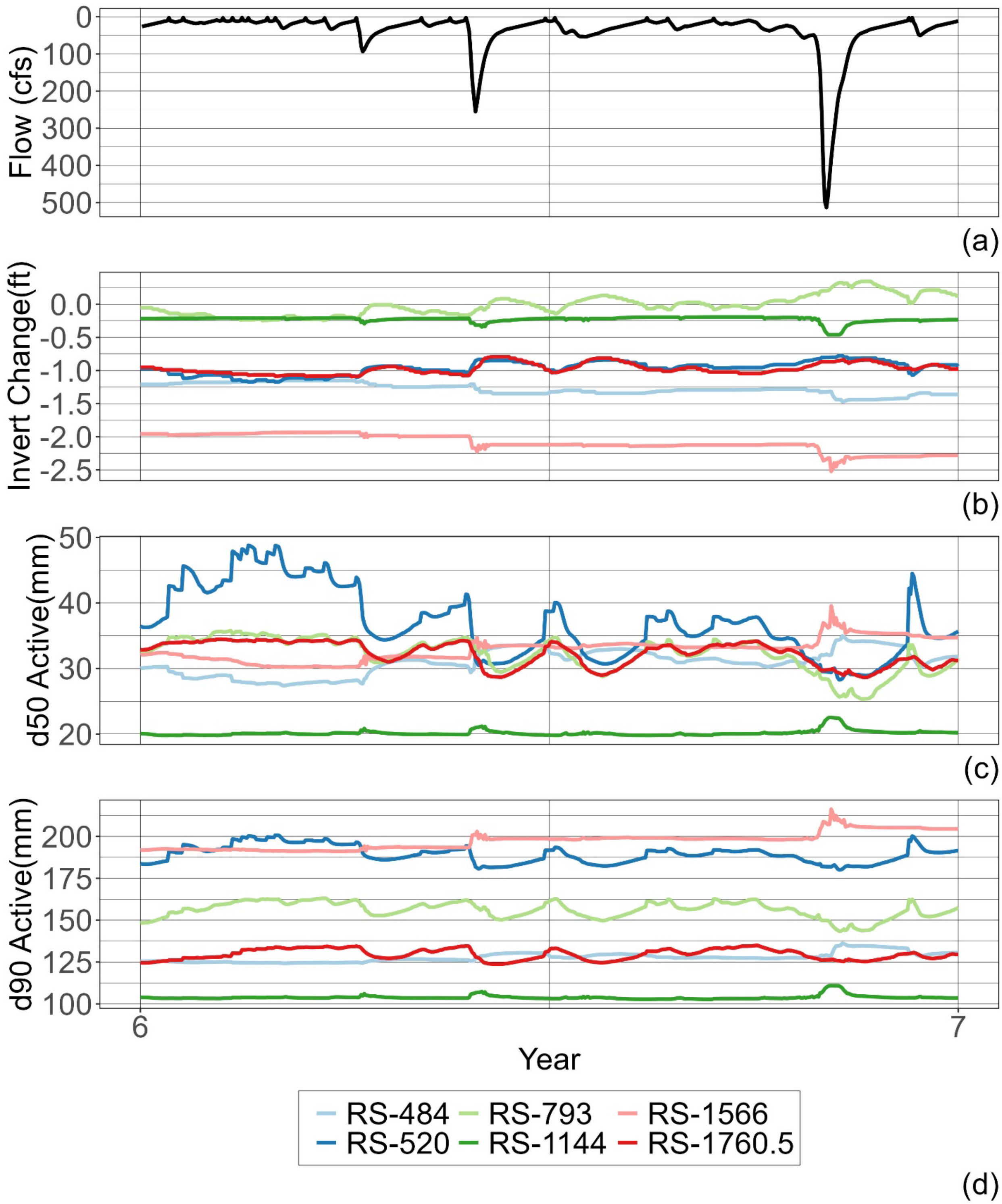

Figure 3-17. Simulated Time Series of a) Flow; b) Channel Invert Elevation Change; c) Bed Material d_{50}; and, d) Bed Material d_{90} for the Current Climate between the 6th and 7th Year

Model results indicate that climate change will accelerate the long-term channel adjustments predicted under the current climate. Figure 3-15 shows the range of channel bed profiles for the 128 CC scenarios (gray shaded region), with the two CC scenarios (CSIRO-Mk3-6-0 MACA RCP 4.5 and MRI-CGCM3 MACA RCP 4.5) having the most and least total rainfall illustrated (truncated data series). Considering the projected climate changes, it is anticipated that the magnitude of the largest 5% of peak flows will increase in the future (Figure 3-10), as compared to the current climate. Consequently, the current cobble and boulder particles found in the channel bed, which are typically mobile within the flow range of 150 and 250 cfs, respectively, are expected to become mobilized and redeposited in areas of reduced bed shear stress. This process gives rise to the formation of steep riffles in the channel, altering the channel morphology in response to the changing hydrological conditions. As demonstrated in Figure 3-15a, the most extreme CC scenario exhibited a notable pattern wherein multiple consecutive storm events with peak flows exceeding 250 cfs occurred during years 11 and 21. These flows led to a discernible coarsening of the channel bed, as evidenced by the increase in bed material d_{90} (Figure 3 15d), specifically observed at two riffle locations (RS 793 and RS 1760). Furthermore, the mild CC scenario (Figure 3-17a), although featuring lower flows compared to the current climate (Figure 3-16a), exhibited a similar trend. Between year 21 and 31, multiple storm events with peak flows exceeding 250 cfs occurred, leading to a comparable pattern of bed coarsening at the same two riffle locations (Figure 3-19d). Upstream of these riffles, aggradation is expected to occur, with channel incision occurring downstream. While the exact predicted channel profile depends on the range and sequence of flows for each scenario, the channel is expected to exhibit regions of bed degradation and aggradation as the channel slope decreases in response to the changing hydrology. As with long-term predictions of channel response to watershed development under the current climate, it is anticipated that the channel will ultimately erode to bedrock, which was estimated as 3 ft. below the initial channel invert elevation, based on the USGS map of bedrock elevations for Montgomery County, MD (Froelich 1975).

The impact of sediment supply on channel stability is illustrated in Figure 3-20 for the CanESM2 - LOCA RCP 4.5 climate scenario. With a continued increase in sediment supply with increasing discharge, it is predicted that two riffles will form (RS 832 and 1760), but a knickpoint will develop at RS 520, similar to the predicted channel change under the current climate. Channel incision occurs downstream of RS 520 and in the section between RS 1300 and RS 1750. If sediment supplies are limited and do not increase significantly with higher discharges, channel degradation is more widespread, with additional bed incision occurring in the middle section of the reach. The coarse material mobilized from the bed deposits further downstream at RS 520 instead of RS 832. This example shows that, regardless of the upstream sediment supply, over time, the channel will continue to erode. As shown in Figure 3-21b for the higher sediment load, the channel bed elevation and d_{50}at RS 520 increase up to approximately year 20. After year 21 and 31, the channel bed elevation and d_{50} decrease, respectively, suggesting the knickpoint at this location is migrating upstream.

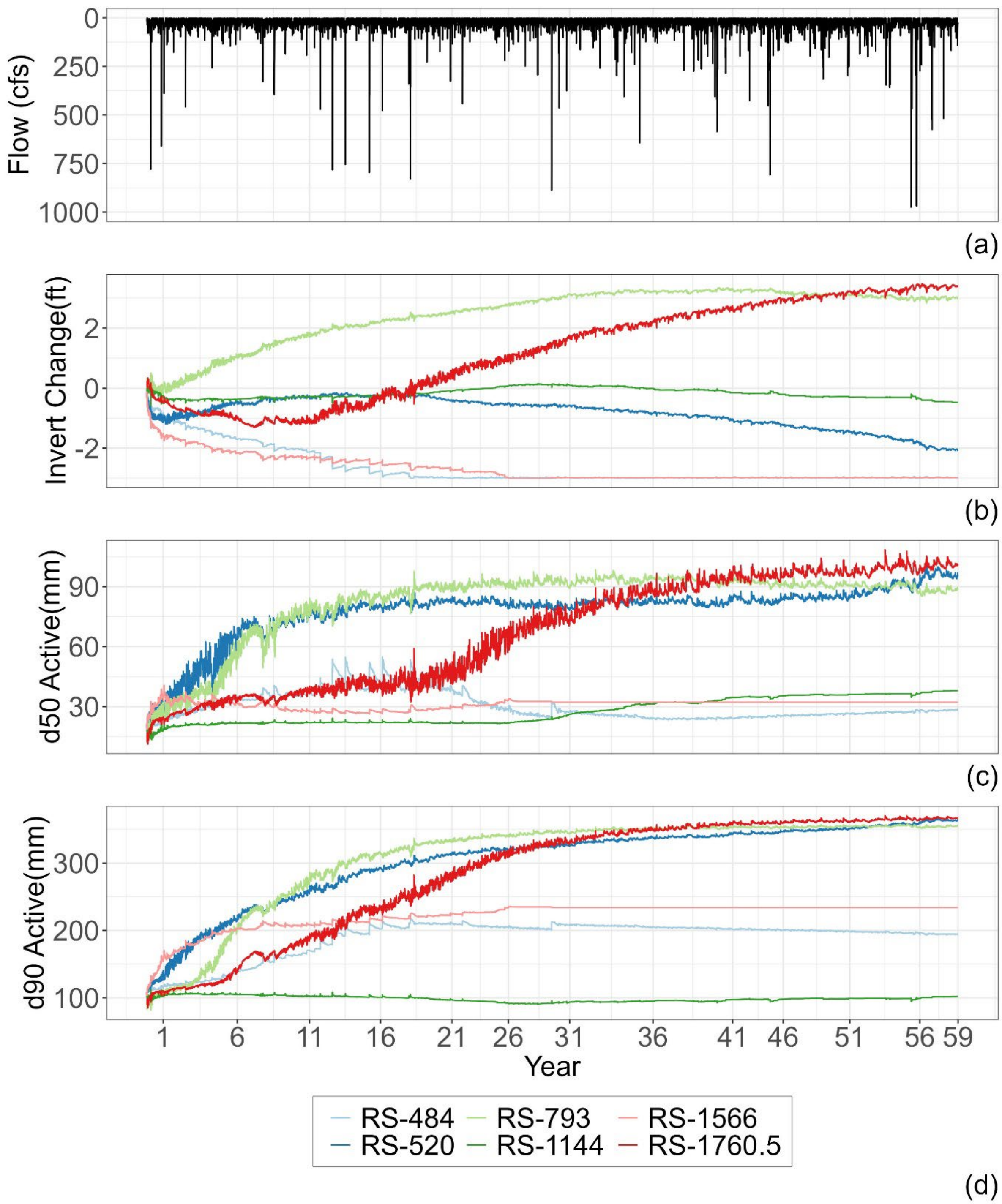

Figure 3-18. Time Series of a) Flow; b) Channel Invert Elevation Change; c) Bed Material d_{50}; and d) Bed Material d_{90} for the Most Extreme CC Scenario (CSIRO-Mk3-6-0 MACA RCP 4.5) without Sediment Exhaustion

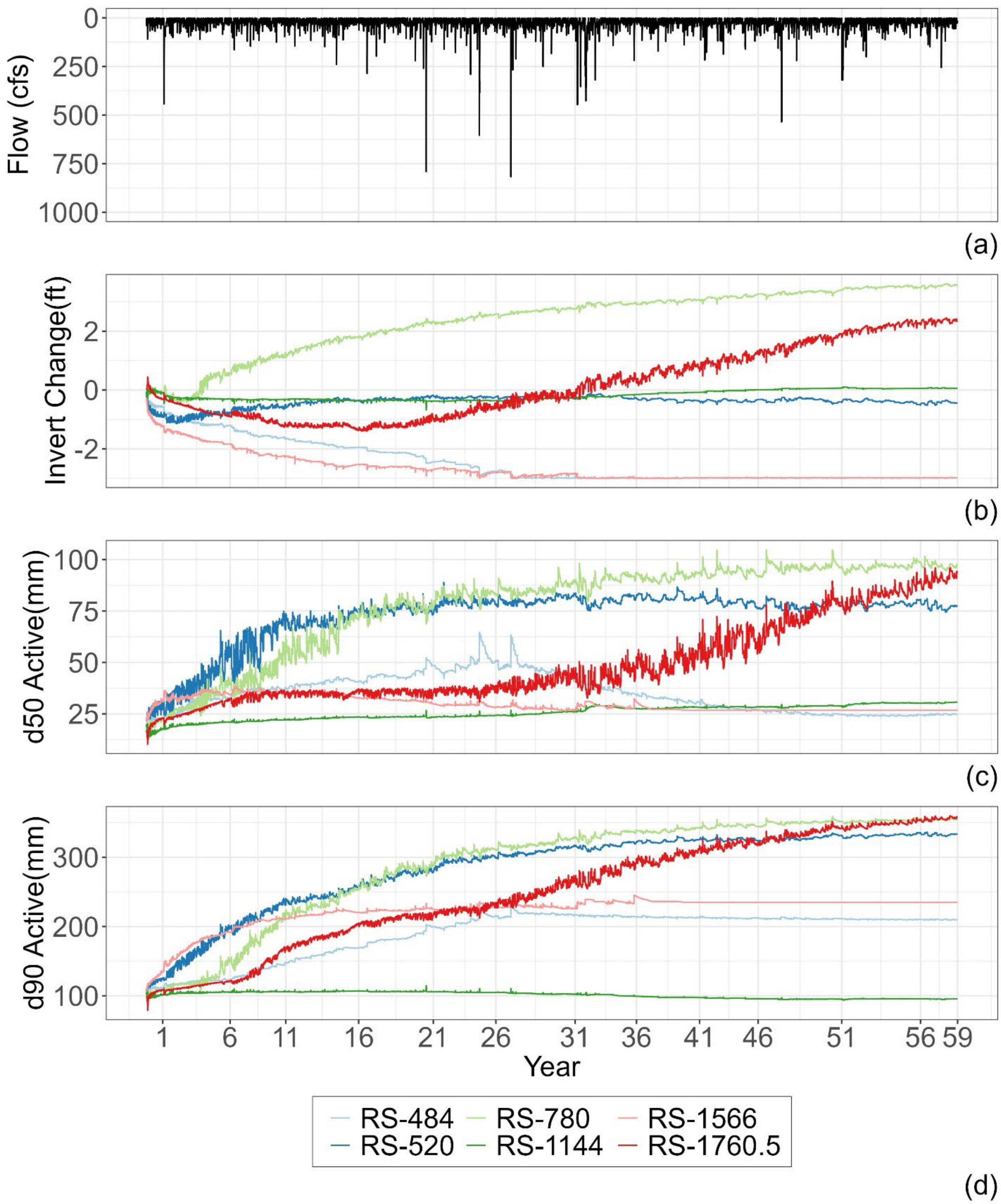

Figure 3-19. Time Series of a) Flow; b) Channel Invert Elevation Change; c) Bed Material d_{50}; and d) Bed Material d_{90} for the Mild CC Scenario (MRI-CGCM3 MACA RCP 4.5) without Sediment Exhaustion

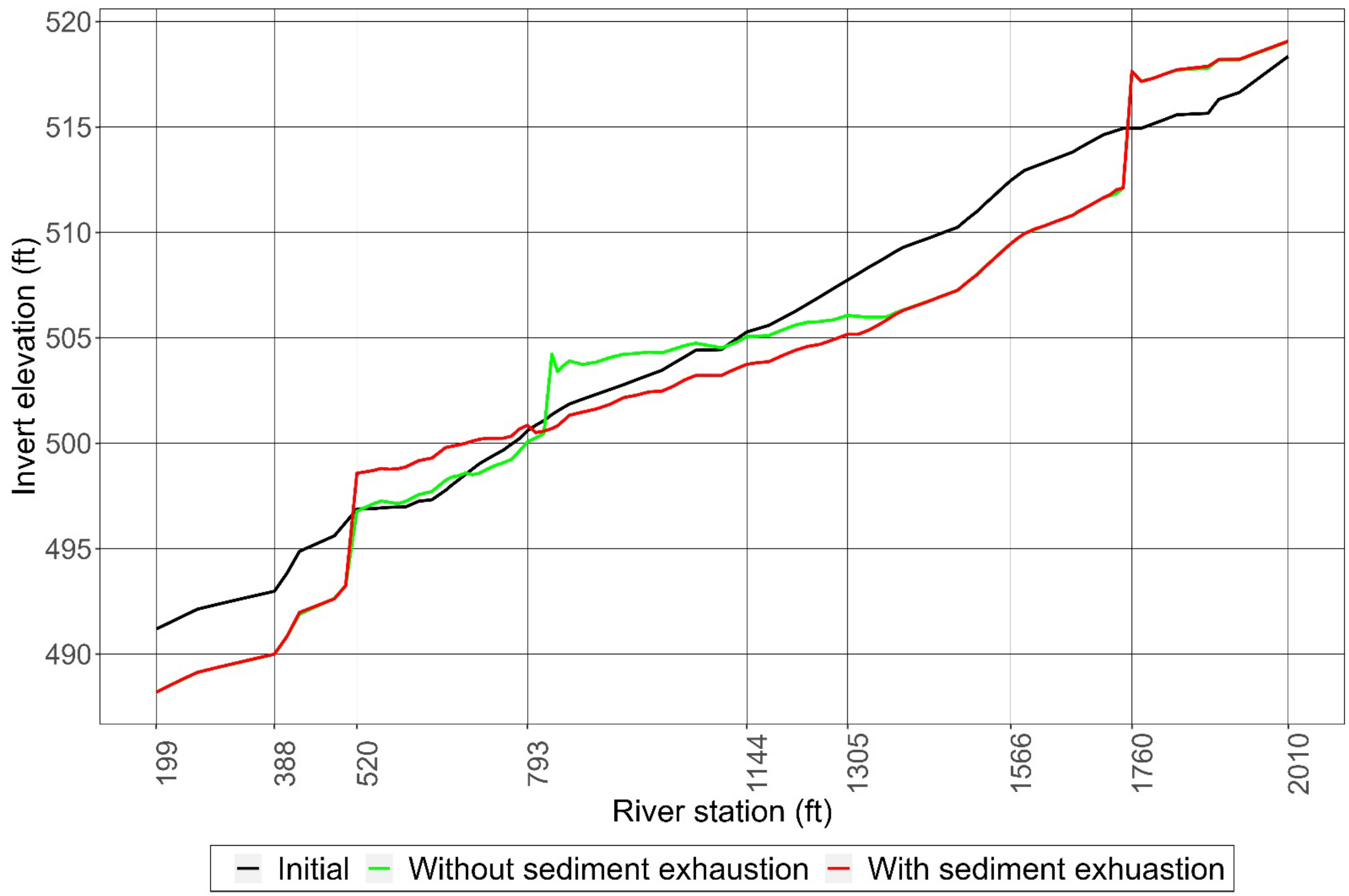

Figure 3-20. Channel Longitudinal Profile for CanESM2 - LOCA RCP 4.5 Climate Change Scenario with and without Sediment Exhaustion.

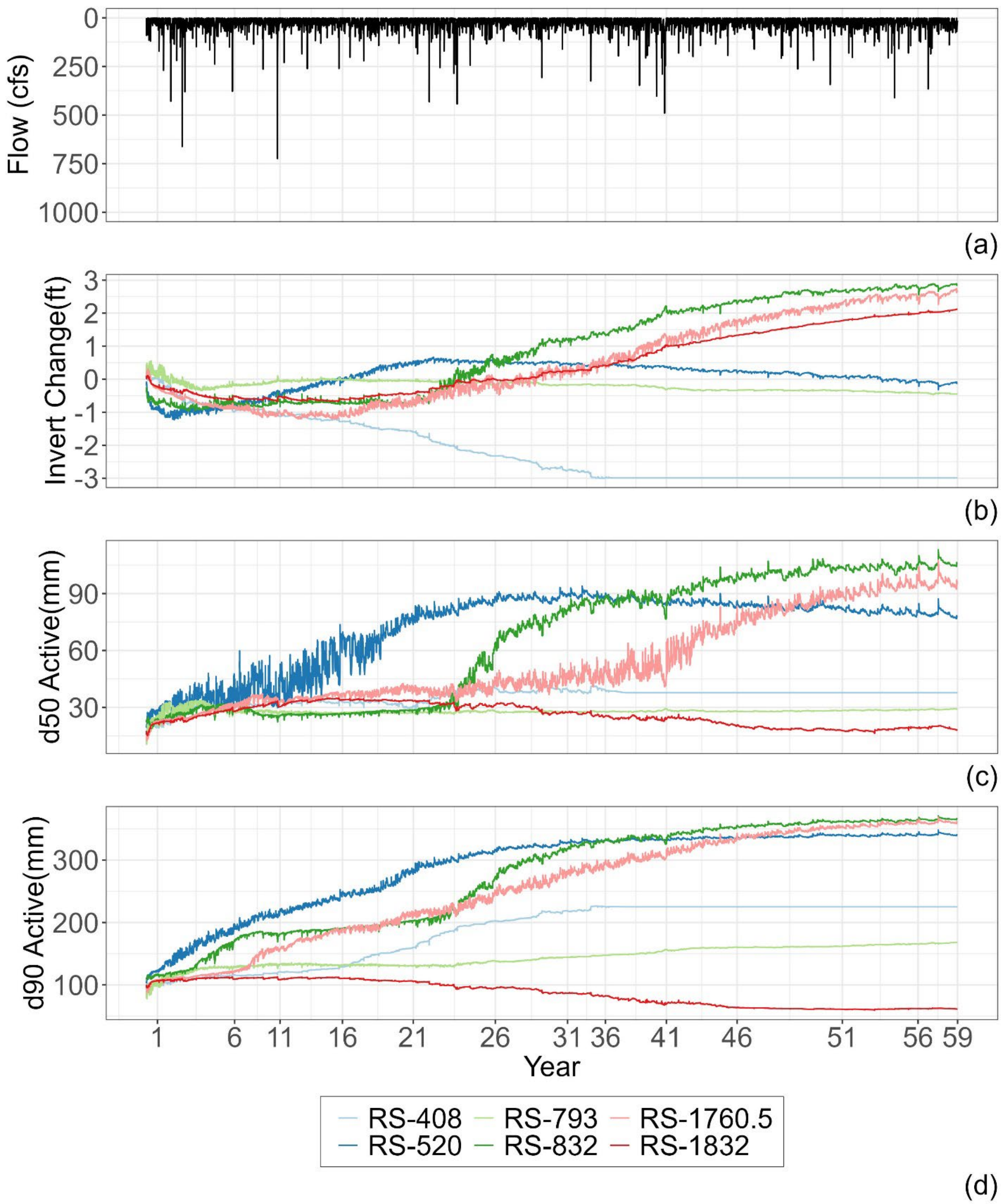

Figure 3-21. Time Deries of a) Flow; b) Channel Invert Elevation Change; c) Bed Material d_{50}; and d) Bed Material d_{90} for CanESM2 - LOCA RCP 4.5 Climate Change Scenario without Sediment Exhaustion

3.2.2.2 Impact of Climate Change on Sediment Transport Dynamics

Channel stability occurs when the incoming sediment load and the sediment transport through the reach are generally balanced or when the channel is resistant to erosion. The incoming sediment load is set by the sediment load rating curve (Figure 3-4) and is a function of the number and magnitude of flood events. As such, the incoming sediment load for each climate scenario varied, depending on the distribution of precipitation and the resulting stream discharge.

The flow volume, total incoming sediment load, and total sediment yield for four distinct flow ranges observed in the current climate, along with the most extreme and mild climate change (CC) scenarios and the bcc-csm1-1-m MACA RCP 8.5 scenario are presented in Figure 3-22. While the greatest volume of flow volume into the reach occurs at discharges less than 40 cfs, the majority of sediment transport into and through the reach occurs during smaller floods, in the range of 40-319 cfs. The range of flows for each scenario has significant impacts on sediment delivery and transport. For example, despite the total flow volume in the current climate exceeding that of the truncated bcc-csm1-1-m MACA RCP 8.5 scenario, the proportion of flow volumes within the discharge range of 319 – 600 cfs is higher, resulting in a greater incoming sediment load for this specific climate scenario compared to the current climate. Additionally, while the mild CC scenario exhibits significantly lower flow volume and incoming sediment load in comparison to the current climate, it is important to note that a portion of flow volumes within the more extreme discharge range of 600 – 1300 cfs occurs, leading to a proportionately higher sediment yield. Even though there is a noticeable difference in incoming sediment load across the different CC scenarios compared with the current climate, the total sediment yield is similar, indicating that even though the channel bed is degrading in some sections, the overall reach is transport-limited, resulting in net sediment deposition within the reach.

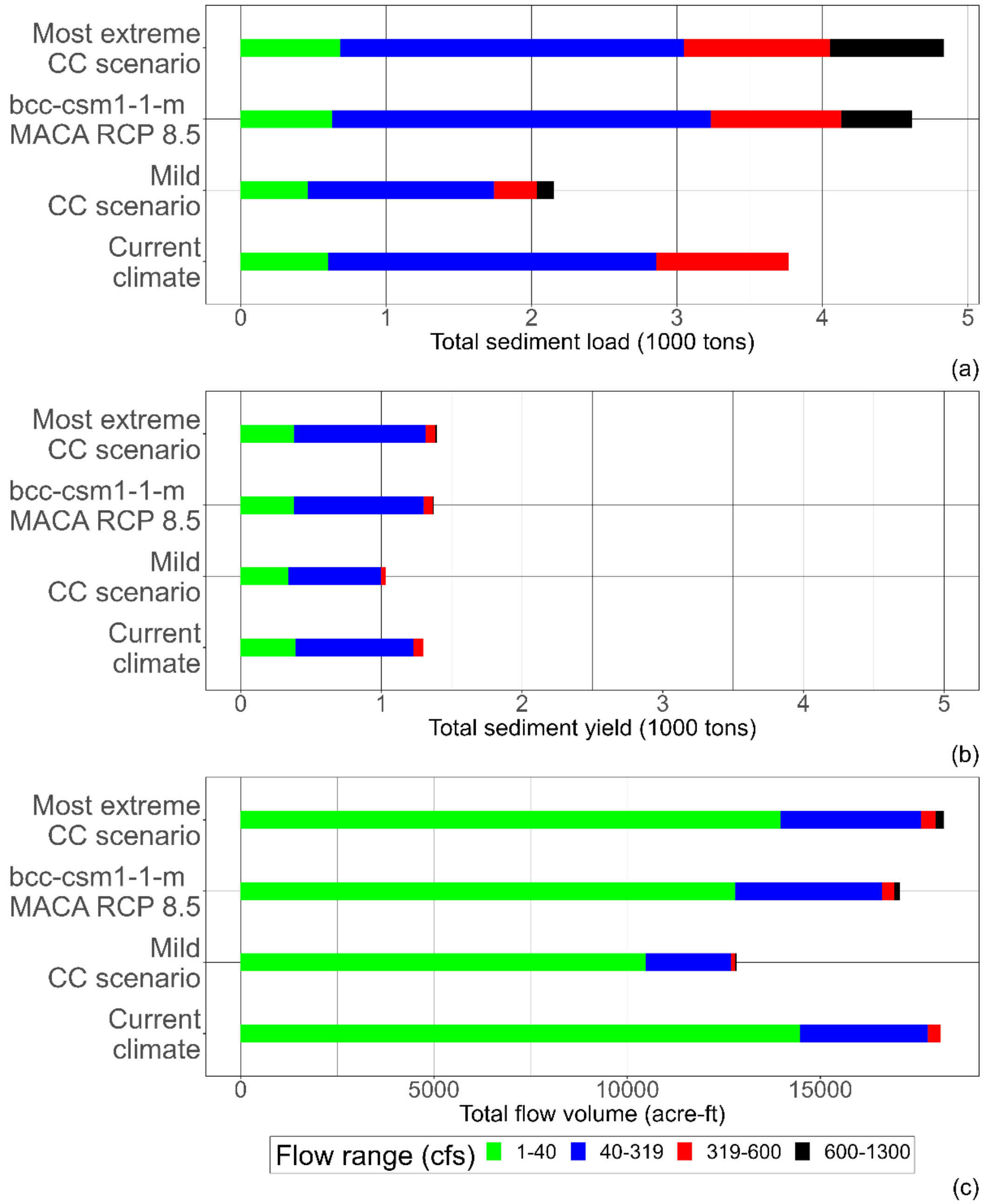

Figure 3-22. Incoming Sediment Load (a), Outgoing Sediment Yield (b) and Flow Volume (c) as a Function of Stream Discharge Class for the Current Climate, the Most Extreme and Mild Climate Change (CC) Scenarios, and the bcc-csm1-1-m MACA RCP 8.5 Scenario

In general, the CC scenarios with the LOCA downscaling had lower incoming sediment loads than the current climate and those CC scenarios with the MACA downscaling (Figure 3-23). This decrease in incoming sediment load for the LOCA scenarios is due to the difference in the distribution of flows and the sediment load associated with different stream discharges, based on the calibrated sediment rating curve (Figure 3-4). As expected, the scenarios that assumed the coarse sediment supply from the watershed decreased with increasing flow magnitude (sediment “starved”) had lower incoming sediment loads than scenarios that assumed the supply of coarse bed sediment continued to increase with increasing discharge. The sediment transport potential of the stream reach is a function of the distribution of flood flows, but also the channel bed slope, changes in channel cross-section, roughness, and bed material size. The coarse riffles that form in the channel decrease the bed slope locally, causing aggradation upstream of the riffles. Under both the current and projected climate, the channel is net aggregational. As seen in Figure 3-23b, all of the CC scenarios had higher sediment yields than expected under the current climate, indicating an increase in sediment transport due to the predicted increase in peak flows of storm events with low percent exceedance. Because the incoming sediment loads were lower for the LOCA CC scenarios, but the sediment yield was similar, less channel aggradation occurred for the LOCA scenarios, as compared to the current climate and the CC scenarios with MACA downscaling.

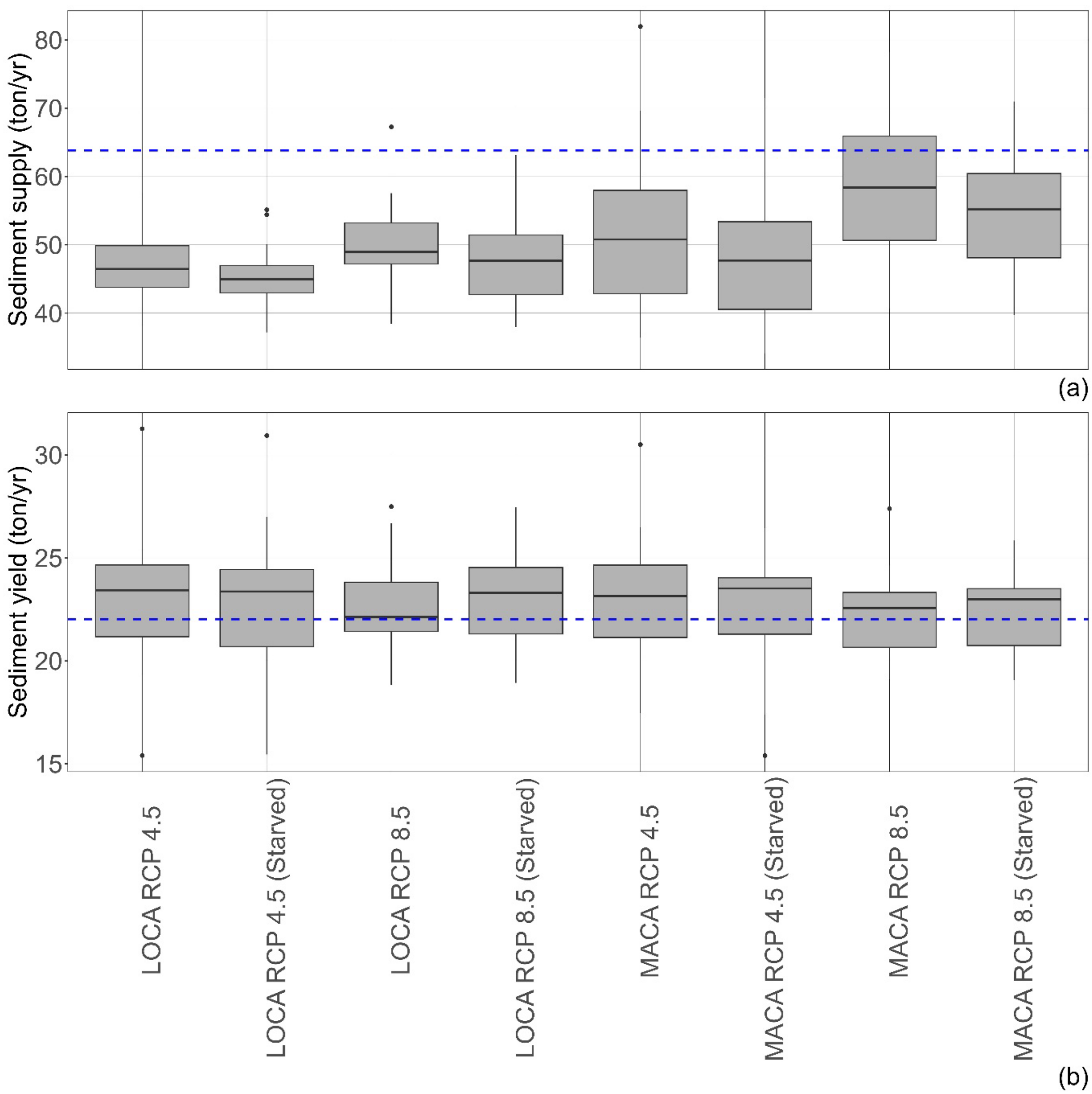

Figure 3-23. Annual Incoming Sediment Supply and Reach Sediment Yield as a Function of Climate Downscaling Technique and Sediment Exhaustion

Note: Blue dashed line represents the sediment supply and reach sediment yield under current climate.

3.2.2.3 Climate Change Impacts on Channel Dimensions

Three indices of channel cross-section change were evaluated, including change in the bed invert elevation, change in the cross-sectional area, and change in the width:depth ratio, evaluated at each cross-section (not including interpolated cross-sections). A positive value of the difference in the median bed invert elevation change indicates the central tendency of the channel is to degrade more due to climate change, as compared to the current climate. Although the channel is predicted to experience areas of degradation and aggradation under the current climate, model results indicated that the median amount of channel incision (negative change in invert elevation) will increase by 0 – 1.5 ft due to climate change (Figure 3-24). If watershed development also reduced coarse sediment loads to the channel (sediment-starved scenarios), channel incision will be exacerbated, as indicated by comparing sediment supply to the reach with sediment yields from the reach in Figure 3-24.

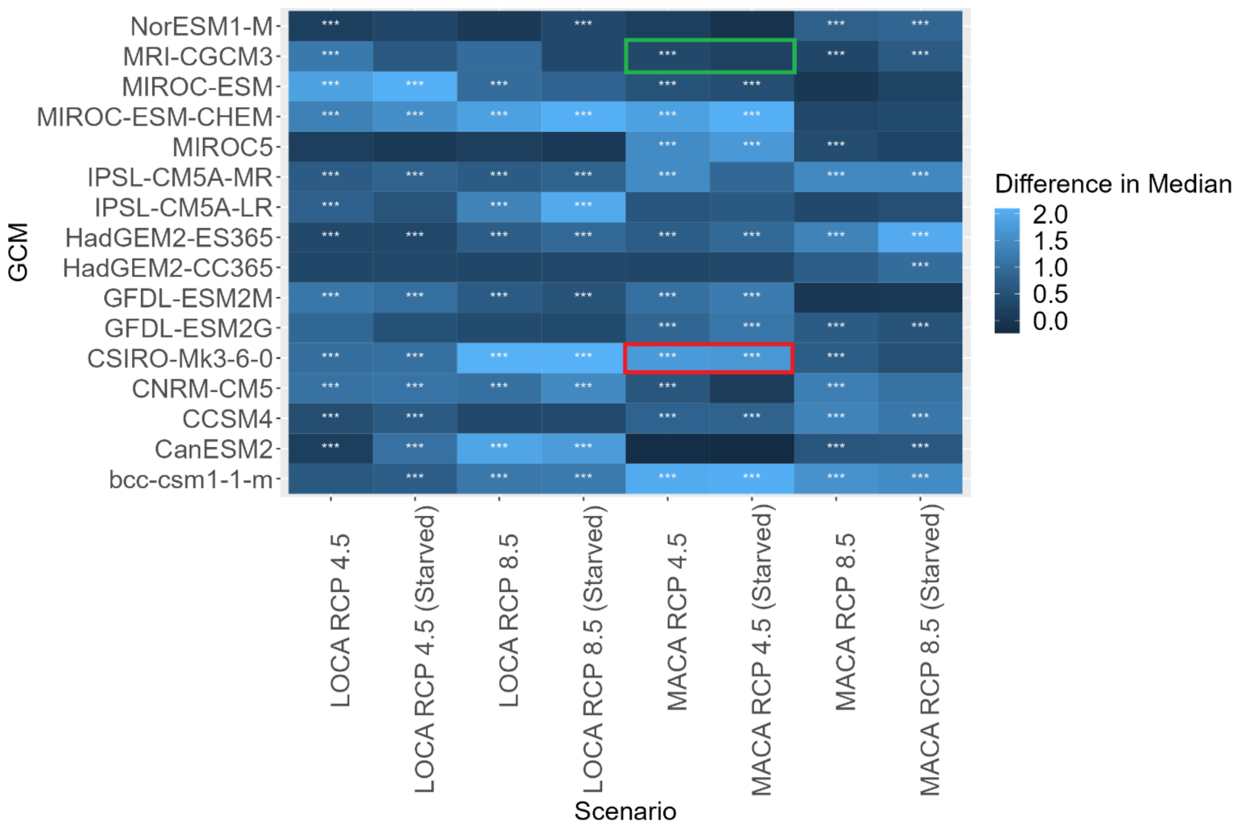

Figure 3-24. Difference in Median Bed Invert Elevation Change (ft) between the Current Climate and Each Climate Change Scenario

Note: A positive value of the difference indicates the central tendency of the channel is to degrade more due to climate change. The most extreme and mild CC scenarios are indicated by red and green boxes, respectively. Significant differences ($\alpha = 0.05$) are indicated by ***.

Another measure of channel change is the change in cross-sectional area. Model predictions indicate that the median difference in the change in cross-sectional area could be as much as 30 ft.^{2} when comparing the impact of development under the current climate versus the future climate (Figure 3-25).

Given the representation of channel dynamics in HEC-RAS, channel erosion first occurs as incision or lowering of the channel bed. Once a resistant layer is reached, such as bedrock, the channel will start to widen. Most of the CC scenarios predict a median difference in cross-sectional area change over 59 years of less than 20 ft^2. Almost 50% of the differences are statistically significant, indicating that future changes in channel dimensions will not be similar to changes that would be expected if the climate remained stationary. However, actual channel degradation under the future climate may be more extensive than predicted in this study since the current conditions period was unusually wet.

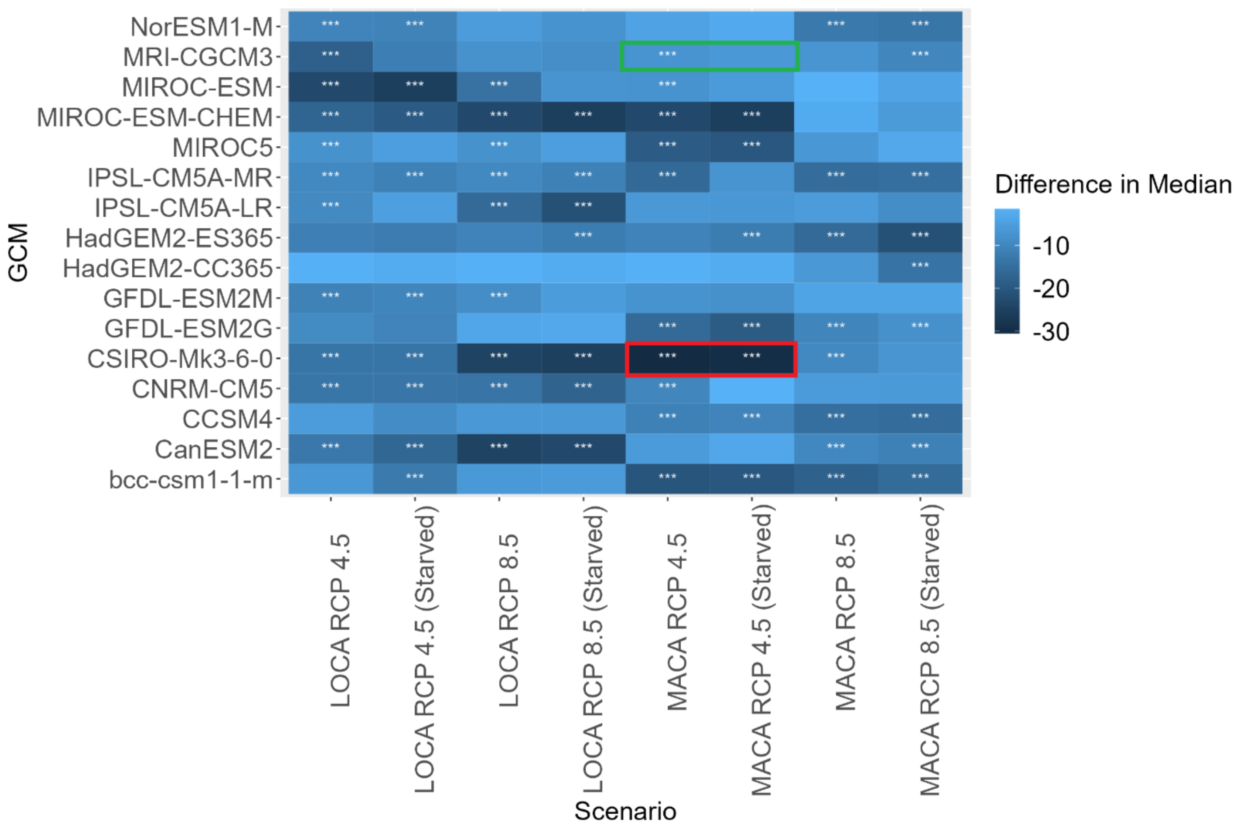

Figure 3-25. Difference in Median Cross-section Area Change (ft^2) between the Current Climate and Each Climate Change Scenario over 59 years

Note: Negative values indicate the median additional increase in channel cross section due to each climate change scenario. The most extreme and mild CC scenarios are indicated by red and green boxes, respectively. Significant differences (α = 0.05) are indicated by ***.

The width:depth ratio (W:D) of a cross-section indicates how incised the channel is. Since the 1-D HEC-RAS model erodes the channel bed until a resistant layer is encountered, simulated channel change is primarily in the vertical direction. As such, the W:D will decrease as the channel incises. A median positive difference between the current and climate change scenarios indicates that the channel will degrade more as a result of climate change. Median predicted decreases in the W:D due to climate change range from 0.5 to over 1.5 (Figure 3-26); however, fewer than 25% of the CC models produced statistically significant differences over the channel impacts predicted under the current climate.

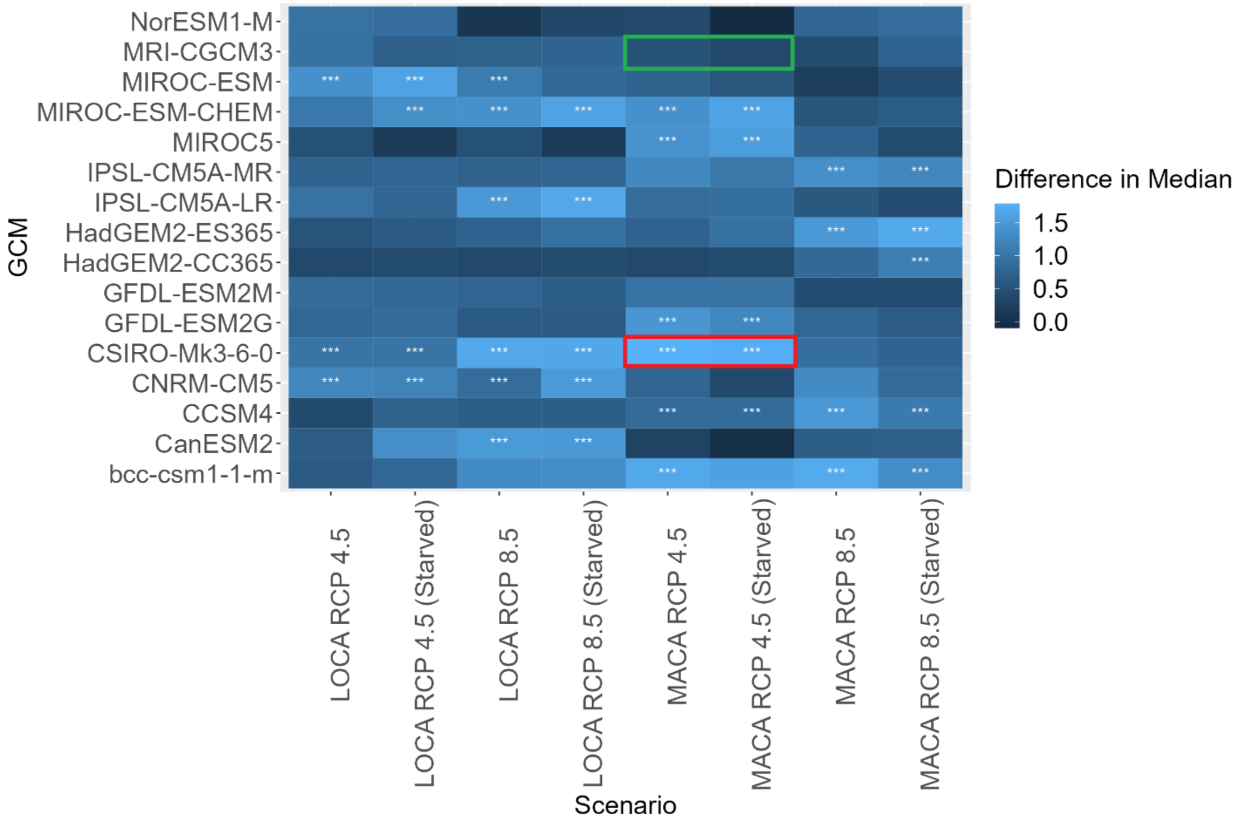

Figure 3-26. Difference in Median Width to Depth Ratio Change between the Current Climate and Each Climate Change Scenario

Note: The most extreme and mild CC scenarios are indicated by red and green boxes, respectively. Significant differences ($\alpha = 0.05$) are indicated by ***.

3.2.3 Stormwater Management Changes to Achieve Channel Stability

3.2.3.1 Performance of Retrofit ESD Scenarios under Design Storms

Despite the widespread implementation of SCMs, the cumulative mass of sediment transported (Q_s) in Tributary 109 was almost double that of the pre-development condition for the 1-yr and 2-yr design storms (Table 3-4). This increased sediment transport is the driving force behind the observed and simulated channel degradation in Tributary 109. To reduce the impact of urban development on channel stability, the existing sediment transport within the receiving stream must be maintained.

Two different methods of designing stormwater management systems that consider sediment transport in the receiving stream were implemented in the Tributary 109 SWMM model and the effect of each method on long-term stream discharge and sediment transport was simulated in HEC-RAS for both the current and predicted future climate. Figure 3-27 presents four simulated hydrographs representing the pre-development, ESD, Erosion Potential, and Shear Stress scenarios for a 1-yr design storm. Although all existing dry ponds were designed to capture and retain the 1-yr design storm runoff for 24 hours, the current implementation of ESD does not replicate pre-development peak flow rates. Maintenance of pre-development peak discharges is required only for some localities; therefore, designs based on simply on retaining the 1-yr design storm runoff volume may not address changes in runoff hydrograph timing or the impacts of runoff from multiple subwatersheds on peak flows at the watershed outlet. This finding illustrates the need for continuous modeling of watersheds in which development takes place. A recent study that compared event-based streamflow metrics using an instantaneous discharge from the study watershed with a nearby forested watershed also pointed out the failure of the ESD to maintain predevelopment hydrology (Hopkins et al. 2020). The Erosion Potential scenario resulted in a much lower 1-yr design storm peak flow than the predevelopment scenario, but the volume and duration of lower flows (hydrograph recession) were significantly increased due to the controlled release of flows from the new and retrofit ponds which decreased the sediment transport below the pre-development scenario (Table 3-4). Because urban development ultimately increases the amount of runoff, to maintain the pre-development mass of sediment transported by the stream, the post-development hydrograph must have lower peak flows and higher baseflows than the pre-development watershed.

The erosional hour (E_h) and effective work (E_w) for the Predeveloped, ESD, and Shear Stress scenarios are also presented in Table 3-4. The magnitude and duration of shear stress exceedance for the pre-development condition is zero for 1- and 2-yr. storm events, which indicates bed particles equal to or larger than the d_{50} are not transported during those events. The Shear Stress scenario resulted in a 1-yr., 24-hr. design storm peak flow close to the pre-development scenario, but the volume and duration of lower flows (hydrograph recession) are greater due to the controlled release of flows from the retrofitted ponds.

3.2.3.2 Evaluation of Retrofit ESD Scenarios

Under the current climate conditions, it is predicted that channel degradation will be significantly reduced over the next 59 years if the existing SCMs are retrofitted as per the two proposed design scenarios, particularly in the middle and lower sections of the reach (Figure 3-28). The Erosion Potential method is more effective in preventing the mobilization of coarse bed materials, as indicated by the reduced number of boulders and cobbles at RS 793, as compared to ESD and the Shear Stress method (Figure 3-29). This improvement can be attributed to a reduction in peak runoff during storm events due to the addition of an in-line pond just upstream of Snowden Farm Parkway. It is important to note that no additional storage-based SCMs were incorporated in the Shear Stress scenario; however, this scenario was not as effective at maintaining the pre-development bed elevations as the Erosion Potential method.

Table 3-4. Values of Erosion Potential (E_p), Erosional Hour (E_h) and Effective Work (E_w) for Different Stormwater Management Scenarios

Storm type	Pre-development			ESD				Erosion Potential		Shear Stress		
	Q_s (tons)	E_h (hr.)	E_w (lb./ ft^2)	Q_s (tons)	E_p	E_h (hr.)	E_w (lb./ft^2)	Q_s (tons)	E_p	Qs (tons	E_h (hr.)	E_w (lb./ft^2)
1-yr., 24-hr.	1.99	0.00	0.00	4.25	2.13	0.42	0.04	1.84	0.92	2.01	0.00	0.00
2-yr., 24-hr.	3.61	0.00	0	6.90	1.91	1.08	1.20	3.47	0.96	3.93	0.00	0.00
5-yr., 24-hr.	8.65	1.75	2.65	11.89	1.38	1.50	5.63	6.22	0.72	9.12	0.42	0.28

Note: ESD= environmental site design. Q_s = total mass of sediment transported per storm event.

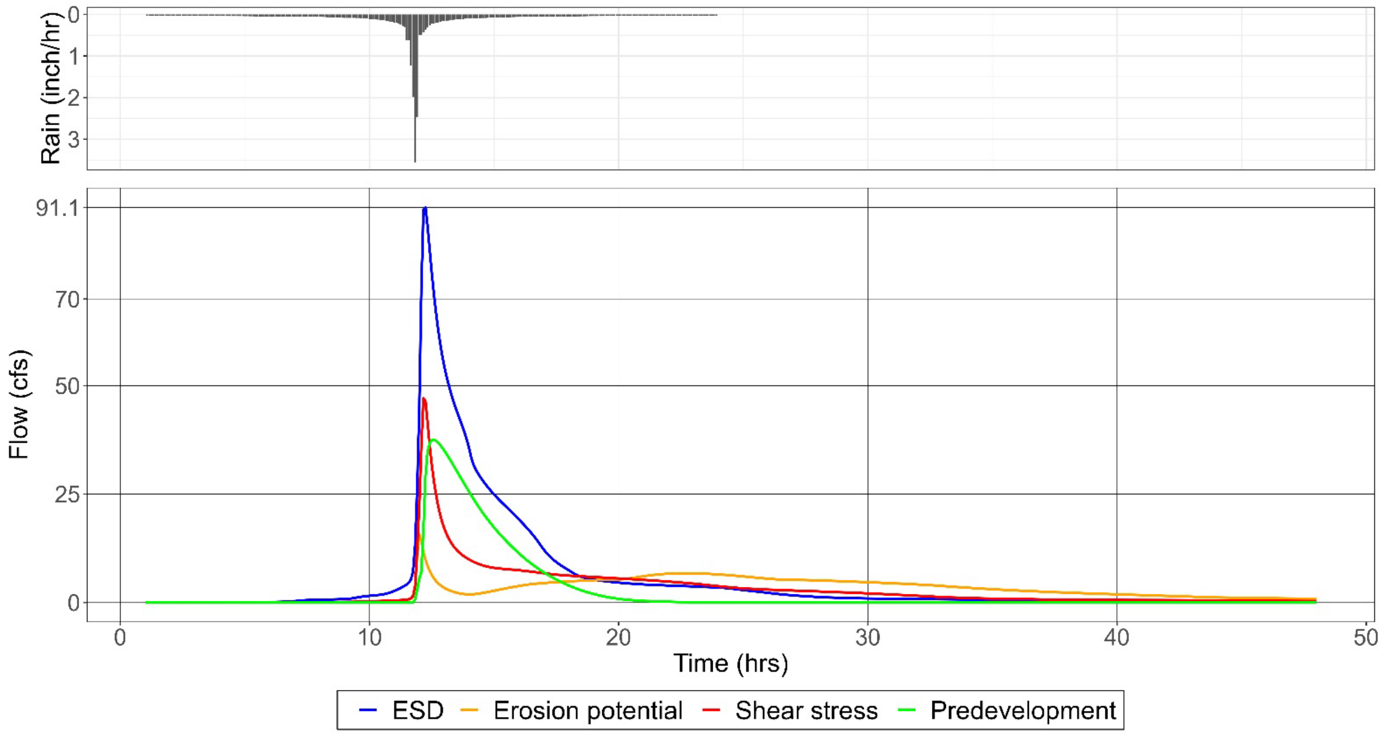

Figure 3-27. Simulated Hydrographs for 1-yr Design Storm

Note: ESD = environmental site design.

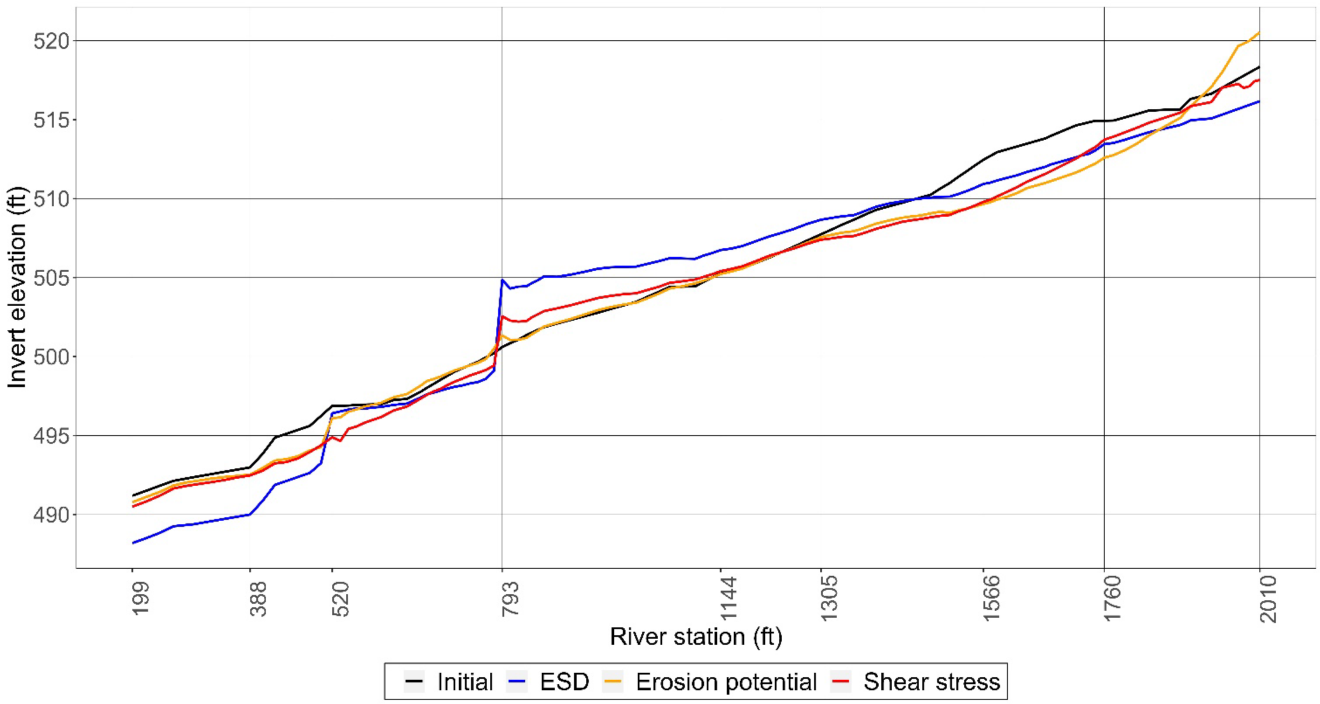

Figure 3-28. Predicted Channel Longitudinal Profile for the Current Climate for the Environmental Site Design (ESD), Erosion Potential, and Shear Stress Scenarios

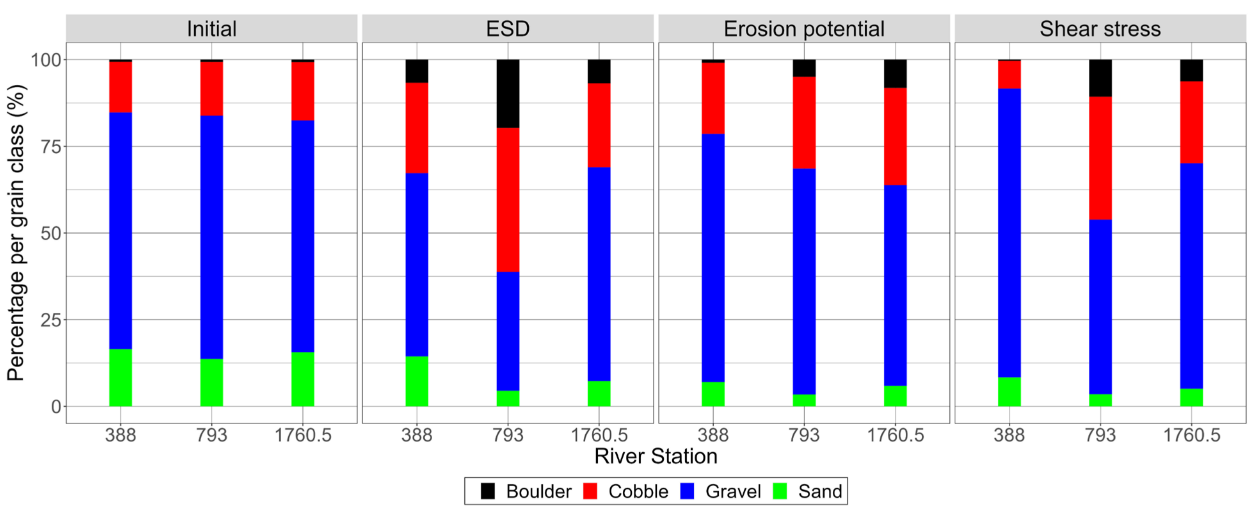

Figure 3-29. Bed Gradation at Three Different Locations for the Current Climate for the Environmental Site Design (ESD), Erosion Potential, and Shear Stress Scenarios

3.2.3.3 Evaluation of Retrofit ESD Scenarios under Climate Change

Model results indicate that the creation of a new storage pond along with the retrofitting of existing ponds in the future would significantly reduce the pattern of channel degradation and aggradation under the most extreme CC scenario when compared to the ESD scenario (Figure 3-30). However, just modifying the outlet configuration of existing ponds to match the duration and magnitude of shear stress exceedance of pre-development conditions may not be able to significantly reduce the pattern of channel degradation and aggradation under the most extreme CC scenario. Additional storage provided by the new pond could reduce the peak flows of low recurrence interval storm events which will decrease the mobilization and subsequent deposition of cobbles and boulders upstream of narrower sections of the reach around RS 793. The Shear Stress scenario will likely not be able to delay and reduce the extent of riffle aggradation at RS 793, since the riffles are formed by high flows which are not controlled by the retrofitted SCMs alone. As a result, it is anticipated that downstream channel incision will occur for the Shear Stress scenario, almost to the same extent as with the ESD scenario.

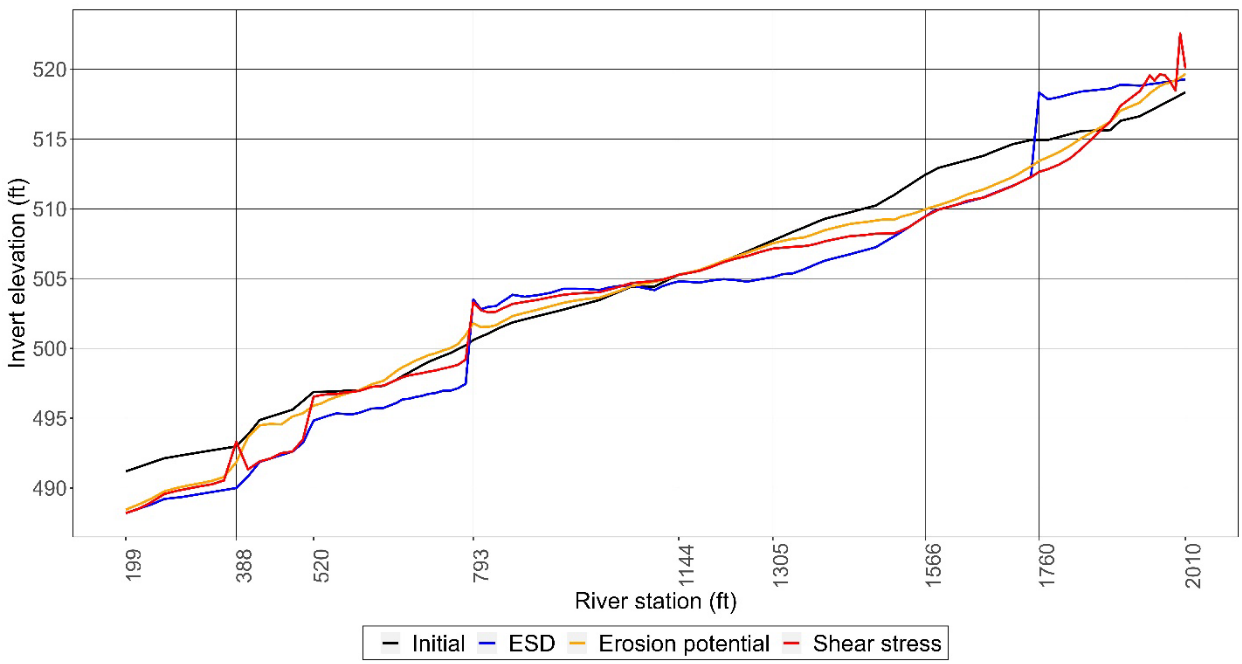

Figure 3-30. Predicted Channel Longitudinal Profile for the Most Extreme Climate Change (CC) Scenario for the Environmental Site Design (ESD), Erosion Potential, and Shear Stress Scenarios

3.2.3.4 Effect of Flow Distribution on Sediment Supply and Yield with ESD Retrofitting

Gravel bed streams like Tributary 109 are characterized by a dynamic sediment transport regime, where the sediment supply and yield are closely linked to the continuous flow regime or flow distribution being delivered to the upstream end of the reach (Downs and Soar 2021). In HEC-RAS, the sediment supply is the incoming sediment load at the upstream end of the reach and is parameterized by the sediment load rating curve. In reality, the incoming sediment load is a function of the upstream watershed and channel and is typically calibrated, since sediment loads are difficult to measure. A typical sediment rating curve increases sediment load with increasing flows because the higher flows can transport more sediment. All storage facilities, particularly those constructed in the mainstem channel capture and retain coarse sediment. This reduction in coarse sediment load to the stream can also lead to channel instability, regardless of hydrologic changes. For the Erosion Potential modeling exercise, because of the discretization of subwatersheds within SWMM, the design requirements could not be met except using an in-line detention pond. In reality, with new development, the design requirements could be met through good site design. For this reason, the effect of the new detention pond on the sediment load to the reach was ignored.

The sediment yield refers to the amount of sediment that is exported from the downstream end of the reach over the simulation time period. The sediment transport within the reach computed by the model is complex and is influenced by several factors. For instance, the size and composition of the sediment within the channel, the stream gradient, and the channel width all influence the sediment transport potential of the individual river stations of the model.

The maximum flow and predicted annual sediment supply and yield of the ESD, Erosion Potential, and Shear Stress scenarios under current and future climate conditions are provided in Table 3-5. In the Erosion Potential scenario, under current climate conditions, the addition of a new in-line pond, combined with modifications to the outlet structures of existing ponds, resulted in a reduction in the highest flow during the simulation period from 589.4 cfs to 193.3 cfs. Due to lower flows, the reduced incoming sediment load shifted the overall sediment mass balance for the reach to a net degradational state due to increased channel incision at the upper section of the reach. In contrast, the alteration of the outlet configurations of existing ponds in the Shear Stress scenario slightly increased the highest flow during the simulation period from 589.4 cfs to 592.5 cfs. This increase is the result of the retrofitted ponds not fully emptying before another storm occurred, due to the smaller outlet structures. These results highlight the need for continuous simulation using actual rainfall data when retrofitting existing ponds to reduce downstream channel erosion. With the pond outlet retrofits for the Shear Stress scenario, the drawdown time for a 5-yr storm event increased to 1.5 days. However, many high magnitude storm events under current climate conditions had inter-event time periods of less than half a day, causing the retrofitted ponds to quickly overflow and generate higher peak flows at the watershed outlet.

Under future climate conditions the magnitude of low RI storm events (100-yr.) is expected to increase (Figure 3-11), reducing the efficacy of the new and retrofitted ponds to mitigate peak flows, and increasing both flow volume and sediment supply, as compared to current conditions. Figure 3-31 depicts the flow volume and total incoming sediment load for four flow ranges under current and future climate conditions for the Erosion Potential, ESD and Shear Stress scenarios. Although the total flow volume for current climate conditions is almost the same as during future climate conditions under the ESD scenario, the proportion of flow volumes in the discharge range of 319 – 600 cfs is higher in the future, resulting in a higher incoming sediment load for future climate than for current climate conditions. The Erosion Potential scenario significantly reduced sediment loads under both the current and projected future climate by reducing discharges greater than 319 cfs. In contrast, the alteration of the outlet configuration in the Shear Stress scenario increased the highest flow of the selected CC scenario by 100 cfs, due to the combined effect of extended detention of the retrofitted ponds and shorter inter-event time periods of high-magnitude storm events. As a result, the proportion of incoming sediment load in the discharge range of >600 cfs was much higher than the ESD scenario (Figure 3-31b). These findings suggest that the design of pond retrofits should be conducted a continuous rainfall-runoff time series to evaluate the impact of multiple storm events on the effectiveness of stormwater management systems.

Table 3-5. Stream Discharge and Sediment Transport for ESD (Environmental Site Design), Shear Stress, and Erosion Potential Scenarios with and without Climate Change (CC)

Scenario	Highest flow (cfs)	Sediment supply (tons/yr.)	Sediment yield (tons/yr.)
ESD - current	589.4	63.84	22.02
Erosion Potential - current	193.3	9.23	11.61
Shear Stress - current	592.5	28.17	18.16
ESD - CC	974.7	81.97	23.62
Erosion Potential - CC	651.3	15.71	8.93
Shear Stress - CC	1076.0	69.77	15.71

[1] Effective discharge is the flow that transports the most sediment over the simulation period (Biedenharn et al. 2000).

[2] Percentile flow is the flow equaled or exceeded for a given percent of time, as determined from the flow duration curve.

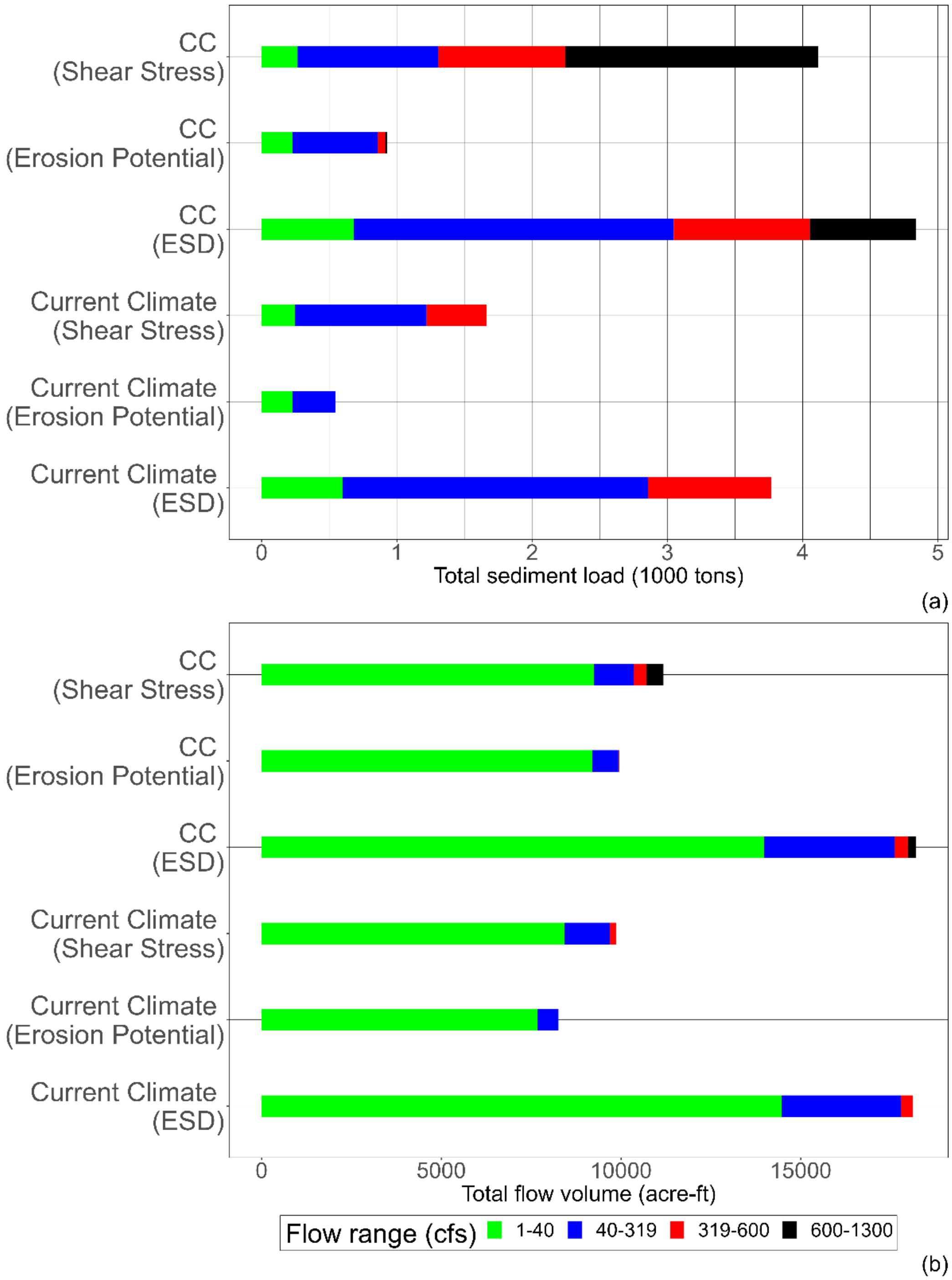

Figure 3-31. Incoming Sediment Load (a) and Flow Volume (b) as a Function of Stream Discharge Class under Current and Future Climate (CC) for Environmental Site Design (ESD), Erosion Potential, and Shear Stress Scenarios

4.0 DISCUSSION

4.1 DOWNSCALING METHODS

Urban stormwater management responds to local, short-duration precipitation and runoff conditions. Global models have limited skill in predicting local and short-term climate, requiring spatial and temporal downscaling. In this summary we see that downscaled climate products typically used for evaluation of future extreme precipitation conditions appear to contain statistically significant systematic biases relative to one another, at least for the CMIP5 round of model experiments.

Currently available dynamical downscaling products using RCMs are attractive because they are physically based and do not directly rely on analogy to historic weather patterns. However, the spatial resolution achieved in the CORDEX experiments is still coarser than is needed to resolve the effects of intense convective storms and the intensity of extreme events appears to increase at finer spatial resolution in these models. As a result, additional local downscaling might need to be applied to results downscaled with RCMs. The biggest limitation with CORDEX remains that, because of the computational effort required to implement these models, there are relatively few GCM-RCM combinations available. This may result in an inappropriate representation of the range of possible futures that are predicted.

For larger precipitation events, MACA statistical downscaling results for a given recurrence interval are higher than those obtained from LOCA. For the 2-year and 10-year events, the results from CORDEX dynamical downscaling are also higher than LOCA; however, the difference between CORDEX and LOCA decreases at higher return intervals, which is the opposite of the trend observed with MACA vs. LOCA and the average difference is negative for the 100-year event centered at 2085.

When comparing CORDEX and MACA, the differences are small for the 2-year event but become larger (with MACA on average greater than CORDEX) for longer recurrence intervals. The RMSE for the 100-yr event is notably larger for CORDEX vs. MACA than for CORDEX vs. LOCA. Taken together these results suggest that LOCA may indeed be biased low for shorter recurrence intervals but, on the other hand, MACA may be biased low for longer recurrence intervals relative to CORDEX. The small sample size available for CORDEX experiments hampers the comparison.

The comparison of methods for CMIP5 makes clear that there is a high amount of variability for predictions of extreme storm events at an individual site. Variability in the analyses arises from a number of sources, including the downscaling method, the differences in predictions between individual GCMs and emission scenarios, uncertainties in the Atlas 14 estimation process, and “luck of the draw” as to whether rare events are sampled within relatively short periods of record. Hierarchical ANOVA suggests that, while downscaling method is a statistically significant contributor to total variability, greater fractions of the total variance are attributable to site-specific variability (i.e., to uncertainties associated with data and the IDF estimation process at individual sites) and to the individual GCM. See Liang et al. (2020) for a detailed examination of design storm uncertainty under future climate for the Chesapeake Bay region. Liang et al. demonstrate how local-scale spatial variability in extreme precipitation is subject to uncertainty associated with both the Atlas 14 regionalization of parameters and the spatial downscaling process.

It may be that the apparent biases between MACA and LOCA methods will diminish if and when downscaling results from both methods from the newer CMIP6 model experiments, with consistent training data, become publicly available. The developers of LOCA downscaled CMIP6 GCM data in late

2022 and announced a plan to release it on the Lawrence Livermore National Laboratory Green Data Oasis, but to date the output has only been readily available from the University of Chicago Globus system, which is free to non-profit research institutions but requires a paid subscription for commercial use. MACA downscaling for CMIP6 has not been announced.

4.2 STREAM STABILITY

The watershed of Tributary 109 in Clarksburg, MD underwent development between 2006 and 2017, incorporating extensive implementation of Environmental Site Design (ESD). To assess the potential impacts of climate change on stream channel stability, a coupled hierarchical modeling approach was employed, utilizing a watershed-scale Storm Water Management Model (SWMM) and a well-calibrated quasi-unsteady 1-D Hydraulic Engineering Center's River Analysis System (HEC-RAS) sediment transport model.

Field observations of the channel following the final build-out condition revealed that, despite the implementation of ESD and the presence of 70 SCMs (1 SCM per 3 acres), the channel is experiencing degradation. Although it is impossible to fully capture the dynamics of channel processes with a 1-D HEC-RAS sediment transport model, it can provide insights into long-term trends in channel behavior.

During large storm events, stream discharge has the potential to mobilize the cobbles and small boulders present in the channel bed, leading to the formation of steep riffles. Upstream of these riffles, aggradation is likely to occur, while downstream areas are prone to bed incision, although the overall channel is experiencing net aggradation. This behavior indicates that the channel is adjusting to the changing hydrology and sediment load of the watershed, resulting in a reduction in channel slope through a combination of bed incision and aggradation.

While the patterns of projected long-term channel changes for each climate scenario are similar to those in the current climate, it is expected that the magnitude of channel degradation will be greater under future conditions. Specifically, the median channel depth may increase by as much as an additional 1.5 ft. as compared to channel changes expected under the current climate. Additionally, the median channel cross-sectional area could increase by as much as an additional 30 $ft.^2$ compared to the channel changes expected under current conditions.

In conclusion, the current stormwater regulations in the State of Maryland are anticipated to be insufficient to protect channel stability, and the anticipated changes in climate will further accelerate channel degradation. Designing stormwater management plans based on design storms only, with no consideration of sediment transport in the receiving stream or a sequence of storm events, will not protect channel stability. However, retrofitting the existing SCMs in the watershed to maintain or restore pre-development sediment transport capacity, as opposed to the critical shear stress exceedance, could significantly reduce the extent of channel degradation in the modeled reach when compared to the original ESD requirements.

4.3 ENVIRONMENTAL SITE DESIGN

Hypothesis 3 for this project stated “ESD concepts and requirements are applicable and appropriate to management of real watersheds under future climate.” The answers to this hypothesis are mixed.

On the one hand, current ESD regulations specify that individual SCMs are designed to treat runoff from the 90th percentile 24-hr rainfall event. Our studies suggest that development that incorporates ESD under guidance based on historic climate will continue to meet the design criteria for individual SCMs under projected changes in climate over the course of the 21st century because only minor changes are projected, on average, in the magnitude of 24-hr events with a recurrence interval of one year or less. Analysis of the predicted performance of individual SCMs suggests that the fraction of urban runoff that is treated under ESD during a 90th percentile event will not change significantly under future climate, which is a positive indicator for achieving Chesapeake Bay water quality mitigation goals, although the total pollutant loading across all events is likely to increase because the baseline of comparison (runoff from woods in good condition for the 1-yr., 24-hr. event) is also likely to increase.

The fact that the design objectives of individual SCMs are likely to be achieved, however, does not necessarily imply that current ESD guidance is sufficient for the management of real watersheds under future climate. The overall goal of ESD is to control runoff from new development or redevelopment sites to levels consistent with runoff from woods in good condition for the 1-yr., 24-hr. event. Our study results indicate that the current ESD design criteria, as implemented in Tributary 109, result in post-development peak discharges and runoff volumes that exceed those of the pre-development watershed, which was primarily agricultural. Because the design criteria are based on controlling runoff volumes and do not consider the response of the entire watershed to storm events, the cumulative impacts of the development on watershed hydrology are not considered in the existing design of stormwater management systems.

ESD includes a requirement to retain a volume of water for channel protection The CP_v was developed based on the underlying assumption that controlling high frequency, low magnitude runoff events will maintain channel stability. This concept is rooted in the widely-accepted idea within the stream restoration community that the bankfull discharge is the channel-forming discharge (a single discharge that stable alluvial channels adjust to carry) and has a recurrence interval of 1-2 years (Doyle et al., 2007). Because bankfull stage can be estimated using field measurements and the bankfull discharge calculated using survey data and Manning's equation (or USGS gage data), the bankfull discharge is commonly used as an estimate of the channel-forming flow. However, these field estimates produce discharge estimates that can vary over an order of magnitude for similarly-sized watersheds. Additionally, the concept of a channel-forming flow is only applicable to alluvial channels in equilibrium. Stream channels in Maryland vary widely, from steep, non-alluvial channels in the western mountains to fully alluvial sand-bed streams in the coastal plain. While it is often stated that bankfull discharge has a typical recurrence interval of 1-2 years, others have shown that bankfull discharge can have a recurrence interval of 1-32 years (Williams, 1978), depending on the size of the channel bed material and watershed hydrology. Research conducted following the development of the ESD regulations (Annable et al., 2011) indicates discharge for urbanized streams exceeds bankfull stage multiple times per year. In reality, channel morphology is determined by the full range of flows in a watershed, as well as the sediment supplied to the channel. The concept that a single discharge can replicate the geomorphic work of a full range of discharges assumes consistent climate and watershed conditions over periods of time that far exceed typical engineering and planning time frames.

Additionally, given the history of impacts to streams in the eastern US and the time required for streams to respond to disturbances, many streams in the Chesapeake Bay watershed are still in a state of adjustment. While widely recognized within the field of fluvial geomorphology, this idea was brought to the mainstream water resources community via the work of Walter and Merritts (2008), after the ESD regulations were adopted. Ultimately, maintaining channel stability is highly dependent on the characteristics of each receiving stream.

An additional assumption of the Cp_v is that detaining the runoff volume from the 1-yr, 24-hr storm event for 24 hours will control bankfull and sub-bankfull discharges following development below erosive levels (in other words, discharge is largely a function of rainfall depth). While runoff rate and rainfall depth are strongly linked, the stream discharge resulting from a given storm event, particularly smaller storms, is also strongly controlled by watershed conditions at the time a storm event occurs (e.g., soil moisture content. As a result, a given depth of precipitation over a 24-hr period could produce a range of peak flood discharges in the receiving stream. Furthermore, the duration and peak of the discharge hydrograph from any stormwater structure is determined only in part by the volume of runoff. The SCM surface area and depth, which control the stage-storage relationship, and the outflow structure design, which controls the stage-discharge relationship, also significantly affect the peak and duration of outflow hydrographs from SCMs.

It should also be recognized that individual SCMs are frequently designed with no consideration for the response of other SCMs in the watershed. However, the peak discharge at any point in a watershed in response to a given storm event depends not only on the peak discharges from upstream subwatersheds but also the time at which those individual subwatershed peaks arrive at that point. While designing each SCM individual greatly simplifies design, the cumulative impact of multiple SCMs on the receiving stream must be considered to effectively protect the stability of small channels.

The limitations of these simplifying assumptions, common in many stormwater regulations, are illustrated by the study results and field observations that the extensive use of ESD is not currently protecting channel stability of Tributary 109. Channel morphology depends not only on the flow of water in stream channels, but also the input of sediment to the channel and the characteristics of the channel itself. Channel degradation is predicted to accelerate in the future because the primary effect of climate change will be to increase the magnitude of low frequency storm events. Given that ESD focuses on high frequency, low magnitude storm events, stormwater management systems designed based on current ESD regulations will not provide adequate control of future extreme storm events.

In summary, while the key design requirements of current ESD regulations aim to control runoff volume at the site level, the existing SCMs within the study watershed have not successfully reproduced the runoff rates observed or modeled in the pre-development condition. These findings highlight the need for further investigation and potential adjustments in SCM design and implementation strategies to account for the effects of antecedent events and potential changes in storm magnitudes in reducing the performance of SCMs. Additionally, the impact of development on sediment transport within the receiving stream should be considered in the design of stormwater management systems to protect channel stability.

4.4 ADAPTING TO FUTURE CLIMATE

Traditional engineering approaches to stormwater management are based on understanding the environmental conditions the project is likely to face, often with the implicit assumption that past experience is an adequate guide to the future, accompanied by the addition of a margin of safety to protect against failure. Climate change introduces a new level of complexity. Despite significant advances in climate science and modeling, it is not currently possible to forecast long-term, local-scale changes in precipitation with accuracy; nor is it clear that the magnitude of uncertainty in such predictions is well understood (Butcher, 2021). Key modeling challenges include differing levels of confidence in projections of future climate changes at spatial and temporal scales relevant to resource managers, variability in projecting the effects of climate change and management activities on the environment, and potential nonlinear or abrupt changes (Dessai and Hulme 2004, West et al. 2012). Even with perfect models, uncertainty regarding the future will remain because changes over time also depend on human political and economic decisions. These uncertainties must be acknowledged, together with the recognition that climate change impacts will present an evolving, moving target throughout the coming century. A key realization is that, while decision-making under large climate change uncertainties can be difficult, uncertainty is not equivalent to knowing nothing (Hoffman et al. 2014).

This research demonstrates the broad range of variability in possible future precipitation conditions at the local level. This presents a dilemma for policy makers who must, as in all decisions, strike a balance between risk avoidance and cost. There is a high, but not certain, probability that runoff from larger rainfall events will increase under future climate. Preparations are warranted for this likely increase, and, while the exact balance between risk and cost is uncertain, it is important to acknowledge that the risk exists. While it may not be possible to agree on which future condition is most likely to occur, it is advisable to pursue solutions that are robust against an uncertain future in that they (1) provide, to the extent possible, direct benefits (in stormwater control) and co-benefits (such as reduction in urban heat islands and greenhouse gas emissions) that will be valuable across a range of possible futures, and (2) employ strategies that can be modified as conditions change, such as emphasizing green infrastructure stormwater management measures for water quality protection over expensive hard structures that are difficult and expensive to modify if conditions differ from expectations.

At this time, it is not possible to determine *a priori* which climate products provide the "best" representation of an uncertain future. Instead, it is important to examine the range of potential futures. Some authors have advocated selecting GCM experiments based on their skill in replicating historic climate. However, the consensus is that good performance on historic climate does not guarantee that a GCM will provide strong predictions of future climate – although notably poor performance on historic climate may suggest eliminating certain GCMs. For the Pacific Northwest, Mote and Salathé (2010) evaluated biases in global climate model predictions and found that no single GCM fell into the best five members of the ensemble for prediction of both temperature and precipitation; likewise, no GCM fell into the worst five for both temperature and precipitation. It is thus not appropriate to select a specific GCM based on its perceived prediction skill for the area; instead, the suite of GCMs is more appropriate for analyzing the potential ensemble range of future climates (Mote et al., 2011). This is consistent with findings of Knutti et al. (2010) and Pierce et al. (2009) that attempts to cull the best GCMs yields little difference in representing likely future change relative to a randomly selected subset of GCMs.

Other authors have attempted to ensure that a selected subset of GCMs provides good coverage of the range of potential future events by selecting GCMs that fall near the median and represent reasonable extremes (e.g., 10th percentile, 90th percentile) on readily available annual average statistics of temperature and precipitation volume change. Our own experience has been that these annual average statistics, while indicative of the general water balance, do not provide a reliable guide to the prediction of extreme precipitation events, with the greatest increase in intensity of events with a recurrence of one year or more often arising from scenarios that are, on average, toward the drier end of the ensemble.

Given these concerns it is advisable to approach analysis relative to stormwater as a stochastic problem by analyzing the full distribution of predictions for relevant endpoints. If individual representative scenarios are needed for illustrative purposes it is best to analyze over the full ensemble of GCMs, emission (or future radiative forcing) scenarios, and statistical downscaling products and then make a post hoc selection of representative scenarios based on the distribution of outcomes of interest (e.g., the 10-year 24-hour storm event intensity) by, for instance, selecting individual GCMs that fall near the median, 10th percentile, and 90th percentile of that outcome. This type of approach requires more analysis but is feasible and manageable with tools that provide automated analysis of climate-modified IDF curves for future conditions.

(This page left intentionally blank.)

5.0 CONCLUSIONS

This research evaluated several important issues relative to projected and adaptation to future climate, stormwater runoff, and management of channel condition. The work is framed by three research hypotheses, summarized below.

H1. Problems in the LOCA methodology introduce biases in the estimation of future 1-year, 24-hour rainfall events used to calculate ESD.

The null hypothesis of no significant differences is not supported, and we conclude that there are relative biases between LOCA, MACA, and other sources of downscaled precipitation data under future climate. The LOCA and MACA products from CMIP5 show relatively small, but statistically significant divergences from one another for extreme precipitation projections and both appear to have some systematic differences from CORDEX dynamically downscaled results for the same GCMs. At this point it is advisable to evaluate the range of results available from both LOCA and MACA as neither is clearly superior to the other as currently implemented. Fortunately, both datasets are available in similar format so that code can readily be adapted to analysis of both products. These conclusions should be revisited as more downscaled products become available for the CMIP6 model runs.

H2. Despite changes in precipitation by mid-century, current ESD requirements will be sufficient to mitigate effects associated with anthropogenic development.

Because there are significant differences between LOCA and MACA this hypothesis needed to be addressed by considering the range of potential futures across both sources. The evaluation of this hypothesis is mixed: Current ESD designs are likely to continue to meet their design requirements regarding change in runoff from natural land cover and treatment of runoff from the one year and 90th percentile rainfall events, respectively. This does not, however, indicate that "current ESD requirements will be sufficient to mitigate effects associated with anthropogenic development." That question must be addressed through a more detailed consideration of runoff and sediment transport processes using continuous simulation, as described under H3.

H3. ESD concepts and requirements are applicable and appropriate for management of real watersheds under future climate.

The ensemble simulation results indicate that the application of ESD concepts and requirements could potentially be effective in mitigating the impacts of increased runoff resulting from changing climate conditions when evaluated on an individual SCM basis. However, when considering the cumulative effects of development using continuous rainfall simulation of the entire Tributary 109 watershed, it is clear that ESD does not replicate the hydrology of a watershed with "woods in good condition" and will not protect channel stability over multiple decades under current or future climate conditions. This conclusion is supported by field observations of channel degradation and analysis of measured stream discharge (Hopkins et al. 2022). Given that climate change is predicted to increase the magnitude of severe storm events, the existing channel degradation is likely to accelerate in the future.

- **H3a. The historical flow duration curve for Tributary 109 will not change under future climate.** Frequency analysis of storm event peak flows indicates that the magnitude of peak flows with low percent exceedance (less than 25%) will increase in future although the more frequent events will likely be less intense. However, this conclusion is based on sub-daily downscaling using quantile mapping to the storm events recorded by a local rain gauge during water years 2005 to 2020, which was an unusually wet period.

- **H3b. Watersheds developed under current stormwater management regulations and climate will not experience increased channel erosion.** Coupled flow-sediment simulation results showed that even with the extensive implementation of ESD, the studied reach is expected to degrade over many decades, developing alternate regions of aggradation and degradation due to the changes in watershed hydrology caused by urbanization under both current and future climate conditions.
- **H3c. Retrofitting existing stormwater management using the future 1-yr., 24-hr. design storm will protect channel stability.** Retrofitting the existing SCMs in the watershed to maintain or restore pre-development sediment transport capacity for the 1-yr., 24-hr. design storm could significantly reduce the extent of channel degradation in the modeled reach when compared to the original ESD requirements under current climate as well the most extreme climate change scenarios.

6.0 REFERENCES

Abatzoglou, J.T., and T.J. Brown. 2012. A comparison of statistical downscaling methods suited for wildfire applications. *Int. J. Climatology*, 32: 772-780.

Alamdari, N., and D. J. Sample. 2019. A multiobjective simulation-optimization tool for assisting in urban watershed restoration planning. *J. Clean. Prod.*, 213:251–261.

Alsmadi, M., T.W. Thompson, D.J. Sample, A. Miller, S. Towsif Khan, and M.S. Behrouz. 2022. Effectiveness of Stormwater Management Practices in Protecting Stream Channel Stability. Virginia Tech, Blacksburg, VA.

Amengual, A., V. Homar, R. Romero, S. Alonso, and C. Ramis. 2012. A statistical adjustment of regional climate model outputs to local scales: Application to Platja de Palma, Spain. J*ournal of Climate*, 25:939-957.

Annable, W. K., C. C. Watson, and P. J. Thompson. 2012. Quasi-equilibrium conditions of urban gravel-bed stream channels in southern Ontario, Canada. *River Res. Appl.*, 28:302–325.

Arnbjerg-Nielsen, K., P. Willems, J. Olsson, S. Beecham, A. Pathirana, I. Bülow Gregersen, H. Madssen, and V.T.-V. Nguyen. 2013. Impacts of climate change on rainfall extremes and urban drainage systems: A review. *Water Science & Technology*, 68: 16-28.

Baker, S. Matt. 2022a. Email message to T. Thompson on 8 February 2022.

Baker, S. Matt. 2022b. Phone conversation with T. Thomposn on 15 February 2022.

Biedenharn, D. S., R. R. Copeland, C. R. Thorne, P. J. Soar, R. D. Hey, and C. C. Watson. 2000. Effective Discharge Calculation : A Practical Guide. U.S. Army Engineer Research and Development Center, Vicksburg, MS.

Bledsoe, B. P. 2002. Stream Erosion Potential and Stormwater Management Strategies. *J. Water Resour. Plan. Manag.*, 128:451–455.

Bonnin, G.M., D. Martin, B. Lin, T. Parzybok, M. Yekta, and D. Riley. 2006. NOAA Atlas 14, Precipitation-frequency Analysis of the United States, Volume 2, Version 3.0: Delaware, District of Columbia, Illinois, Indiana, Kentucky, Maryland, New Jersey, North Carolina, Ohio, Pennsylvania, South Carolina, Tennessee, Virginia, West Virginia. Silver Spring, MD: National Oceanic and Atmospheric Administration.

Bonnin, G.M., D. Martin, B. Lin, T. Parzybok, M. Yekta, D. Riley, D. Brewer, and L. Hiner. 2007. Updates to NOAA Precipitation Frequency Atlases. World Environmental and Water Resources Congress 2007 : Restoring Our Natural Habitat. Doi: 10.1061/40927(243)413.

Box, G.E.P. and G.C. Tiao. 1992. *Bayesian Inference in Statistical Analysis*. John Wiley and Sons, New York.

Brunner, G. W. 2022. HEC-RAS User's Manual Version 6.3. US Army Corps of Engineers, Hydrologic Engineering Center, Davis, California.

Butcher, J.B. 2021. Storm intensification: Implications for environmental design in Maryland. *Journal of Water Resources Planning and Management*, 147(10), doi: 10.1061/(ASCE)WR.1943-5452.0001448. https://ascelibrary.org/doi/abs/10.1061/%28ASCE%29WR.1943-5452.0001448.

Butcher, J.B. 2022. Downscaling Methods for Stormwater Response to Climate Change. Grant 19278 Deliverable 7. Prepared by Tetra Tech, Inc. for Chesapeake Bay Trust Restoration Research Program.

Butcher, J.B., T. Zi, B. Pickard, S. Job, T.E. Johnson, and B. Groza. 2021. IDF Curves for precipitation and runoff under future climate: Efficient statistical generation approach. *Climatic Change,* 164, 3. DOI:10.1007/s10584-021-02963-y. https://rdcu.be/cd0qS.

Cannon, A.J., and S. Innocenti. 2019. Projected intensification of sub-daily and daily rainfall extremes in convection-permitting climate model simulations over North America: Implications for future intensity-duration-frequency curves. *Natural Hazards and Earth System Sciences*, 19: 421-440.

Corder, G.W., and D.I. Foreman. 2009. Nonparametric Statistics for Non-Statisticians: A Step-by-Step Approach. Wiley.

Dessai, S., and M. Hulme. 2004. Does climate adaptation policy need probabilities? *Climate Policy*, 4(2):107-128.

Downs, P. W., and P. J. Soar. 2021. Beyond stationarity: influence of flow history and sediment supply on coarse bedload transport. *Water Resour. Res.*, 57:1–19.

Doyle, M.W., D. Shields, K.F Boyd, P.B Skidmore, and D. Dominick. 2007. Channel-forming discharge selection in river restoration design. *Journal of Hydraulic Engineering* 133 (7): 831–37. https://doi.org/10.1061/(ASCE)0733-9429(2007)133:7(831).

Edwards, P. J., E. A. Watson, and F. Wood. 2019. Toward a Better Understanding of Recurrence Intervals, Bankfull, and Their Importance. *J. Contemp. Water Res. Educ.*, 166:35–45.

England Jr., J. F., T. A. Cohn, B. A. Faber, J. R. Stedinger, W. O. Thomas Jr., A. G. Veilleux, J. E. Kiang, and J. Mason Robert R. 2019. Guidelines for determining flood flow frequency — Bulletin 17C (ver. 1.1, May 2019). U.S. Geological Survey Techniques and Methods, Reston, VA.

Froelich, A. J. 1975. Thickness of overburden map, Annandale Quadrangle, Virginia. Page Open-File Report.

Gibson, S., B. Comport, and Z. Corum. 2017. Calibrating a Sediment Transport Model through a Gravel-Sand Transition: Avoiding Equifinality Errors in HEC-RAS Models of the Puyallup and White Rivers. Pages 179–191 World Environmental and Water Resources Congress 2017: Hydraulics and Waterways and Water Distribution Systems Analysis - Selected Papers from the World Environmental and Water Resources Congress 2017.

Hamzah, F. M., H. Tajudin, and O. Jaafar. 2021. A comparative flood frequency analysis of high-flow between annual maximum and partial duration series at Sungai Langat Basin. *Sains Malaysiana*, 50:1843–1856.

Hayhoe, K., D.J. Wuebbles, D.R. Easterling, D.W. Fahey, S. Doherty, J. Kossin, W. Sweet, R. Vose, and M. Wehner. 2018: Our changing climate. In *Impacts, Risks, and Adaptation in the United States: Fourth National Climate Assessment, Volume II* [Reidmiller, D.R., C.W. Avery, D.R. Easterling, K.E. Kunkel, K.L.M. Lewis, T.K. Maycock, and B.C. Stewart (eds.)]. U.S. Global Change Research Program, Washington, DC. doi: 10.7930/NCA4.2018.CH2.

Hoffman, J., E. Rowland, C. Hawkins Hoffman, J. West, S. Herrod-Julius, and M. Hayes. 2014. Decision making under uncertainty. Chapter 12 in *Climate-Smart Conservation: Putting Adaptation Principles into Practice*, ed. B.A. Stein, P. Glick, N. Edelson, A. Staudt. National Wildlife Federation, Washington, DC.

Hood, M. J., J. C. Clausen, and G. S. Warner. 2007. Comparison of stormwater lag times for low impact and traditional residential development. *J. Am. Water Resour. Assoc.*, 43:1036–1046.

Hopkins, K. G., A. S. Bhaskar, S. A. Woznicki, and R. M. Fanelli. 2020. Changes in event-based streamflow magnitude and timing after suburban development with infiltration-based stormwater management. *Hydrol. Process.*, 34:387–403.

Hopkins, K. G., S. A. Woznicki, B. M. Williams, C. C. Stillwell, E. Naibert, M. J. Metes, D. K. Jones, D. M. Hogan, N. C. Hall, R. M. Fanelli, and A. S. Bhaskar. 2022. Lessons learned from 20 y of monitoring suburban development with distributed stormwater management in Clarksburg, Maryland, USA. *Freshw. Sci.*, 41:459–476.

Jakob, D. 2013. Nonstationarity in extremes and engineering design. *Extremes in a Changing Climate: Detection, Analysis and Uncertainty*. AghaKouchak, A., D. Easterling, K. Hsu, S. Schubert, and S. Sorooshian, Eds., Springer, Dordrecht, 363–417.

Janssen, E., R. L. Sriver, D. J. Wuebbles, and K. E. Kunkel. 2016. Seasonal and regional variations in extreme precipitation event frequency using CMIP5. *Geophysical Research Letters*, 43, 5385–5393, doi:10.1002/2016GL069151.

Jarnagin, S. T., and D. B. Jennings. 2004. COLLABORATIVE HYDROLOGIC RESEARCH IN THE CLARKSBURG SPECIAL PROTECTION AREA. Presented at Maryland Water Monitoring Council Workshop on Integrated Hydrologic Monitoring, Baltimore, MD, August 30, 2004.

Job, S., M. Harris, S. Julius, J.B. Butcher, and J.T. Kennedy. 2020. Adapting urban BMPs for resilience to long-term environmental changes. *Water Environment Research*, 92(12): 2178-2192. http://dx.doi.org/10.1002/wer.1302.

Kahane, J.P., and J. Peyriere. 1976. Sur certaines martingales de Benoit Mandelbrot. *Advances in Mathematics*, 22: 131–145.

Knutti, R., R. Furrer, C. Tebaldi, J. Cermak, and G.A. Meehl. 2010. Challenges in combining projections from multiple climate models. *Journal of Climatology*, 23(10):2739–2758.

Kristvik, E., B.G. Johannessen, and T.M. Muthanna. 2019. Temporal downscaling of IDF curves applied to future performance of local stormwater measures. *Sustainability*, 11, 1231; doi:10.3390/su11051231.

Kullback, S., and R. A. Leibler. 1951. On Information and Sufficiency. *Ann. Math. Stat.*, 22:79–86.

Kumar, S., M. Sekhar, D. Reddy, I. Cluckie, Y. Chen, V. Babovic, L. Konikow, et al. 2009. Improving the disaggregation of daily rainfall into hourly rainfall using hourly soil moisture. Hydroinformatics in Hydrology, Hydrogeology and Water Resources (Proc. of Symposium JS.4, Joint IAHS & IAH Convention, Hyderabad, India, September 2009). IAHS Publ. 331.

Li, J., J. Evans, F. Johnson, and A. Sharma. 2017. A comparison of methods for estimating climate change impact on design rainfall using a high-resolution RCM. *Journal of Hydrology*, 547: 413-427.

Liang, M.S., S. Julius, Z. Dong, J. Neal, and Y.F. Yang. 2020. Assessing and managing design storm variability and projection uncertainty in a changing coastal environment. *Journal of Environmental Management*, 264, 110494.

Livneh, B., T. J. Bohn, D. W. Pierce, F. Muñoz-Arriola, B. Nijssen, R. Vose, and L. Brekke. 2015. A spatially comprehensive, hydrometeorological data set for Mexico, the US, and Southern Canada 1950–2013. *Sci. Data*, 2, 150042.

Mandelbrot, B.B. 1974. Intermittent turbulence in self-similar cascades: Divergence of high moments and dimension of the carrier. *Journal of Fluid Mechanics*, 62, 331– 358.

MDE. 2009. 2000 Maryland Stormwater Design Manual, Volumes I and II (Revised May 2009). Maryland Dept. of the Environment (MDE).

Mearns, L.O., et al., 2017: The NA-CORDEX dataset, version 1.0. NCAR Climate Data Gateway, Boulder CO, https://doi.org/10.5065/D6SJ1JCH.

Menabde, M., D. Harris, A. Seed, G. Austin, and D. Stow. 1997. Multiscaling properties of rainfall and bounded random cascades. *Water Resources Research*, 33(12): 2823-2830.

Metes, M. J., and D. K. Jones. 2021. Lidar-derived digital elevation models in Clarksburg, MD representing the years 2002, 2008, 2013, and 2018. U.S. Geological Survey.

Molnar, P., and P. Burlando. 2005. Preservation of rainfall properties in stochastic disaggregation by a simple random cascade model. *Atmospheric Research*, 77:137-151, doi:10.1016/j.amosres.2004.10.024.

Mote, P., L. Brekke, P.B. Duffy, and E. Maurer. 2011. Guidelines for constructing climate scenarios. *Eos, Transactions of the American Geophysical Union*, 92(31):257–258.

Mote, P.W., and E.P. Salathé. 2010. Future climate in the Pacific Northwest. *Climatic Change*, 102(1–2):29–50. doi:10.1007/s10584-010-9848-z.

NRCS. 1986. Urban Hydrology for Small Watersheds. TR-55. U.S. Dept. of Agriculture, Natural Resources Conservation Service.

NWS. 2022. Analysis of Impact of Nonstationary Climate on NOAA Atlas 14 Estimates, Assessment Report. Office of Water Prediction, National Weather Service. https://hdsc.nws.noaa.gov/files25/NA14_Assessment_report_202201v1.pdf, accessed 6/13/23.

Papalexiou, S.M., and A. Montanari. 2019. Global and regional increase of precipitation extremes under global warming. *Water Resources Research*, 2019, 55, 4901–4914.

Pierce, D. W., D. R. Cayan, and B. L. Thrasher. 2014. Statistical downscaling using localized constructed analogs (LOCA). *J. Hydrometeorol.*, 15:2558–2585.

Pierce, D.W., D.R. Cayan, and B.L. Thrasher. 2014. Statistical downscaling using localized constructed analogs (LOCA). *J. Hydrometeorol.*, 15:2558-2585.

Pierce, D.W., T.P. Barnett, B.D. Santer, and P.J. Gleckler. 2009. Selecting global climate models for regional climate change studies. *Proceedings of the National Academy of Sciences*, 106(21):8441–8446.

Pomeroy, C. A., N. A. Postel, P. A. O'Neill, and L. A. Roesner. 2008. Development of storm-water management design criteria to maintain geomorphic stability in Kansas city metropolitan area streams. *J. Irrig. Drain. Eng.*, 134:562–566.

Ragno, E., A. AghaKouchak, C.A. Love, L. Cheng, F. Vahedifard, and C.H.R. Lima. 2018. Quantifying changes in future intensity-duration-frequency curves using multimodel ensemble simulations. *Water Resources Research*, 54(3): 1751-1764.

Rey, D., and M. Neuhäuser. 2011. Wilcoxon-Signed-Rank Test. Pages 1658–1659 *in* M. Lovric, editor. International Encyclopedia of Statistical Science. Springer Berlin Heidelberg, Berlin, Heidelberg.

Rosburg, T. T., P. A. Nelson, and B. P. Bledsoe. 2017. Effects of urbanization on flow duration and stream flashiness: a case study of Puget Sound streams, Western Washington, USA. *J. Am. Water Resour. Assoc.*, 53:493–507.

Rossman, L. A. 2015. Storm Water Management Model User's Manual Version 5.1. U.S. Environmental Protection Agency, Washington, DC, EPA/600/R-14/413b, 2015, Washington, DC.

Sample, D. J., T. Wynn-Thompson, S. Towsif Khan, and M. Al-Smadi. 2022. Evaluation of ESD hydrology: Tributary 109 - Technical memorandum 8A. Prepared for Chesapeake Bay Trust, Restoration Research Program, Request #19278. Blacksburg.

Shapiro, S. S., and M. B. Wilk. 1965. An analysis of variance test for normality (complete samples)†. *Biometrika*, 52:591–611.

Towsif Khan, S., M. Al-Smadi, T. Thompson, D. Sample, and A. Miller. 2023. Effectiveness of stormwater management practices in protecting stream channel stability in Tributary 109 of Little Seneca Creek. Report to the Chesapeake Bay Trust, Annapolis, MD.

Trenberth, K.E., A. Dai, R.M. Rasmussen, and D.B. Parsons. 2003. The changing character of precipitation. *Bulletin of the American Meteorological Society*, (September 2003): 1205-1217.

Van Campenhout, J., G. Houbrechts, A. Peeters, and F. Petit. 2020. Return Period of Characteristic Discharges from the Comparison between Partial Duration and Annual Series, Application to the Walloon Rivers (Belgium). *Water*, 12:792.

Vose, R. S., S. Applequist, M. Squires, I. Durre, C. J. Menne, C. N. Williams, C. Fenimore, K. Gleason, and D. Arndt. 2014. Improved historical temperature and precipitation time series for U.S. climate divisions. *J. Appl. Meteorol. Climatol.*, 53:1232–1251.

Vu, M.T., S.V. Raghavan, J. Liu, and S.-Y. Liong. 2018. Constructing short-duration IDF curves using coupled dynamical-statistical approach to assess climate change impacts. *International Journal of Climatology*, 38(6): 2662-2671.

Walter, R.C., and D.J. Merritts. 2008. Natural streams and the legacy of water-powered mills. *Science*, 319:299-304. https://doi.org/10.1126/science.1151716.

Wang, G., C. Kirchhoff, A. Seth, J.T. Abatzoglou, B. Livneh, D.W. Pierce, L. Fomenko, and T. Ding. 2020. Projected changes of precipitation characteristics depend on downscaling method and training data: MACA vs. LOCA using the U.S. Northeast as an example. *J. Hydrometeorol.*, https://doi.org/10.1175/JHM-D-19-0275.1.

West, J.M., S.H. Julius, and C.P. Weaver. 2012. Assessing confidence in management adaptation approaches for climate-sensitive ecosystems. *Environmental Research Letters*, 7(1):1-8.

Wickham, H., M. Averick, J. Bryan, W. Chang, L. McGowan, R. François, G. Grolemund, A. Hayes, L. Henry, J. Hester, M. Kuhn, T. Pedersen, E. Miller, S. Bache, K. Müller, J. Ooms, D. Robinson, D. Seidel, V. Spinu, K. Takahashi, D. Vaughan, C. Wilke, K. Woo, and H. Yutani. 2019. Welcome to the Tidyverse. *J. Open Source Softw.*, 4:1686.

Wilcock, P. R., and J. C. Crowe. 2003. Surface-based transport model for mixed-size sediment. *J. Hydraul. Eng.*, 129:120–128.

Williams, B. M., H. M. Tarekegn, D. M. Hogan, T. S. Jarnagin, S. A. Woznicki, and K. G. Hopkins. 2018. Land use land cover, 1998 - 2013, Clarksburg (Montgomery County, MD). U.S. Geological Survey.

Williams, B. M., K. G. Hopkins, M. J. Metes, D. K. Jones, S. Gordon, and W. Hamilton. 2022. Tracking geomorphic changes after suburban development with a high density of green stormwater infrastructure practices in Montgomery County, Maryland. *Geomorphology*, 414:108399.

Williams, G. P. 1978. Bank-full discharge of rivers. *Water Resources Research,* 14 (6): 1141–54. https://doi.org/10.1029/WR014i006p01141.

Wohl, E. 2018. Geomorphic context in rivers. *Prog. Phys. Geogr.*, 42:841–857.

Wood, A.W., L. Leung, V. Sridhar, and D.P. Lettenmaier. 2004. Hydrologic implications of dynamical and statistical approaches to downscaling climate model outputs. *Climatic Change*, 62: 189-216, doi: 10.1023/B:CLIM.0000013685.99609.9e.